AN ABSTRACT OF THE DISSERTATION OF

Susan Genualdi for the degree of Doctor of Philosophy in Chemistry presented on September 18, 2008.
Title: Semi-volatile Organic Compounds as Molecular Markers for Atmospheric and Ecosystem Transport

APPROVED :

Staci L. Simonich

The use of semi-volatile organic compounds (SOCs) as molecular markers to identify the contributions of regional and long-range atmospheric transport, as well as current and historic sources, and contaminant deposition in remote ecosystems of the Western U.S. was investigated. Trans-Pacific air masses influenced by Siberian biomass burning events had elevated concentrations of polycyclic aromatic hydrocarbons (PAHs) and the historic use pesticides dieldrin and alpha-HCH, while air masses influenced by regional fires in the Pacific Northwestern U.S. had enhanced concentrations of PAHs and the current-use pesticides dacthal and endosulfan. This suggests that previously deposited SOCs, such as pesticides, revolatilize to the atmosphere during forest fires. In addition, forest soils collected from a burned area in the Pacific Northwestern U.S. had significantly lower SOC concentrations (34 to 100 %) than soils collected from an un-burned area separated only by a two lane road. This confirms that SOCs re-volatilize and/or degrade from soils and vegetation during the burning process. The chiral signatures of alpha-HCH in air masses at three sites in the Pacific Northwestern U.S. indicated that the boundary layer has a non-racemic alpha-HCH signature likely due to re-volatilization of alpha-HCH from the Pacific Ocean and that the free troposphere is a source of racemic alpha-HCH. Racemic alpha-HCH was also associated with Asian and

trans-Pacific air masses. Racemic cis and trans-chlordane in Pacific Northwestern U.S. air masses indicated that U.S. urban areas continue to be a source of chlordane to the atmosphere. The deposition of non-racemic alpha-HCH in seasonal snowpack in continental Western U.S. national park high elevation ecosystems reflected regional transport, while the high latitude, Alaskan national parks were influenced by long-range atmospheric transport of racemic alpha-HCH. The chiral signature of alpha-HCH in fish collected from high elevation and high latitude ecosystems in Western U.S. national parks reflected the chiral signature of the seasonal snowpack in the lake catchment. This indicates that the fish in these ecosystems do not enantioselectively biotransform alpha-HCH. Racemic cis-chlordane was measured in seasonal snowpack and lake sediments in Sequoia National Park due to the high population density surrounding the park and the past use of chlordane as a termiticide in urban areas. Non-racemic cis-chlordane was measured in sediment collected from Rocky Mountain National Park because this park receives chlordane due to re-volatilization from regional agricultural soil.

SEMI-VOLATILE ORGANIC COMPOUNDS AS MOLECULAR MARKERS FOR ATMOSPHERIC AND ECOSYSTEM TRANSPORT

by
Susan Genualdi

A DISSERTATION

submitted to

Oregon State University

in partial fulfillment of
the requirements for the
degree of

Doctor of Philosophy

Presented September 18, 2008
Commencement June 2009

Doctor of Philosophy dissertation of Susan Genualdi presented on September 18, 2008.

APPROVED :

Major Professor, representing Chemistry

Chair of the Department of Chemistry

Dean of the Graduate School

I understand that my dissertation will become part of the permanent collection of Oregon State University libraries. My signature below authorizes release of my dissertation to any reader upon request.

Susan Genualdi, Author

ACKNOWLEDGEMENTS

The author is extremely grateful to her family and friends for their constant love and support throughout the years. The author also wishes to thank her major advisor, Staci Simonich for her guidance and encouragement, and all of the current and past members of the Simonich laboratory who aided in her teaching and development as a scientist. The author is also grateful to all her committee members (Bernd Simoneit, Doug Barofsky, Jennifer Field, and Greg Rorrer) for their time and advice. The author is also extremely thankful for the opportunity to participate in the NSF EAPSI - China program and their financial support.

CONTRIBUTION OF AUTHORS

Dr. Staci L. Simonich provided advice and support in all aspects of this dissertation. Jim Woods assisted in the sample collection at Cheeka Peak, while Robert Killin assisted with sample collection at both Cheeka Peak and Mary's Peak (Chapter 2). Dr. Toby Primbs assisted in the air sampling method development and the collection and analysis of air samples from Okinawa, Japan and Mt. Bachelor, Oregon (Chapter 3). Dr. Terry Bidleman and Dr.Liisa Jantunen trained the author in the methods of chiral analysis (Chapter 3). David Schmedding and Glenn Wilson assisted in the sampler installation at Mary's Peak (Chapter 2), and Glenn Wilson also assisted in maintenance and repair of the sites along with training in analytical methods and instrumental analysis. Tong Zhu and Wang Feng assisted in the soil sample collection in China. Keon-Sang Ryoo collected and performed SOC analysis on soils samples from South Korea. Kim Hageman, Sascha Usenko, and Luke Ackerman all assisted in the SOC extraction and analysis of the WACAP samples.

TABLE OF CONTENTS

TABLE OF CONTENTS (Continued)

TABLE OF CONTENTS (Continued)

LIST OF FIGURES

LIST OF FIGURES CONTINUED

LIST OF TABLES

SEMI-VOLATILE ORGANIC COMPOUNDS AS MOLECULAR MARKERS FOR ATMOSPHERIC AND ECOSYSTEM TRANSPORT

CHAPTER 1. INTRODUCTION

Goals

The goals of this research were to (1) measure semi-volatile organic compounds (SOCs) in Pacific Northwestern U.S. air masses and use them to distinguish between regional and trans-Pacific atmospheric transport; (2) measure the enantiomer fractions (EFs) of chiral organochlorine pesticides (OCPs) in Asian, trans-Pacific and regional North American air masses and use them to determine if these air masses are influenced by current or historic use of these compounds; and (3) measure the EFs of OCPs in seasonal snowpack, sediment, and fish collected from high elevation and high latitude ecosystems in Western U.S. national parks and use these to understand the sources and fate of these compounds in the ecosystems.

Long-Range Atmospheric Transport

The long-range atmospheric transport of SOCs, including organochlorine pesticides (OCPs) and other persistent organic pollutants (POPs), to remote locations such as the Arctic has been identified (1-5). The physiochemical properties of SOCs enable them to be transported distances far from their sources and deposit in locations where they have never been used (6) . The sources of SOCs to remote ecosystems are of concern, because some of them have toxic and bioaccumulative properties.

There is evidence of trans-Pacific atmospheric transport of volatile organic compounds (VOCs) and SOCs from Asia to the West Coast of the United States, and it has been shown to occur in as little as 5 days (3,7-13). HYSPLIT back trajectories,

satellite images, and models have all been used to identify time periods when trans-Pacific transport is occurring to the Pacific Northwest (12-14).

Semi-Volatile Organic Compounds (SOCs)

SOCs have a wide range of physiochemical properties, and range in vapor pressures from $10^{-4}$to 10^{-11} atm, half-lives in the environment from hours to years, and come from a variety of sources including industry (polychlorinated biphenyls (PCBs)), combustion (polycyclic aromatic hydrocarbons (PAHs)), and agriculture (pesticides, both current-use (CUPs) and historic-use (HUPs)) (13,15,16). Because of their wide range of physical chemical properties (17) and emission sources, SOCs have been shown to be good molecular markers for distinguishing between regional and long-range atmospheric transport (13,16).

POPs include OCPs, polychlorinated biphenyls (PCBs), and polychlorinated dibenzo-p-dioxins and furans (6,18). POPs are of global concern because they have been shown to bioaccumulate through the food chain, are toxic, and have endocrine-disrupting properties (6,18). The United Nations Environmental Progam (UNEP) met in 1998 to seek worldwide elimination of these compounds. In order to eliminate these compounds from the world's atmosphere, their sources, fate, and transport in the environment must first be identified (18).

It is unclear as to whether the sources of OCPs to the environment are from the continued use of these compounds in developing countries or re-volatilization from environmental compartments that have been previously contaminated. Chiral pesticides have been used to distinguish between current and historic sources to air, water, soil, and biota (18-27).

Chiral pesticides have two enantiomers and racemic mixtures have equal amounts of each enantiomer. The ratio of the enantiomers is preferably written as a fraction (EF), where the EF is equal to: area (+) enantiomer/(area (+) enantiomer + area (-) enantiomer) (28). Racemic signatures have EFs equal to 0.5, while non-racemic signatures are greater than or less than 0.5, depending on the enantiomer that is selectively degraded (28). EFs typically increase in their deviations from racemic as the complexity of the enzymatic system increases, with the degree of deviation from racemic being air < soil < biota (29).

The enantiomers have the same physical chemical properties so abiotic processes (volatilization, deposition, photolysis) do not affect the ratio of the enantiomers (18). However, microorganisms and enzymatic processes can selectively degrade one enantiomer over the other, resulting in a non-racemic signature (18). The EF of an OCP in soil is reflected in air above the soil due to revolatilization (18).

SOCs as molecular markers for atmospheric transport

Biomass burning has been shown to produce a variety of atmospheric pollutants such as particulate matter, carbon monoxide, and polycyclic aromatic hydrocarbons (PAHs) (10,30-34). Enhancements of ozone and carbon monoxide have been observed on the West coast of the U.S. due to the influence of Siberian biomass burning emissions. (7,10) During these enhancements, ozone air quality standards were exceeded in the Pacific Northwestern U.S (7,10).

It has recently been suggested that biomass burning can re-volatilize pesticides from previously contaminated soil (12,35). For example, enhancements in PCB concentrations in the Arctic atmosphere have been attributed to biomass burning emissions from agricultural fires in Eastern Europe (35). Alpha and gamma-

hexachlorocyclohexane (HCH), hexachlorobenzene (HCB), and trifluralin concentrations were all significantly positively correlated (p-value < 0.05) with markers of regional fires (including gas-phase PAHs and retene) in air masses sampled at Mt. Bachelor Observatory (MBO), Oregon (12). Trans-Pacific air masses sampled at MBO were associated with enhanced particulate phase PAH concentrations, while air masses influenced by regional transport had enhanced concentrations of gamma-HCH, dacthal, endosulfan, metribuzin, triallate, trifluralin, and chlorpyrifos (12).

SOCs as molecular markers for source age

Chiral SOCs have been previously measured in the air above agricultural soils, oceans, lakes, and urban areas (19-26,36-40). A passive air sampling study across North America observed the spatial variation in alpha-HCH EFs based on their proximity to different bodies of water and agricultural fields (26). This study observed that the Pacific and Atlantic oceans have different enantioselectivities of alpha-HCH (26). Alpha-HCH has been measured in the air at increasing heights above agricultural soils (21). The signatures were more non-racemic near the soil surface and tended toward racemic as the height above the soil increased (21). Other studies noticed the same trend with the air-water exchange of alpha-HCH in the Bering Sea, Chukchi Sea, and the Arctic Ocean (22,38,41,42).

Non-racemic chlordane signatures have been measured in agricultural soils in Sweden, England, Alabama, Connecticut, Hawaii, Ontario, and British Columbia, Canada (19). In agricultural soils, trans-chlordane is typically depleted in the (+) enantiomer, while cis-chlordane is typically depleted in the (-) enantiomer (19). Urban air in South Carolina and Alabama and house foundation soils in Connecticut had racemic chlordanes,

which are attributed to the previous use of chlordane as a termiticide around the foundations of homes (19).

Fate of chiral SOCs in ecosystems

Chiral SOCs have been previously measured in Arctic food webs consisting of seawater, zooplankton, fish, and marine mammals (29,43,44). The EFs of chiral OCPs were near racemic in seawater, zooplankton, and fish, but were non-racemic in marine mammals due to enantioselective biotransformation of one enantiomer over the other (45). The enantioselectivity of biota is dependent on the complexity of the enzymatic system and the EFs deviate from racemic to a greater degree at higher trophic levels (29). EFs of chiral OCPs have also been used to evaluate the effects of habitat, diet, and geographic location on enantioselective biotransformation (43).

LITERATURE CITED

(1) Bailey, R.; Barrie, L. A.; Halsall, C. J.; Fellin, P.; Muir, D. C. G. *Journal of Geophysical Research-Atmospheres* **2000**, *105*, 11805-11811.

(2) Harner, T.; Shoeib, M.; Kozma, M.; Gobas, F. A. P. C.; Li, S. M. *Environmental Science & Technology* **2005**, *39*, 724-731.

(3) Killin, R. K.; Simonich, S. L.; Jaffe, D. A.; DeForest, C. L.; Wilson, G. R. *Journal of Geophysical Research-Atmospheres* **2004**, *109*.

(4) Liang, Q.; Jaegle, L.; Jaffe, D. A.; Weiss-Penzias, P.; Heckman, A.; Snow, J. A. *Journal of Geophysical Research-Atmospheres* **2004**, *109*.

(5) Van Drooge, B. L.; Grimalt, J. O.; Camarero, L.; Catalan, J.; Stuchlik, E.; Garcia, C. J. T. *Environmental Science & Technology* **2004**, *38*, 3525-3532.

(6) Wania, F.; Mackay, D. *Environmental Science & Technology* **1996**, *30*, A390-a396.

(7) Bertschi, I. T.; Jaffe, D. A. *Journal of Geophysical Research-Atmospheres* **2005**, *110*.

(8) Jaffe, D.; Anderson, T.; Covert, D.; Kotchenruther, R.; Trost, B.; Danielson, J.; Simpson, W.; Berntsen, T.; Karlsdottir, S.; Blake, D.; Harris, J.; Carmichael, G.; Uno, I. *Geophysical Research Letters* **1999**, *26*, 711-714.

(9) Jaffe, D.; Anderson, T.; Covert, D.; Trost, B.; Danielson, J.; Simpson, W.; Blake, D.; Harris, J.; Streets, D. *Journal of Geophysical Research-Atmospheres* **2001**, *106*, 7449-7461.

(10) Jaffe, D.; Bertschi, I.; Jaegle, L.; Novelli, P.; Reid, J. S.; Tanimoto, H.; Vingarzan, R.; Westphal, D. L. *Geophysical Research Letters* **2004**, *31*.

(11) Jaffe, D.; McKendry, I.; Anderson, T.; Price, H. *Atmospheric Environment* **2003**, *37*, 391-404.

(12) Primbs, T., Wilson, G., Schmedding, D., Higginbotham, C., Simonich, Staci Massey *Environ. Sci. Technol.* **2008**, *ASAP online*.

(13) Primbs, T.; Piekarz, A.; Wilson, G.; Schmedding, D.; Higginbotham, C.; Field, J.; Simonich, S. M. *Environ. Sci. Technol.* **2008**, *ASAP Online*.

(14) Genualdi, S.; Primbs, T.; Killin, R.; Woods, J.; Wilson, G.; Schmedding, D.; Simonich, S. *Submitted to ES&T* **2008**.

(15) Bidleman, T. F. *Environmental Science & Technology* **1988**, *22*, 361-367.

(16) Primbs, T., Wilson, G., Schmedding, D., Higginbotham, C., Simonich, Staci Massey *Environ. Sci. Technol.* **2008**, *ASAP online*

(17) Mackay, D.; Shiu, W.-Y.; Ma, K.-C. *Illustrated Handbook of Physical-Chemical Properties and Environmental Fate for Organic Chemicals*; Lewis Publishers, 1997 Vol. Pesticide Chemicals.

(18) Bidleman, T. F.; Falconer, R. L. *Environmental Science & Technology* **1999**, *33*, 206A-209A.

(19) Bidleman, T. F., Leone, A.D. Falconer, R.L., Harner, T., Jantunen, L.M., Wiberg, K., Helm, P.A., Diamond, M.L., Loo, B. *The Scientific World* **2002**, *2*, 357-373.

(20) Falconer, R. L.; Bidleman, T. F.; Szeto, S. Y. *Journal of Agricultural and Food Chemistry* **1997**, *45*, 1946-1951.

(21) Finizio, A.; Bidleman, T. F.; Szeto, S. Y. *Chemosphere* **1998**, *36*, 345-355.

(22) Jantunen, L. M. M.; Bidleman, T. F. *Archives of Environmental Contamination and Toxicology* **1998**, *35*, 218-228.

(23) Kurt-Karakus, P. B.; Bidleman, T. F.; Jones, K. C. *Environmental Science & Technology* **2005**, *39*, 8671-8677.

(24) Leone, A. D.; Ulrich, E. M.; Bodnar, C. E.; Falconer, R. L.; Hites, R. A. *Atmospheric Environment* **2000**, *34*, 4131-4138.

(25) Li, J.; Zhang, G.; Qi, S. H.; Li, X. D.; Peng, X. Z. *Science of the Total Environment* **2006**, *372*, 215-224.

(26) Shen, L.; Wania, F.; Lei, Y. D.; Teixeira, C.; Muir, D. C. G.; Bidleman, T. F. *Environmental Science & Technology* **2004**, *38*, 965-975.

(27) Shen, L.; Wania, F.; Lei, Y. D.; Teixeira, C.; Muir, D. C. G.; Bidleman, T. F. *Environmental Science & Technology* **2005**, *39*, 409-420.

(28) Harner, T.; Wiberg, K.; Norstrom, R. *Environmental Science & Technology* **2000**, *34*, 218-220.

(29) Hegeman, W. J. M.; Laane, R. W. P. M. *Reviews of Environmental Contamination and Toxicology, Vol 173* **2002**, *173*, 85-116.

(30) Bush, P. B.; Neary, D. G.; McMahon, C. K. In *Fire and Forest Ecology: Innovative Silviculture and Vegetation Management. Tall Timbers Fire Ecology*: Tall Timbers Research Station, Tallahassee, FL, 2000; pp 132-136.

(31) Friedli, H. R., Radke, L.F, Prescott, R. *Global Biogeochemical Cycles* **2003**, *17*, 1-8.

(32) Simoneit, B. R. T. *Applied Geochemistry* **2002**, *17*, 129-162.

(33) Simoneit, B. R. T.; Elias, V. O. *Marine Pollution Bulletin* **2001**, *42*, 805-810.

(34) Simoneit, B. R. T.; Schauer, J. J.; Nolte, C. G.; Oros, D. R.; Elias, V. O.; Fraser, M. P.; Rogge, W. F.; Cass, G. R. *Atmospheric Environment* **1999**, *33*, 173-182.

(35) Eckhardt, S.; Breivik, K.; Mano, S.; Stohl, A. *Atmospheric Chemistry and Physics Discussions* **2007**, *7*, 6229-6254.

(36) Bidleman, T. F.; Leone, A. D.; Falconer, R. L.; Harner, T.; Jantunen, L. M.; Wiberg, K.; Helm, P. A.; Diamond, M. L.; Loo, B. *Environmental Fate and Effects of Pesticides* **2003**, *853*, 196-225.

(37) Bidleman, T. F.; Wong, F.; Backe, C.; Sodergren, A.; Brorstrom-Lunden, E.; Helm, P. A.; Stern, G. A. *Atmospheric Environment* **2004**, *38*, 5963-5970.

(38) Jantunen, L. M.; Bidleman, T. *Journal of Geophysical Research-Atmospheres* **1996**, *101*, 28837-28846.

(39) Jantunen, L. M. M.; Bidleman, T. F.; Harner, T.; Parkhurst, W. J. *Environmental Science & Technology* **2000**, *34*, 5097-5105.

(40) Ridal, J. J.; Bidleman, T. F.; Kerman, B. R.; Fox, M. E.; Strachan, W. M. J. *Environmental Science & Technology* **1997**, *31*, 1940-1945.

(41) Jantunen, L. M.; Bidleman, T. F. *Environmental Science & Technology* **1995**, *29*, 1081-1089.

(42) Jantunen, L. M.; Kylin, H.; Bidleman, T. F. *Deep-Sea Research Part Ii-Topical Studies in Oceanography* **2004**, *51*, 2661-2672.

(43) Borga, K.; Fisk, A.; Hoekstra, P.; Muir, D. C. G. *Environmental Toxicology and Chemistry* **2004**, *23*, 2367-2385.

(44) Wiberg, K.; Letcher, R. J.; Sandau, C. D.; Norstrom, R. J.; Tysklind, M.; Bidleman, T. F. *Environmental Science & Technology* **2000**, *34*, 2668-2674.

(45) Hoekstra, P. F.; O'Hara, T. M.; Karlsson, H.; Solomon, K. R.; Muir, D. C. G. *Environmental Toxicology and Chemistry* **2003**, *22*, 2482-2491.

CHAPTER 2. TRANS-PACIFIC AND REGIONAL U.S. ATMOSPHERIC TRANSPORT OF PAHS AND PESTICIDES IN BIOMASS BURNING EMISSIONS

Susan A. Genualdi[1], Robert K. Killin[2], Jim Woods[3], Glenn Wilson[4], David Schmedding[4], Staci L. Massey Simonich[1,4]*

[1]Department of Chemistry, Oregon State University, Corvallis, Oregon
[2]Department of Chemistry, Lewis and Clark College, Portland, OR
[3]Makah Tribe Air Quality Project
[4]Department of Environmental and Molecular Toxicology, Oregon State University, Corvallis, Oregon

ABSTRACT

The trans-Pacific and regional U.S. atmospheric transport of polycyclic aromatic hydrocarbons (PAHs) and pesticides in biomass burning emissions was measured in air masses from April to September 2003 at two remote sites in the Pacific Northwestern United States. Mary's Peak Observatory (MPO) is located in Oregon's Coast Range and Cheeka Peak Observatory (CPO) is located on the tip of the Olympic Peninsula in Washington State. During this time period, both remote sites were influenced by PAH and pesticide emissions from forest fires in Siberia and regional fires in Oregon and Washington State. Concurrent samples were taken at both sites on June 2 and August 4, 2003. On these dates, CPO had elevated gas phase PAH, alpha-hexachlorocyclohexane and retene concentrations ($p<0.05$) and MPO had elevated retene, particulate phase PAH and levoglucosan concentrations due to trans-Pacific transport of emissions from fires in Siberia. In addition, during the April to September 2003 sampling period, CPO and MPO were influenced by emissions from regional fires that resulted in elevated levoglucosan, dacthal, endosulfan and gas phase PAH concentrations. Burned and unburned forest soil samples collected from the regional forest fire area showed that 34 to 100% of the pesticide mass was lost from soil due to burning. These data suggest that the trans-Pacific and regional atmospheric transport of biomass burning emissions results in elevated PAH and pesticide concentrations in the western United States. The elevated pesticide concentrations are likely due to re-emission during the fire event of historically deposited pesticides from the soil and vegetation.

INTRODUCTION

Biomass burning, including forest fires, produces atmospheric pollutants such as particulate matter, carbon monoxide, mercury, volatile organic compounds (VOCs), and semi-volatile organic compounds (SOCs) [1-5]. Because biomass burning emissions are expected to increase significantly with global warming, the effect that biomass burning emissions have on the global radiation budget, the production of greenhouse gas emissions, and air quality is a growing concern [6].

The air quality of the Pacific Northwestern U.S. is influenced by biomass burning emissions from both regional and trans-Pacific atmospheric transport [4, 5, 7]. In addition, during some periods of trans-Pacific atmospheric transport, the concentrations of carbon monoxide and ozone in the Pacific Northwest increase and sometimes exceed air quality standards [7].

During the summer of 2003, large-scale biomass burning occurred throughout Siberia, with the most intense fires occurring from May to early June and during the month of August [8]. Approximately 18.9 million hectares of land were burned during the entire 2003 fire season in Russia, and, on average, approximately 8 to 10 million hectares burn there each year [7]. In the summer of 2003, elevated concentrations of carbon monoxide and $PM_{2.5}$ had a significant impact on air quality in the Pacific Northwestern U.S. and were linked to two separate trans-Pacific events of Siberian fire emissions [7, 8]. On June 6, 2003, the U.S. EPA's 8-hour standard for ozone was exceeded in Enumclaw, WA (55 km southeast of Seattle) and, during the first week of August in 2003, the 24-hour average PM2.5 standard was exceeded in Seattle, WA [7, 8]. During these time periods, we measured polycyclic aromatic hydrocarbons (PAHs) and

pesticides concurrently in air masses at both Cheeka Peak Observatory (CPO), a remote site located on the Olympic Peninsula of Washington, and at Mary's Peak Observatory (MPO), a remote site located in Oregon's Coast Range. The two sites are located approximately 500 km from each other and have an elevation difference of 769 m. Concurrently sampling at these two remote sites provides a unique opportunity to investigate the spatial and altitudinal variation of PAH and pesticide concentrations in trans-Pacific and regional air masses. In addition to these trans-Pacific event time periods, PAHs and pesticides were also measured at these two sites from April to September 2003 in air masses influenced by several regional U.S. fires. The objectives of this research were to measure PAH and pesticide concentrations in trans-Pacific and regional air masses influenced by biomass burning events and to assess the influence that these fire events have on their concentrations in the Pacific Northwestern United States.

EXPERIMENTAL SECTION

Chemicals

Eighty-four targeted SOCs, including polycyclic aromatic hydrocarbons (PAHs) and historic and current-use pesticides, were measured in hi-volume air samples [9]. These SOCs span several orders of magnitude in vapor pressure; exist in both the gas and particle phases of the atmosphere, and their atmospheric half-lives range from hours to months. Isotopically labeled surrogates and internal standards were used to recovery correct and quantify the SOC concentrations over the entire analytical method [9]. A complete list of the SOC standards, their manufacturers and storage conditions have been previously reported [10].

Sampling Sites

Air samples were collected from two remote sites located in the Pacific Northwestern United States. Mary's Peak Observatory (MPO) (44.5^{o}N, 123.6^{o}W, 1249 m) is the highest peak in Oregon's coast range, while Cheeka Peak Observatory (CPO) (48.3^{o}N, 124.6^{o}W, 480 m) is a coastal site located on the tip of the Olympic Peninsula in Washington State (Figure 2.1). The annual precipitation at both MPO and CPO is ~250 cm [11] and the predominant wind direction at both sites is westerly (from the Pacific Ocean).

CPO is a well-established site for the study of trans-Pacific atmospheric transport to the United States and is located ~240 km West of Seattle and 3 km from the Pacific Ocean [7, 8, 12-14]. Previous studies have identified that, during westerly flow, this site is primarily influenced by clean marine air masses and Asian air masses containing anthropogenic emissions [7, 12, 14]. MPO is located ~26 km from the Pacific Ocean and ~30 km west of the agriculturally intensive Willamette Valley and Interstate 5 (Figure 2.1). Concurrently sampling at CPO and MPO provided a unique opportunity to investigate the spatial and altitudinal variation of PAH and pesticide concentrations in trans-Pacific and regional air masses.

Sample Collection

From April to September 2003, twenty-two high volume air samples were collected at MPO and CPO (Table 2.1). During this time period, eight 48-hour air samples and 2 field blanks were collected at CPO using a modified hi-volume air sampler (Tisch Environmental, Cleves, OH). At CPO, an 11cm diameter sampling head with two glass fiber filters (GFFs) was used to collect the particulate phase SOCs and two 5.5 cm diameter polyurethane foam (PUF) plugs were used to collect the gas phase SOCs. This

sampler had an average flow rate of approximately 14 m^3/hour and, during a 48-hour period, an average of 650 m^3 of air was sampled.

At MPO, eleven 48-hour and three 24-hour air samples, as well as 2 field blanks, were collected using a modified hi-volume air sampler (Tisch Environmental, Cleves, OH) (Table 2.1). At MPO, a 20.3 cm by 25.4 cm rectangular sampling head with a GFF (Whatman, Maidstone England) was used to collect the particulate-phase SOCs and two 6.5 cm diameter PUF plugs, with ~50 grams of Amberlite XAD-2 resin (Supelco, Bellefonte, PA) placed between the two PUF plugs was used to collect the gas-phase SOCs. In a 48 hour sampling period, ~ 2500m^3 of air was sampled and, in a 24 hour sampling period, ~900m^3 of air was sampled. The sampling flow rate decreased when the sampling period changed from 48 to 24 hours because the brush motor (higher flow rate) was replaced with a brushless motor (lower flow rate). The air sampling media was pre-cleaned before deployment in the field. Details of the cleaning procedure and solvents used have been previously reported [9, 15].

A composite soil sample was collected from an un-burned (100 m^2) and burned (100 m^2) area in the Deschutes National Forest, located 6 miles west of Sisters, Oregon at the edge of the area burned by the B&B complex forest fire. The burned and unburned areas were adjacent to each other but separated by a two lane road which stopped the forest fire. Each composite soil sample consisted of 7 random surface (20 cm deep) samples for each 100 m^2 area.

Measurement of SOCs

The extraction of SOCs from the air sampling media was conducted using an Accelerated Solvent Extractor (ASE) 300 (Dionex, Sunnyvale, CA). The ASE conditions

and solvent compatibility with the sampling media has been described elsewhere [9]. The average percent SOC recoveries (%RSD) from the entire analytical method were 76.7(6.2), 79.3(8.1), and 93.4(2.9) for the QFF, PUF, and XAD-2, respectively and are reported elsewhere [9]. The extracts were concentrated to 300 uL with a stream of nitrogen using a Turbo Vap II (Caliper Life Sciences, Hopkinton, MA) and were analyzed using gas chromatography/mass spectrometry (GC-MS) in selected ion monitoring (SIM) mode [9, 10]. Levoglucosan was measured in the air samples using the method described in Mederios et al [16].

SOCs were extracted from the forest soil samples using the same method for PUF as described elsewhere [9]. The soil extracts were further purified using silica gel adsorption chromatography (Varian, Palo Alto, CA) and a 75:25 hexane:acetone solvent mixture as the elution solvent. The extracts were concentrated with nitrogen and analyzed by GC-MS.

The GC-MS consisted of an Agilent 6890 GC interfaced with an Agilent 5973N mass selective detector. A DB-5ms column (30m, 0.25mm id., 0.25um film thickness, J&W Scientific, USA) was used with an oven temperature program that varied based on the ionization mode of the mass selective detector [10]. Details on the GC temperature programs for both electron capture negative ionization (ECNI) and electron impact ionization (EI), as well as the ions monitored were previously reported [10]. The mode of ionization chosen for each SOC was based on which ionization technique gave the lowest detection limit [10]. EPA method 8280A was used to calculate the estimated detection limits (EDLs) for each SOC in the air samples [17]. For a typical air sample, EDLs ranged from 0.0078 pg/m^3 to 0.19 pg/m^3 in ECNI mode and 0.059 pg/m^3 to

0.73pg/m^3 in EI mode. All reported concentrations were surrogate recovery corrected and field blank subtracted.

Quality Assurance/Quality Control

Each air sample consisted of both a top and bottom quartz fiber filter (QFF) and the bottom QFF was analyzed separately to check for sorption of gas phase SOCs to the QFF. All SOCs were below the limits of quantification on the bottom QFF and no correction for SOC sorption was done. The CPO air samples consisted of a two PUF system and the bottom PUF was analyzed separately to check for breakthrough of gas phase SOCs in ~50% of the air samples. Only hexachlorobenzene (HCB) had the potential for gas phase breakthrough and 39 to 44% of the total HCB concentration was measured on the bottom PUF. No correction for the potential breakthrough of HCB was done. However, this suggests that the HCB concentration at CPO may be slightly underestimated. At MPO, a PUF/XAD/PUF gas phase sampling system was used and HCB breakthrough was not observed in the bottom PUF.

Field blanks were collected at both MPO and CPO. At CPO, phenanthrene, fluorene, pyrene, and retene were measured slightly above the quantification limit, while at MPO, dacthal, chlorpyrifos, HCB, endosulfan I, endosulfan II, endosulfan sulfate, phenanthrene, fluorene, pyrene, and retene were measured slightly above the quantification limit. All reported concentrations were field blank subtracted.

Air Mass Back Trajectory Calculation and Satellite Image Analysis

10-day air mass back trajectories were calculated using NOAA's Hybrid Single-Particle Lagrangian Integrated Trajectory model (HYSPLIT) to assess potential source regions [18]. For each sampling period, a 10-day back trajectory was calculated every 4

hours at the site elevation and location and at 8 points located in a 1^0 by 1^0 grid surrounding the site. This resulted in approximately 162 trajectories calculated for each sampling period. At CPO and MPO, trajectories were calculated at the site elevations of 500 m and 1249 m, respectively. HYSPLIT data was imported into ArcGIS and was used to calculate the percent of time the trajectory spent in the boundary layer (below 1000 m) and above the boundary layer (above 1000 m) for each sample.

The Moderate Resolution Imaging Spectroradiometer (MODIS) flies onboard NASA satellites and collects global fire activity in a 1^o by 1^o grid [19]. The Navy Aerosol and Analysis Prediction System (NAAPs) model estimates smoke emissions based on satellite and MODIS fire product data [20]. The MODIS fire detects, the NAAPs model, and the 10-day air mass back trajectories were used to help determine the location of both the regional and Siberian fires during the sampling periods.

RESULTS

Identification of Air Mass Source Regions and Biomass Burning events

HYSPLIT back trajectories were used to calculate source region impact factors (SRIFs) for each air mass sampled at MPO and CPO. The SRIF was calculated by determining the percentage of time the back trajectories spent in a given source region compared to the total trajectory time, and details of these calculations are reported elsewhere [4, 5, 15]. The defined source regions included agriculturally intensive areas in the Western U.S., including Eastern Washington, the Willamette Valley in Oregon, and the Central Valley in California (Figure SI.1) [4]. Two other potential source regions in Asia and Siberia were identified and used to assess the influence of these source regions on the SOC concentrations in the sampled air masses [4]. The SRIFs for

each sampling date are listed in Table 2.1. The SRIFs do not add up to 100% because they do not account for the significant time the trajectories spent over the Pacific Ocean. However, during trans-Pacific transport, Asian dust and smoke plumes may be present over the Pacific Ocean. In order to account for this, the percentage of time the air mass trajectories spent over the Pacific Ocean as opposed to continental land was calculated (Table 2.1).

Levoglucosan, a combustion byproduct of cellulose that exists in the particulate phase in the atmosphere, is often used as a molecular marker for biomass burning emissions [21-24] The levoglucosan concentrations measured at both sites are listed in Table 2.2. For sampling dates that had elevated levoglucosan concentrations (greater than 10,000 pg/m^3) or NAAPs model images that indicated smoke emissions, air mass back trajectories and satellite images were used to determine the fire locations. The NAAPs model images for the concurrent CPO and MPO sampling start dates of June 2 (Figure 2.2) and August 4 (Figure 2.3) show smoke emissions from large scale fires burning in Siberia being transported across the Pacific Ocean to the Pacific Northwestern United States. The NAAPs model images also indicated that CPO was influenced by Siberian biomass burning emissions during the June 16 sampling period (Figure 2.4) and MPO was influenced by regional fire emissions in Eastern Oregon during the September 4 sampling period (Figure 2.5).

To determine if biomass burning emissions influenced individual air samples, the following were considered; (1) the levoglucosan concentration in the air sample was elevated (greater than 10,000pg/m^3) (2) the smoke emissions estimated by the NAAPS

model passed over the sampling site, and (3) the 10-day air mass back trajectories for the sample passed near MODIS fire detects.

Polycyclic Aromatic Hydrocarbons

Siberian Fires

During the June 2-4 concurrent sampling at CPO and MPO, elevated particulate phase PAH concentrations were measured at MPO, while elevated gas phase PAH concentrations were measured at CPO (Figure 2.2 and Table 2.2). Previous studies have shown that elevated particulate phase PAH concentrations are associated with trans-Pacific air masses at Mt. Bachelor Observatory (MBO), which is located at 2800m in Oregon's Cascade Range [5], while elevated gas phase PAH concentrations were measured in trans-Pacific air masses at CPO [7]

To determine if the sampled air mass represented the boundary layer or tropospheric air, the HYSPLIT back trajectories were used to calculate the amount of time the air mass time spent above (>1000 m) or below (<1000 m) the boundary layer in the 10 days prior to sampling (Table SI.1). In the June 2 air masses, 96% of the trajectory time was spent above the boundary layer prior to reaching MPO, while only 68% of the trajectory time was spent above the boundary layer prior to reaching CPO (Table 2.1). At CPO, the concentrations of retene, a biomarker for the incomplete combustion of soft wood [2], fluoranthene, and pyrene were elevated (p-value < 0.05) in the June 2 air mass, while, at MPO, the levoglucosan concentration was elevated (>10,000 pg/m^3). However, the levoglucosan concentration at CPO was below the detection limit. Levoglucosan is particle bound and water-soluble and the relatively wet boundary layer air mass at CPO may partly explain the loss of levoglucosan at CPO. In

addition, the average relative humidity CPO and MPO during the June 2 sampling was 79% and 60%, respectively. Due to CPO's higher relative humidity and closer proximity to the Pacific Ocean, fog formation is greater at CPO than at MPO. Fog is an efficient scavenger of SOCs and may explain the removal of levoglucosan and particle bound PAHs from the sampled air mass at CPO.

The NAAPs model images indicate that, during the June 2 concurrent sampling, smoke plumes from Siberian fires crossed the Pacific Ocean and passed over CPO and MPO (Figure 2.6). In addition, Figures 2.2 and 2.3 show the air mass back trajectories for the June 2 concurrent sampling at CPO and MPO overlaid onto MODIS 10-day fire start images. The MODIS images are generated by satellite data over 10-day periods and the image shown in Figure 2.2 represents the June 1-10 time period. In Figures 2.2 and 2.3, each red dot represents a fire that burned during the 10-day period, while the yellow dots indicate areas of more intense burning [19]. By comparing the MPO and CPO trajectories in Figure 2.2, it is clear that the MPO air mass spent more time over the Siberian and Asian source regions (13.2%) than the CPO air mass (1.4%) (Table 2.1). This indicates that, during the June 2 concurrent sampling, MPO was influenced to a greater extent by Siberian biomass burning emissions than CPO. This, along with different site characteristics, such as relative humidity and elevation, may explain the different observations at CPO and MPO.

The ratios of individual PAH isomers have been used for source apportionment by comparing the PAH ratio of the combustion source to the PAH ratio measured in air [7, 25, 26]. During the June 2 concurrent sampling, the ratio of indeno-[1,2,3-cd]-pyrene/(indeno-[1,2,3-cd]-pyrene +benzo-[ghi]-perylene) was 0.65 at MPO. This PAH

ratio for wood combustion is 0.64 ± 0.07 [26], suggesting that the MPO air mass contained biomass burning emissions from the Siberian fires. The same PAH ratio could not be calculated in the concurrent June 2 CPO air mass or the CPO and MPO concurrent August 4 air masses because the concentrations of both indeno-[1,2,3-cd]-pyrene and benzo-[ghi]-perylene were below the detection limits (Table 2.2).

Similar to the June 2 concurrent sampling, during the August 4 concurrent sampling, MPO had elevated particulate phase PAH concentrations and CPO had elevated gas phase PAH concentrations (Figure 2.3). A previous study reported low total aerosol scattering/carbon monoxide concentration ratios during the August 4 time period at CPO and the affect of precipitation in transit to CPO was explored to explain this low ratio [8]. The HYSPLIT model indicated that relatively low precipitation, 1.4 mm at CPO and 15.1mm at MPO, fell along the 10-day air mass back trajectory of the June 2 sampled air mass. However, for the August 4 sampled air mass the precipitation that fell in transit was 9.5 mm at CPO and 38.6 mm at MPO. Because wet deposition is a primary removal mechanism of submicron aerosols from the atmosphere, precipitation in transit across the Pacific Ocean may explain why the particulate phase PAH concentrations in the August 4 air mass were lower than the June 2 air mass at CPO and MPO (Figure 2.1). The NAAPs model image for the August 4 concurrent sampling confirms the influence of Siberian biomass burning emissions at CPO and MPO (Figure 2.7)

Principal component analysis (PCA) was used to further evaluate the differences in PAH profiles in the CPO and MPO air masses. Individual PAH concentrations were normalized to total PAH concentrations in each air sample to allow direct comparison of the PAH profile between samples. The PCA biplot in Figure 2.8 confirms that the June 2

and August 4 air masses sampled concurrently at MPO and CPO contained different PAH profiles even though both air masses were influenced by the same Siberian biomass burning emissions. The PCA biplot indicates that the CPO (10S and 17S) and MPO (8S and 16S) air masses influenced by the Siberian biomass burning emissions had elevated pyrene and retene concentrations.

Regional Fires

Fluorene concentrations were elevated at CPO in the April 11 air mass compared to the rest of 2003 and it was the only sampled air mass at CPO that was from an easterly rather than westerly direction (Tables 2.1 and 2.2). The atmospheric lifetime of fluorene is relatively short (22 hours) [27], suggesting that this CPO air mass may have been influenced by local sources.

From August 19 to September 26, approximately 90,789 acres of U.S. National Forest burned in the Oregon Cascade Range located 150 miles east of MPO (referred to as the B&B complex fire). An air mass was sampled at MPO on September 4-6, during one of the most intense periods of burning. The predominant wind direction at MPO during this time period was from the southwest (Table 2.1). However, the NAAPs model image shows that smoke emissions from this forest fire influenced a large portion of Oregon (Figure 2.5). This air mass had elevated concentrations of all gas phase PAHs, including anthracene and retene, and levoglucosan (Table 2.2). The relatively high anthracene concentrations in this air mass, along with its relatively short atmospheric half-life of 1.5 hours [27], is consistent with an air mass influenced by a regional combustion source and the elevated retene and levoglucosan concentrations indicate it was the B&B complex fire.

Pesticides

Siberian Fires

The fate of pesticides in fires depends on their physiochemical properties and the temperature of the fire [28]. At temperatures greater than 500^{o}C, most pesticides thermally degrade [28]. However, under smoldering conditions (300^{o}C to 500^{o}C), pesticides volatilize to the atmosphere [28]. Experiments on the combustion of insecticide treated wood showed that stable pesticides with higher vapor pressures, such as gamma-HCH (lindane), volatilized under smoldering conditions and 43% of the gamma-HCH was recovered in the smoke stream [28]. For pesticides with lower vapor pressures, such as chlorpyrifos, 28% was recovered in the smoke stream under smoldering conditions [28]. When gamma-HCH and chlorpyrifos were burned at temperatures greater than 500 ^{o}C, both pesticides thermally degraded [28]. Because the physiochemical properties of gamma-HCH are similar to its isomer alpha-HCH, it is possible that alpha-HCH and other SOCs volatilize from soil and vegetation during biomass burning.

The highest dieldrin concentrations at CPO were measured in the June 2, June 16, and August 4 air masses (Table 2.3). The PCA biplot of normalized pesticide concentrations confirmed these elevated concentrations in the June 2 and June 16 air masses (Figure 2.9). At CPO, the dieldrin concentration was significantly correlated with alpha- and gamma- HCH, fluoranthene, pyrene, and retene concentrations (Table 2.4). The NAAPs model indicated these three CPO air masses were influenced by the trans-Pacific transport of Siberian biomass burning emissions (Figures 2.4, 2.6, 2.7). The highest dieldrin concentrations at MPO were measured in the Sept. 21 air mass. On this

day, air mass back trajectories and elevated particulate phase PAH concentrations indicated influence from trans-Pacific transport at MPO. This suggests that dieldrin, banned in the U.S in 1987, was transported during these trans-Pacific events to CPO and MPO.

Dieldrin use in China has not been reported however, dieldrin has been measured in sediments from Lake Taihu and in air in Beijing and Qingdao [25, 29-31]. Dieldrin was also measured in air on Okinawa, Japan, a site located downwind of Asian source regions, but no single Asian source region could be identified [15]. The CPO and MPO data suggest that dieldrin undergoes trans-Pacific transport to the U.S. West Coast.

The alpha-HCH concentration was also elevated at CPO in the June 2, June 16, and August 4 air masses that were influenced by the Siberian biomass burning emissions (Figure 2.1 and Table 2.3). Technical HCH (containing alpha-HCH and gamma-HCH) was banned in the U.S in 1974, in China in 1983, and in the former Soviet Union in 1990 [32]. Emission inventories for alpha-HCH were developed for both China and the former Soviet Union based on production and usage in these countries [33-35]. From these inventories, it is evident that most of the land burned in Siberia during the summer of 2003 had minimal direct use of alpha-HCH [34, 35]. However, the burned area in Siberia was near the areas of intense alpha-HCH use in China and the Soviet Union and was likely a receptor region for these alpha-HCH emissions for many years [36].

At CPO, alpha-HCH concentrations were significantly ($p < 0.05$) positively correlated with dieldrin concentrations and negatively correlated with dacthal concentrations. Dacthal (or DCPA) is a current use pesticide in the U.S. These correlations suggest that the elevated alpha-HCH and dieldrin concentrations at CPO are

due to trans-Pacific transport, while the elevated dacthal concentrations are due to regional transport. The alpha to gamma-HCH ratio did not appear to be indicative of trans-Pacific or regional atmospheric transport (Table 2.3). In addition, this ratio was not correlated with SOC concentrations at MPO or CPO (Table 2.5).

Regional Fires

The highest CPO concentrations of dacthal and endosulfan I, both current use pesticides, were in the April 11 easterly air mass (Table 2.3). Pesticide-use maps indicate dacthal and endosulfan use in Eastern Washington on wheat [37]. Because the air mass back trajectories passed over Eastern Washington and the highest concentration of levoglucosan at CPO was measured in this air mass, it is likely that the April 11 air mass was influenced by agricultural field burning in Eastern Washington. The most prevalent agricultural burning of wheat fields (89% of the total acres burned in Washington) occurs in April and May and also in September and October [38]. Also, the dacthal concentration at CPO was significantly negatively correlated with the alpha-HCH concentration, providing further evidence that the dacthal at CPO was from regional, and not trans-Pacific, sources.

The highest dacthal and endosulfan sulfate concentrations at MPO were measured in the Sept. 4 air mass that was influenced by the B&B complex fire (Table 2.3). The concentration of dacthal and endosulfan sulfate at MPO were significantly positively correlated with each other and gas-phase PAH concentrations. In addition, the PCA biplot of normalized pesticide concentrations confirms the elevated dacthal concentrations in the Sept. 4 air mass at MPO (Figure 2.9). This suggests that these

current use pesticides were volatilized and transported to MPO during regional fire events, including the B&B complex fire.

Pesticide Loss from Soil Due to Forest Fires

Composite forest soil samples from a burned and unburned area of the B&B complex forest fire discussed above were collected and analyzed to investigate the potential loss of SOCs from soil due to re-volatilization and/or degradation from a forest fire. The pesticides with elevated concentrations in air masses influenced by the Siberian and regional biomass burning emissions, dieldrin, alpha-HCH, dacthal, and endosulfan sulfate, had concentrations in burned forest soil that were decreased by 100%, 97%, 90%, and 97%, respectively, compared to unburned forest soil (Figure 2.10, Table 2.6). These four pesticides also had some of the highest concentrations in unburned soil among the pesticides measured (Figure 2.10, Table 2.6). Other pesticides measured in the unburned forest soils included trifluralin, HCB, gamma-HCH, heptachlor, chlorpyrifos oxon, heptachlor epoxide, trans-chlordane, trans-nonachlor, and endosulfan II. Their losses from forest soil ranged from 34 to 100% (Figure 2.10, Table 2.6). The losses of PCBs from forest soil ranged from 80 to 85% (Figure 2.10, Table 2.6). However, the PCB concentrations in unburned forest soil were significantly lower than the dieldrin, alpha-HCH, and endosulfan sulfate concentrations. These results confirm that pesticides and other SOCs may re-volatilize and/or degrade during biomass burning.

ACKNOWLEDMENTS

We would like to thank Will Hafner and Dan Jaffe at the University of Washington – Bothell for use of their trajectory analysis programs and access to meteorological data from Cheeka Peak Observatory. This work was made possible by

funding from the National Science Foundation CAREER (ATM-0239823) grant and also the National Institutes of Health (P30ES00210).

LITERATURE CITED

1. Friedli, H. R., Radke, L.F, Prescott, R., Mercury emissions from the August 2001 wildfires in Washington State and an agricultural waste fire in Oregon and atmospheric mercury budget estimates. *Global Biogeochemical Cycles* **2003,** *17*, (2), 1-8.
2. Simoneit, B. R. T.; Rogge, W. F.; Mazurek, M. A.; Standley, L. J.; Hildemann, L. M.; Cass, G. R., Lignin pyrolysis products, lignans, and resin acids as specific tracers of plant classes in emissions from biomass combustion. *Environ. Sci. Technol.* **1993,** *27*, (12), 2533-2541.
3. Eckhardt, S.; Breivik, K.; Mano, S.; Stohl, A., Record high peaks in PCB concentrations in the Arctic atmosphere due to long-range transport of biomass burning emissions. *Atmospheric Chemistry and Physics Discussions* **2007,** *7*, 6229-6254.
4. Primbs, T., Wilson, G., Schmedding, D., Higginbotham, C., Simonich, Staci Massey, Influence of Asian and Western United States Agricultural Areas and Fires on the Atmospheric Transport of Pesticides in the Western United States. *Environ. Sci. Technol.* **2008,** *ASAP online*.
5. Primbs, T.; Piekarz, A.; Wilson, G.; Schmedding, D.; Higginbotham, C.; Field, J.; Simonich, S. M., Influence of Asian and Western United States Urban Areas and Fires on the Atmospheric Transport of Polycyclic Aromatic Hydrocarbons, Polychlorinated Biphenyls, and Fluorotelomer Alcohols in the Western United States. *Environ. Sci. Technol.* **2008,** *ASAP online*.
6. Penner, J. E., Dickinson, R.E., O'Neill, C.A Effects of Aerosol from Biomass Burning on the Global Radiation Budget *Science* **1992,** *256*, (5062), 1432.
7. Killin, R. K.; Simonich, S. L.; Jaffe, D. A.; DeForest, C. L.; Wilson, G. R., Transpacific and regional atmospheric transport of anthropogenic semivolatile organic compounds to Cheeka Peak Observatory during the spring of 2002. *Journal of Geophysical Research-Atmospheres* **2004,** *109*, (D23).
8. Bertschi, I. T.; Jaffe, D. A., Long-range transport of ozone, carbon monoxide, and aerosols to the NE Pacific troposphere during the summer of 2003: Observations of smoke plumes from Asian boreal fires. *Journal of Geophysical Research-Atmospheres* **2005,** *110*, (D5).
9. Primbs, T.; Genualdi, S.; Simonich, S., Solvent Selection for Pressurized Liquid Extraction of Polymeric Sorbents Used in Air Sampling. *Environmental Toxicology and Chemistry* **2008,** *27*, (2008), 1267-1272.
10. Usenko, S.; Hageman, K. J.; Schmedding, D. W.; Wilson, G. R.; Simonich, S. L., Trace analysis of semivolatile organic compounds in large volume samples of snow, lake water, and groundwater. *Environmental Science & Technology* **2005,** *39*, (16), 6006-6015.
11. Anderson, H. G., Growth Form and Distribution of Vine Maple (Acer Cirinatum) on Marys Peak, Western Oregon. *Ecology* **1969,** *50*, (1), 127-130.
12. Jaffe, D.; Anderson, T.; Covert, D.; Kotchenruther, R.; Trost, B.; Danielson, J.; Simpson, W.; Berntsen, T.; Karlsdottir, S.; Blake, D.; Harris, J.; Carmichael, G.; Uno, I.,

Transport of Asian air pollution to North America. *Geophysical Research Letters* **1999,** *26*, (6), 711-714.
13. Jaffe, D.; Anderson, T.; Covert, D.; Trost, B.; Danielson, J.; Simpson, W.; Blake, D.; Harris, J.; Streets, D., Observations of ozone and related species in the northeast Pacific during the PHOBEA campaigns 1. Ground-based observations at Cheeka Peak. *Journal of Geophysical Research-Atmospheres* **2001,** *106*, (D7), 7449-7461.
14. Jaffe, D.; McKendry, I.; Anderson, T.; Price, H., Six 'new' episodes of trans-Pacific transport of air pollutants. *Atmospheric Environment* **2003,** *37*, (3), 391-404.
15. Primbs, T.; Simonich, S.; Schmedding, D.; Wilson, G.; Jaffe, D.; Takami, A.; Kato, S.; Hatakeyama, S.; Kajii, Y., Atmospheric Outflow of Anthropogenic Semivolatile Organic Compounds from East Asia in Spring 2004. *Environ. Sci. Technol.* **2007,** *41*, (10), 3551-3558.
16. Medeiros, P. M.; Simoneit, B. R. T., Analysis of sugars in environmental samples by gas chromatography-mass spectrometry. *Journal of Chromatography A* **2007,** *1141*, (2), 271-278.
17. Method 8280A, E.P.A. The analysis of polycholorinated dibenzo-p-dioxins and polychlorinated dibenzofurans by high-resolution gas chromatography/low resolution mass spectrometry (HRGC/LRMS). In Vol. http://www.epa.gov/epaoswer/hazwaste/test/pdfs/8280a.pdf.
18. Draxler, R. R.; Rolph, G. D., HYSPLIT (HYbrid Single-Particle Lagrangian Integrated Trajectory) Model. In NOAA Air Resources Laboratory Silver Spring, MD: 2003 http://www.arl.noaa.gov/ready/hysplit4.html.
19. Descloitres, J. MODIS Rapid Response System Global Fire Maps. http://rapidfire.sci.gsfc.nasa.gov/firemaps/
20. NRL Monterey Aerosol Page. http://www.nrlmry.navy.mil/aerosol/
21. Simoneit, B. R. T.; Schauer, J. J.; Nolte, C. G.; Oros, D. R.; Elias, V. O.; Fraser, M. P.; Rogge, W. F.; Cass, G. R., Levoglucosan, a tracer for cellulose in biomass burning and atmospheric particles. *Atmospheric Environment* **1999,** *33*, (2), 173-182.
22. Simoneit, B. R. T., Biomass burning - A review of organic tracers for smoke from incomplete combustion. *Applied Geochemistry* **2002,** *17*, (3), 129-162.
23. Simoneit, B. R. T.; Elias, V. O., Detecting organic tracers from biomass burning in the atmosphere. *Marine Pollution Bulletin* **2001,** *42*, (10), 805-810.
24. Simoneit, B. R. T.; Elias, V. O.; Kobayashi, M.; Kawamura, K.; Rushdi, A. I.; Medeiros, P. M.; Rogge, W. F.; Didyk, B. M., Sugars - Dominant water-soluble organic compounds in soils and characterization as tracers in atmospheric particulate matter. *Environmental Science & Technology* **2004,** *38*, (22), 5939-5949.
25. Li, J.; Zhang, G.; Qi, S. H.; Li, X. D.; Peng, X. Z., Concentrations, enantiomeric compositions, and sources of HCH, DDT and chlordane in soils from the Pearl River Delta, South China. *Science of the Total Environment* **2006,** *372*, (1), 215-224.
26. Yunker, M. B.; Macdonald, R. W.; Vingarzan, R.; Mitchell, R. H.; Goyette, D.; Sylvestre, S., PAHs in the Fraser River basin: a critical appraisal of PAH ratios as indicators of PAH source and composition. *Organic Geochemistry* **2002,** *33*, (4), 489-515.
27. Brubaker, W. W.; Hites, R. A., OH Reaction Kinetics of Polycyclic Aromatic Hydrocarbons and Polychlorinated Dibenzo-p-dioxins and Dibenzofurans. *J. Phys. Chem. A* **1998,** *102*, (6), 915-921.

28. Bush, P. B.; Neary, D. G.; McMahon, C. K. In *Fire and Pesticides: A Review of Air Quality Considerations,* Fire and Forest Ecology: Innovative Silviculture and Vegetation Management. Tall Timbers Fire Ecology, Tall Timbers Research Station, Tallahassee, FL, 2000; Tall Timbers Research Station, Tallahassee, FL, 2000; pp 132-136.
29. *Regionally Based Assessment of Persistent Toxic Substances*; Global Environmtal Facility: 2002 http://www.chem.unep.ch/pts/regreports/C&NE%20Asia%20full%20report.pdf.
30. Lammel, G.; Ghim, Y. S.; Grados, A.; Gao, H. W.; Huhnerfuss, H.; Lohmann, R., Levels of persistent organic pollutants in air in China and over the Yellow Sea. *Atmospheric Environment* **2007,** *41*, (3), 452-464.
31. Wang, X.; Li, X.; Cheng, H.; Xu, X.; Zhuang, G.; Zhao, C., Organochlorine pesticides in particulate matter of Beijing, China. *Journal of Hazardous Materials* **2007,** *155*, (1-2), 350-357.
32. Willett, K. L.; Ulrich, E. M.; Hites, R. A., Differential Toxicity and Environmental Fates of Hexachlorocyclohexane Isomers. *Environ. Sci. Technol.* **1998,** *32*, (15), 2197-2207.
33. Li, Y. F.; Cai, D. J.; Shan, Z. J.; Zhu, Z. L., Gridded usage inventories of technical hexachlorocyclohexane and lindane for china with 1/6 degrees latitude by 1/4 degrees longitude resolution. *Archives of Environmental Contamination and Toxicology* **2001,** *41*, (3), 261-266.
34. Li, Y. F.; Cai, D. J.; Singh, A., Technical hexachlorocyclohexane use trends in China and their impact on the environment. *Archives of Environmental Contamination and Toxicology* **1998,** *35*, (4), 688-697.
35. Li, Y. F.; Zhulidov, A. V.; Robarts, R. D.; Korotova, L. G., Hexachlorocyclohexane use in the former Soviet Union. *Archives of Environmental Contamination and Toxicology* **2005,** *48*, (1), 10-15.
36. Tsydenova, O.; Batoev, V.; Weissflog, L.; Klaus-Dieter, W., Pollution of the Lake Baikal Basin: Organochlorine Pesticides. *Chemistry for Sustainable Development* **2003,** *11*, 349-352.
37. U.S. Geological Survey, Pesticide National Synthesis Project. http://ca.water.usgs.gov/pnsp/pesticide_use_maps_1997
38. Bidleman, T. F.; Leone, A. D.; Falconer, R. L.; Harner, T.; Jantunen, L. M.; Wiberg, K.; Helm, P. A.; Diamond, M. L.; Loo, B., Air-soil and air-water exchange of chiral pesticides. *Environmental Fate and Effects of Pesticides* **2003,** *853*, 196-225.

Figure 2.1. Map of air sampling locations (Cheeka Peak Observatory – CPO and Mary's Peak Observatory –MPO) in relation to source regions (boxes) in (A) Asia, Siberia, and the U.S. and (B) urban and agricultural source regions in the United States

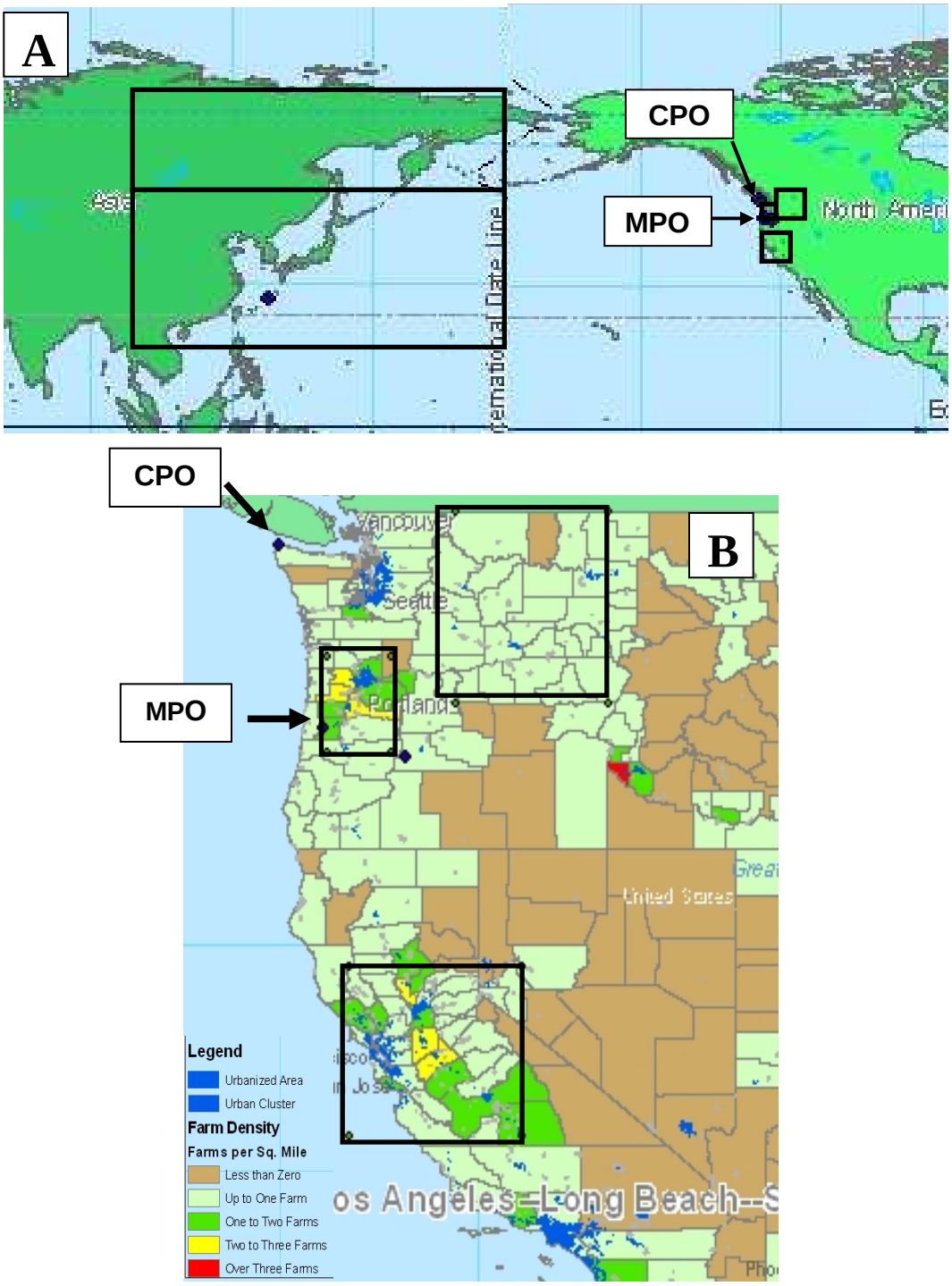

Figure 2.2: MODIS 10-day fire detects overlaid with 10-day air mass back trajectories and corresponding PAH and pesticide concentrations measured at MPO (purple) and CPO (orange) for the concurrent sampling on June 2, 2003 and. Smoke plumes extended across the Pacific Ocean to the Western U.S. (Figures 2.6 and 2.7).

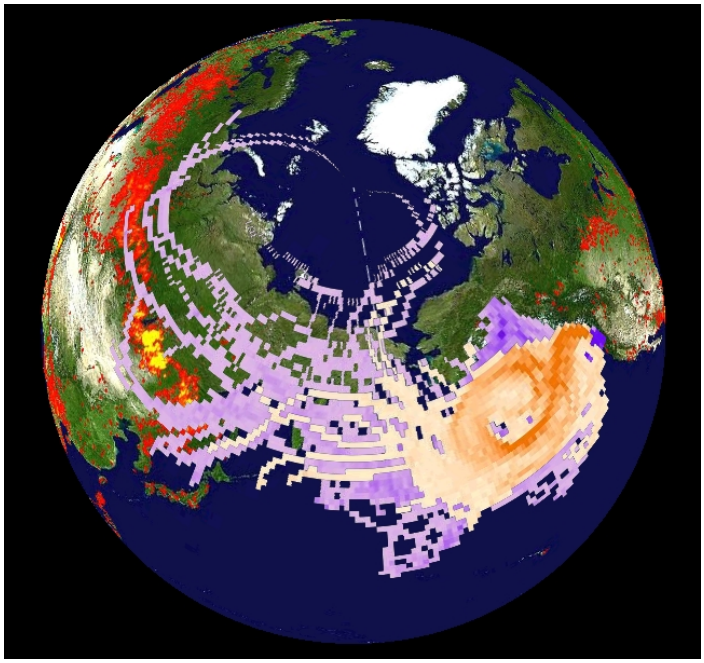

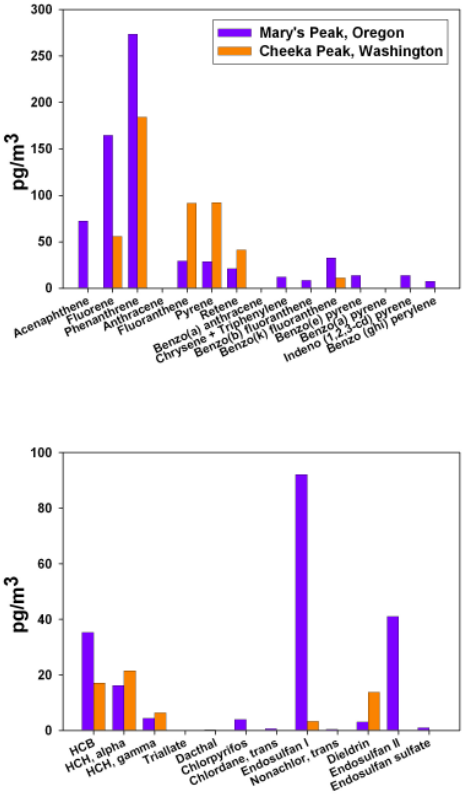

Figure 2.3: MODIS 10-day fire detects overlaid with 10-day air mass back trajectories and corresponding PAH and pesticide concentrations measured at MPO (purple) and CPO (orange) for the concurrent sampling on August 4, 2003. Smoke plumes extended across the Pacific Ocean to the Western U.S. (Figures 2.6 and 2.7).

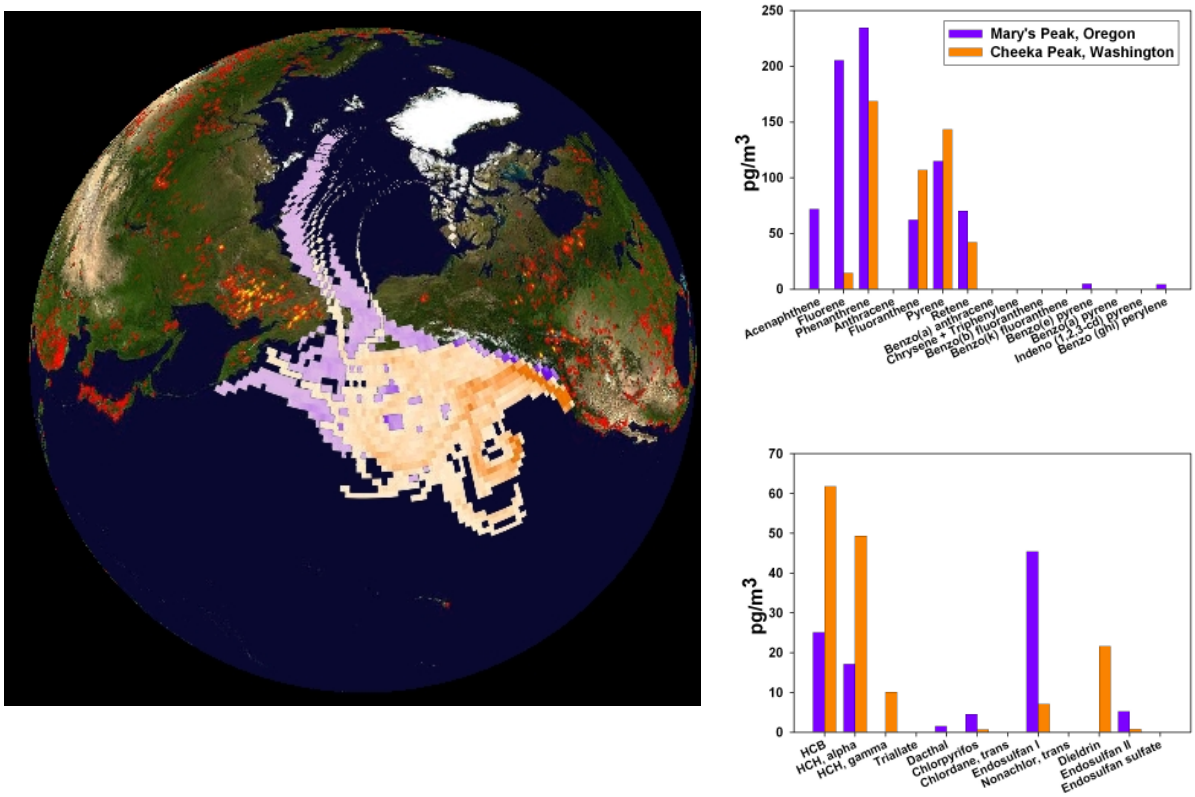

Figure 2.4 NAAPs model images depicting the smoke optical depth during the June 16 sampling at CPO. The legend represents the smoke mass mixing ratio (ug / m^3) at the surface. The contouring begins at 0.1 ug / m^3 and doubles in magnitude for each successive contour [20].

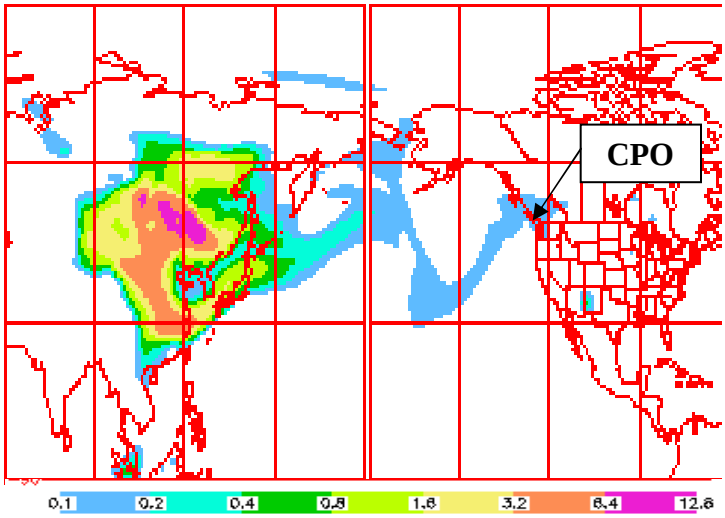

Figure 2.5 NAAPs model images depicting the smoke optical depth during the September 4 sampling at MPO. The legend represents the smoke mass mixing ratio (ug / m^3) at the surface. The contouring begins at 0.1 ug / m^3 and doubles in magnitude for each successive contour [20].

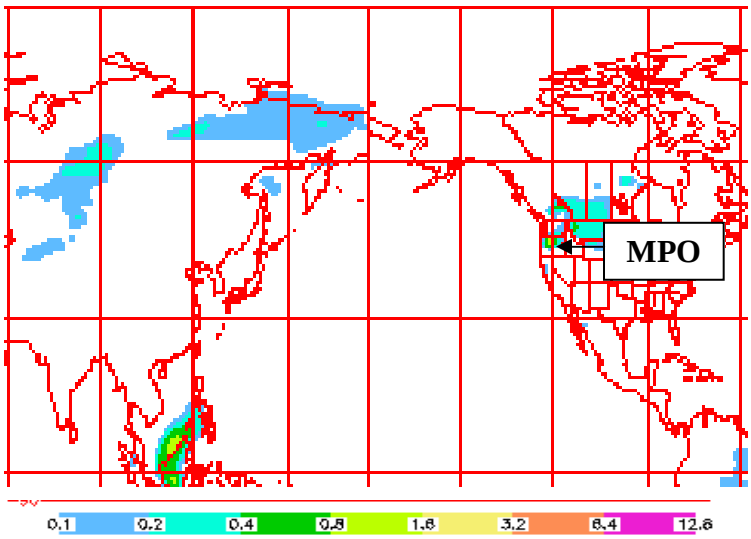

Figure 2.6 NAAPs model images depicting the smoke optical depth during the June 2 concurrent sampling at CPO and MPO. The legend represents the smoke mass mixing ratio (ug / m^3) at the surface. The contouring begins at 0.1 ug / m^3 and doubles in magnitude for each successive contour [20].

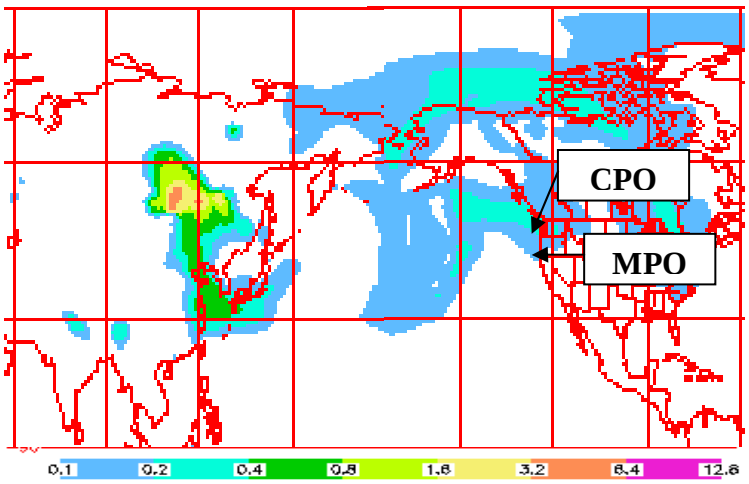

Figure 2.7 NAAPs model images depicting the smoke optical depth during the August 4 concurrent sampling at CPO and MPO. The legend represents the smoke mass mixing ratio (ug / m^3) at the surface. The contouring begins at 0.1 ug / m^3 and doubles in magnitude for each successive contour [20].

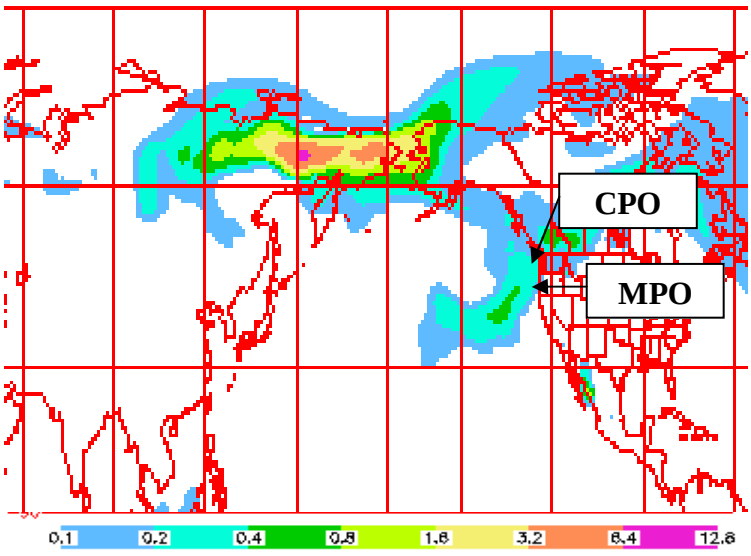

Figure 2.8. PCA biplot of normalized PAH and concentrations measured at MPO and CPO during 2003. The numbers correspond to sample numbers in Tables 2.1. The letters next to the sample number indicate samples influenced by Siberian biomass burning emissions (S) and regional fires (R).

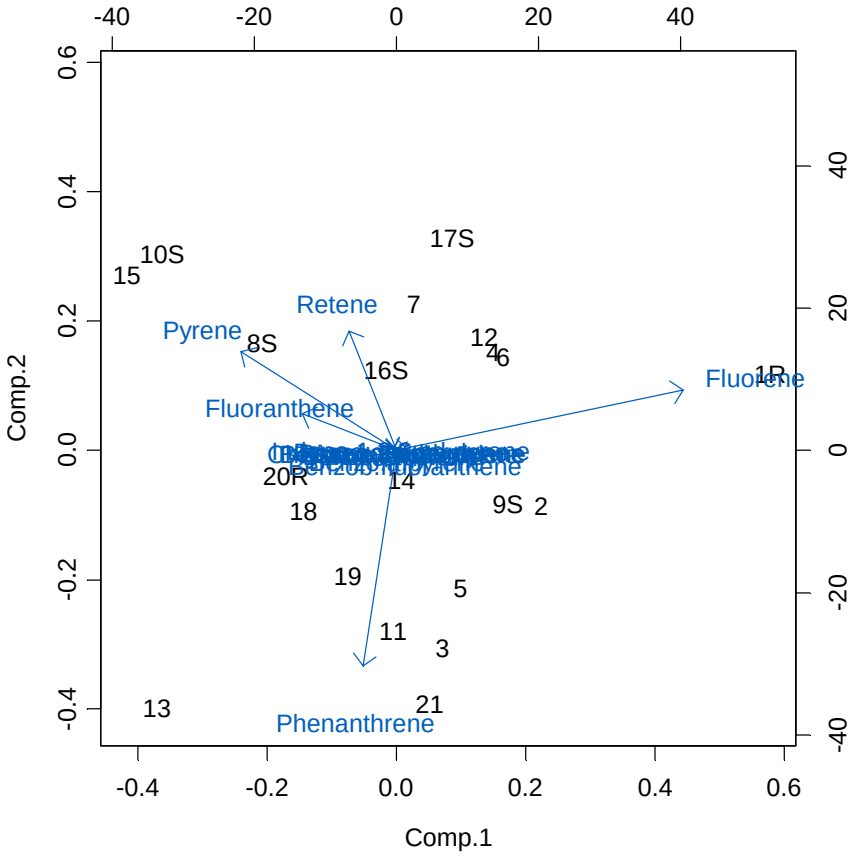

Figure 2.9. PCA biplot of normalized Pesticide concentrations measured at MPO and CPO during 2003. The numbers correspond to sample numbers in Table 2.1. The letters next to the sample number indicate samples influenced by Siberian biomass burning emissions (S) and regional fires (R).

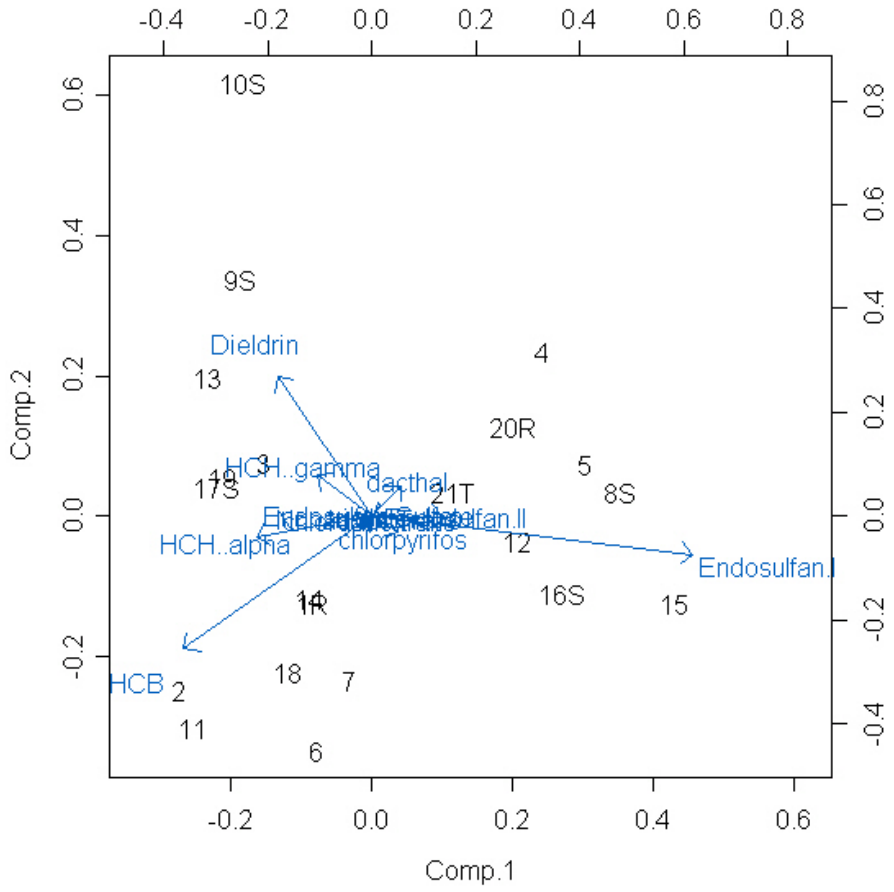

Figure 2.10. Concentrations of pesticides and polychlorinated biphenyls (PCBs) (pg/g dry weight) in burned and un-burned forest soil collected from the B&B complex forest fire in the Deschutes National Forest, Oregon.

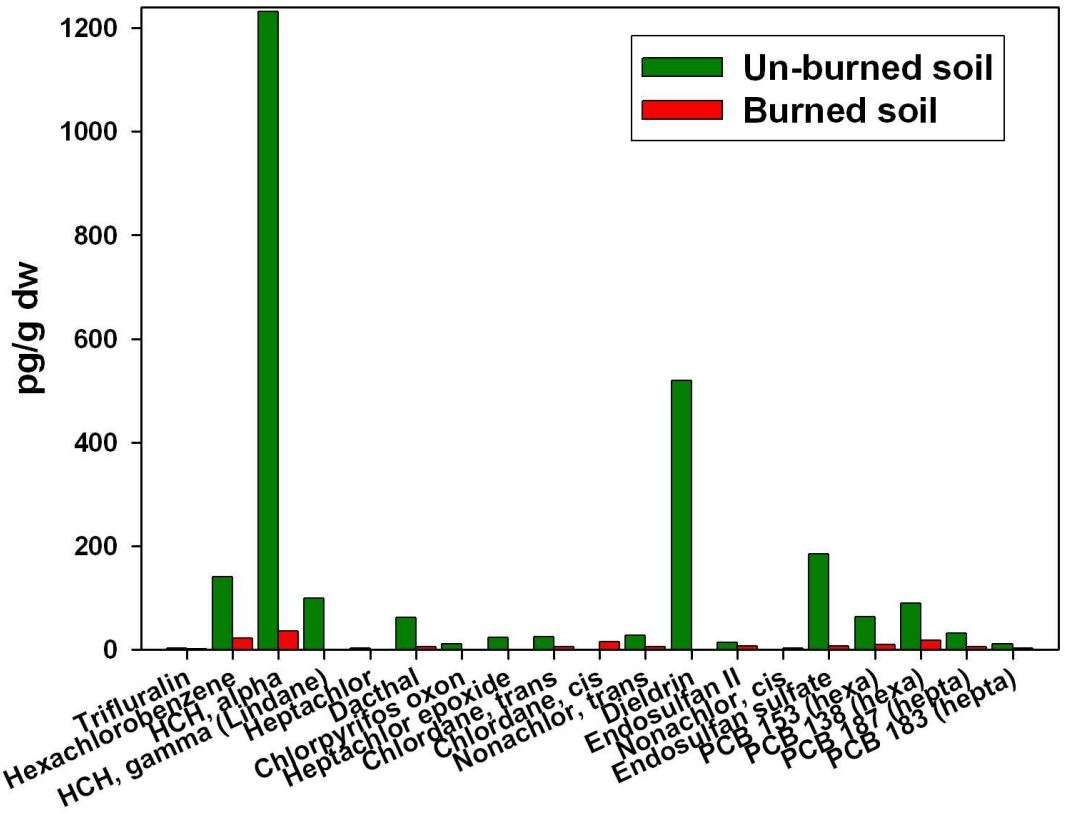

Table 2.1. Sample, meteorological, and SRIF information for air samples collected at MPO and CPO during 2003. The %PO indicates the percent of time the air mass spent over the Pacific Ocean relative to land masses along the 10 day back trajectory.

Sample #	Sampling Location	Start	Stop	Hours Sampled	m3 of air	Avg Temp (oC)	Average Wind Speed (m/s)	Primary Wind Direction	% Pacific Ocean	%<BL	%>BL	%Siberia	% Asia	% Eastern Oregon and Washington	% Western Oregon	% Central California
1R	CPO	11-Apr	13-Apr	48	675	9.1*	5*	NE*	87.7	81.4	18.6	17.8	17.9	1.5	0.7	0.0
2	CPO	21-Apr	23-Apr	48	664	8.3*	8*	W*	85.0	58.4	41.6	22.1	5.4	0.0	1.1	0.0
3	CPO	2-May	4-May	48	661	9.1*	3.0	W	56.8	71.2	28.8	0.0	0.0	0.0	0.0	0.2
4	MPO	11-May	13-May	48	3041	5.0	5.3	W	29.2	18.9	81.1	0.0	0.0	4.0	7.1	0.0
5	MPO	21-May	23-May	48	3207	12.1	2.5	SW	96.0	16.5	83.5	1.9	5.1	0.0	0.5	0.0
6	MPO	26-May	28-May	48	3207	NA	3.9	NE	94.7	26.5	73.5	0.1	8.9	0.0	0.5	0.0
7	MPO	30-May	1-Jun	48	3207	7.7	5.2	NE	89.2	40.5	59.5	4.8	2.8	0.0	1.8	0.0
8S	MPO	2-Jun	4-Jun	48	3207	9.4	9.1	NE	78.1	3.8	96.2	8.5	4.7	0.0	2.2	0.0
9S	CPO	2-Jun	4-Jun	48	643	12.9*	2.7	W	88.7	32.0	68.0	1.2	0.2	0.0	0.0	0.0
10S	CPO	16-Jun	18-Jun	48	636	14.5*	2.0	W	93.3	45.8	54.2	8.8	4.4	0.0	0.0	0.0
11	MPO	22-Jun	24-Jun	48	2867	4.0	6.8	NE	89.2	25.3	74.7	3.8	2.4	0.0	0.7	0.0
12	MPO	4-Jul	6-Jul	48	2867	13.4	4.9	NE	88.7	33.1	66.9	0.1	1.7	0.0	0.9	0.0
13	CPO	7-Jul	9-Jul	48	636	13.8*	3.2	SW	92.2	83.5	16.5	3.9	6.9	0.0	0.0	0.0
14	MPO	22-Jul	24-Jul	48	1794	18.4	4.4	N	90.4	16.5	83.5	2.9	21.4	0.0	1.8	0.0
15	MPO	2-Aug	4-Aug	48	1794	15.0	2.6	S	95.0	39.9	60.1	0.8	0.6	0.0	0.8	0.0
16S	MPO	4-Aug	5-Aug	24	897	17.0	3.8	SW	87.1	52.9	47.1	4.2	0.0	0.0	0.6	0.0
17S	CPO	4-Aug	6-Aug	48	647	13.9*	2.5	SW	83.5	80.6	19.4	1.7	0.0	0.0	0.0	0.0
18	MPO	8-Aug	10-Aug	48	1794	11.9	4.9	SW	86.2	25.8	74.2	2.6	0.2	0.0	0.8	0.0
19	MPO	12-Aug	14-Aug	48	1794	12.0	4.6	SW	82.2	26.6	73.4	0.0	0.0	0.0	2.9	0.0
20R	MPO	4-Sep	5-Sep	24	897	23.4	2.8	SW	77.5	56.2	43.8	3.3	0.3	2.5	2.5	0.0
21T	MPO	21-Sep	22-Sep	24	897	11.6	13.5	NE	78.2	6.0	94.0	12.6	20.9	0.0	1.9	0.0

*** CPO data from met station in Quillayute, WA**

S = influenced by Siberian biomass burning

R = influenced by regional biomass burning

T = influenced by trans-Pacific transport

Table 2.2. PAH concentrations (pg/m^3) in MPO and CPO air samples collected during 2003

Sample #	Sampling Location	Sampling start date	ACE	FLO	PHE	ANT	FLA	PYR	RET	BaA	CHR	BbF	BkF	BeP	BaP	IcdP	BghiP	LEV
1R	CPO	11-Apr	<DL	256	170	<DL	41.0	1.71	<DL	14.8	6.98	<DL	<DL	<DL	<DL	<DL	<DL	16000
2	CPO	21-Apr	<DL	54.3	75.9	<DL	18.8	12.2	<DL	<DL	<DL	4.96	<DL	1.73	<DL	<DL	<DL	654
3	CPO	2-May	<DL	49.81	125	<DL	23.2	16.3	<DL	<DL	<DL	9.94	<DL	<DL	<DL	<DL	<DL	381
4	MPO	11-May	<DL	155	199	<DL	38.1	69.2	38.8	4.47	4.00	<DL	<DL	<DL	<DL	<DL	3.98	<DL
5	MPO	21-May	<DL	258	558	<DL	81.9	93.6	66.4	5.43	3.83	<DL	<DL	<DL	<DL	<DL	4.75	22600
6	MPO	26-May	<DL	43.5	55.2	<DL	8.71	19.0	11.3	<DL	<DL	<DL	<DL	<DL	<DL	<DL	1.03	<DL
7	MPO	30-May	<DL	21.5	27.4	<DL	0.74	25.7	<DL	<DL	<DL	<DL	<DL	1.63	<DL	2.42	1.01	<DL
8S	MPO	2-Jun	72.4	165	274	<DL	29.5	28.8	21.0	<DL	12.0	8.47	32.6	13.8	<DL	13.7	7.47	32300
9S	CPO	2-Jun	<DL	55.7	184	<DL	91.5	92.2	41.2	<DL	<DL	<DL	11.2	<DL	<DL	<DL	<DL	<DL
10S	CPO	16-Jun	<DL	51.5	306	<DL	200	236	84.5	<DL	<DL	<DL	<DL	<DL	<DL	<DL	<DL	<DL
11	MPO	22-Jun	<DL	38.4	121	<DL	13.4	23.6	23.3	<DL	<DL	<DL	<DL	<DL	<DL	<DL	0.89	3440
12	MPO	4-Jul	<DL	97.7	127	<DL	28.4	41.8	27.2	5.43	<DL	<DL	<DL	<DL	<DL	2.31	3.05	<DL
13	CPO	7-Jul	<DL	<DL	68.5	<DL	20.2	21.2	<DL	<DL	<DL	<DL	<DL	<DL	<DL	<DL	<DL	<DL
14	MPO	22-Jul	149	522	1120	<DL	246	376	156	<DL	<DL	<DL	<DL	<DL	<DL	<DL	<DL	3980
15	MPO	2-Aug	3.69	56.5	91.6	<DL	29.6	57.0	<DL	<DL	<DL	<DL	<DL	2.97	<DL	3.10	2.00	<DL
16S	MPO	4-Aug	72.0	205	235	<DL	62.3	115	70.3	<DL	<DL	<DL	<DL	4.90	<DL	<DL	4.23	33800
17S	CPO	4-Aug	<DL	14.6	169	<DL	107	143	42.1	<DL	<DL	<DL	<DL	<DL	<DL	<DL	<DL	1980
18	MPO	8-Aug	137	153	656	25.5	102	263	74.7	<DL	<DL	<DL	<DL	52.2	<DL	<DL	2.38	2750
19	MPO	12-Aug	88.0	240	824	<DL	103	261	80.1	<DL	<DL	<DL	<DL	<DL	<DL	4.30	4.07	0
20R	MPO	4-Sep	431	483	2230	125	330	1070	303	<DL	<DL	<DL	<DL	321	20.1	<DL	5.96	17100
21T	MPO	21-Sep	<DL	215	682	<DL	52.8	69.2	48.0	19.9	5.11	<DL	<DL	10.7	35.0	8.91	9.43	472

indicates concurrent samples

Abbreviations: **ACE=acenapthene, FLO = fluorene, PHE = phenanthrene, ANT = anthracene, FLA = fluoranthene, PYR = pyrene, RET = retene, BaA = Benzo(a)anthracene = chrysene and triphenylene, BbF = Benzo(b)fluoranthene, BkF = Benzo(k)fluoranthene, BeP = Benzo(e)pyrene, BaP = Benzo(a)pyrene, IcdP = Indeno(1,2,3-cd)pyrene, BghiP = Benzo(ghi)perylene, LEV = levoglucosan, 1,3,5 TPB = 1,3,5 triphenylbenzene**

S= influenced by Siberian biomass burning emissions

R= influenced by regional biomass burning emissions

T= inlfuenced by trans-Pacific transport

Table 2.3. Pesticide concentrations (pg/m^3) in MPO and CPO air samples collected during 2003

Sample #	Sampling Location	Sampling start date	HCB	HCH, alpha	HCH, gamma	alpha / gamma ratio	Triallate	Dacthal	Chlorpyrifos	Chlordane, trans	Endosulfan I	Nonachlor, trans	Dieldrin	Endosulfan II	Endosulfan sulfate
1R	CPO	11-Apr	38.6	13.6	4.57	2.96	6.31	9.44	<DL	0.28	12.1	<DL	3.00	<DL	<DL
2	CPO	21-Apr	43.3	15.6	5.06	3.08	<DL	<DL	<DL	<DL	2.53	<DL	6.46	<DL	<DL
3	CPO	2-May	36.2	14.4	6.70	2.15	2.40	8.79	<DL	0.22	6.49	<DL	11.7	<DL	<DL
4	MPO	11-May	30.1	12.6	5.27	2.39	5.85	32.6	1.88	0.64	62.4	0.56	13.9	6.66	0.62
5	MPO	21-May	29.0	13.3	3.30	4.04	<DL	2.07	4.49	0.96	64.9	0.67	6.38	26.6	1.12
6	MPO	26-May	9.82	3.84	0.96	4.01	<DL	<DL	0.37	0.23	3.86	0.16	<DL	<DL	<DL
7	MPO	30-May	11.3	5.76	1.09	5.27	<DL	0.05	2.49	<DL	5.30	<DL	<DL	0.84	<DL
8S	MPO	2-Jun	35.2	16.2	4.32	3.74	<DL	0.16	3.91	0.61	92.1	0.41	3.03	41.0	0.96
9S	CPO	2-Jun	17.1	21.5	6.35	3.38	<DL	<DL	<DL	<DL	3.24	<DL	13.7	<DL	<DL
10S	CPO	16-Jun	26.2	29.9	14.9	2.00	<DL	2.04	<DL	<DL	3.50	<DL	40.1	<DL	<DL
11	MPO	22-Jun	37.5	25.3	2.51	10.1	<DL	0.51	0.63	0.52	2.81	0.36	1.05	0.35	0.16
12	MPO	4-Jul	13.2	6.41	1.00	6.41	0.31	0.42	12.7	0.37	18.9	0.25	<DL	4.16	0.30
13	CPO	7-Jul	13.7	<DL	4.64	NA	<DL	0.29	<DL	<DL	0.83	<DL	7.13	<DL	<DL
14	MPO	22-Jul	81.1	37.0	7.20	5.13	<DL	3.67	4.16	1.79	24.8	1.42	11.0	14.2	3.23
15	MPO	2-Aug	22.8	9.30	<DL	NA	<DL	0.03	<DL	<DL	61.8	<DL	<DL	4.53	0.30
16S	MPO	4-Aug	25.1	17.1	<DL	NA	<DL	1.48	4.54	<DL	45.4	<DL	<DL	5.23	<DL
17S	CPO	4-Aug	61.7	49.3	10.1	4.91	<DL	<DL	0.70	<DL	7.09	<DL	21.6	0.73	<DL
18	MPO	8-Aug	84.3	53.1	3.91	13.6	<DL	5.65	2.42	0.75	26.2	0.67	4.75	3.26	0.30
19	MPO	12-Aug	28.6	22.9	4.66	4.91	<DL	<DL	0.32	<DL	3.29	<DL	10.0	0.34	2.31
20R	MPO	4-Sep	82.6	29.9	4.99	5.99	<DL	101	3.46	1.37	117	1.41	9.57	9.95	8.16
21T	MPO	21-Sep	80.1	50.4	8.33	6.05	<DL	<DL	2.60	2.45	91.0	1.66	26.7	8.65	1.87

indicates concurrent samples

<DL = below detection limit

NA = not applicable

S= influenced by Siberian biomass burning emissions

R= influenced by regional biomass burning emissions

T = influenced by trans-Pacific transport

Table 2.4. Significant Pearson correlation coefficients (R) (p-value <0.05) between PAH and pesticide concentrations measured at CPO: Hexachlorobenzene(HCB), alpha and gamma Hexachlorocyclohexane (a-HCH, g-HCH), Dacthal (Dac), Endosulfan 1(Endo 1), Dieldrin (Dield), Endosulfan II(Endo2), Endosulfan Sulfate (EndoS), Sum Chlordanes (ΣChlor), Sum Endosulfans (ΣEndos), Fluorene (FLO), Phenanthrene (PHE), Anthracene (ANT), Fluoranthene (FLA), Pyrene (PYR), Retene (RET), and Levoglucosan (Lev).

	HCB	***aHCH***	***gHCH***	***a/g ratio***	***Dact***	***Endo1***	***Dield***	***Endo2***	***EndoS***	***Σ Chlor***	***Σ Endo***	***FLO***	***PHE***	***ANT***	***FLA***	***PYR***	***RET***	***Lev***
HCB	NA				0.95													
aHCH		NA	0.83		-0.99		0.89								0.92	0.98	0.93	
gHCH		0.83	NA				0.98						0.82		0.83	0.79		
a/g ratio				NA														
Dact	0.95	-0.99			NA												.	
Endo1						NA												0.89
Dield	2.00	0.89	0.98				NA								0.83	0.87	0.99	
Endo2																		
EndoS																		
Σ Chlor																		
Σ Endo																		
FLO												NA						0.96
PHE			0.82										NA					
ANT																		
FLA		0.92	0.83				0.83								NA	0.95	0.99	
PYR		0.98	0.79				0.87								0.95	NA	0.95	
RET		0.93					0.99								0.99	0.95	NA	
Lev						0.89						0.96						NA

Table 2.5 Significant Pearson correlation coefficients (R) (p-value <0.05) between PAH and pesticide concentrations measured at MPO: Hexachlorobenzene (HCB), alpha and gamma Hexachlorocyclohexane (a-HCH, g-HCH), Dacthal (Dac), Endosulfan 1(Endo 1), Dieldrin (Dield), Endosulfan II(Endo2), Endosulfan Sulfate (EndoS), Sum Chlordanes (ΣChlor), Sum Endosulfans (ΣEndos), Fluorene (FLO), Phenanthrene (PHE), Anthracene (ANT), Fluoranthene (FLA), Pyrene (PYR), Retene (RET), and Levoglucosan (Lev), NA = not applicable.

	HCB	***aHCH***	***gHCH***	***a/g ratio***	***Dac***	***ENDO1***	***DIELD***	***ENDO2***	***ENDOS***	***Σ Chlor***	***Σ Endo***	***FLO***	***PHE***	***ANT***	***FLA***	***PYR***	***RET***	***Lev***
HCB	NA	0.94	0.78							0.78		0.72	0.79		0.70	0.65	0.66	
aHCH	0.94	NA	0.71							0.65								
gHCH	0.78	0.71	NA				0.87			0.89	0.58	0.70	0.58					
a/g ratio				NA														
Dac					NA	0.66			0.86			0.63	0.82	0.93	0.79	0.86	0.83	
ENDO1			0.60			NA					0.97		0.59					
DIELD			0.87				NA			0.77								
ENDO2								NA			0.66							0.57
ENDOS					0.86				NA			0.87	0.96	0.87	0.94	0.95	0.96	
Σ Chlor	0.78	0.65	0.89				0.77			NA								
Σ Endo			0.58			0.97		0.66			NA	0.56	0.58					0.54
FLO	0.72		0.70						0.87	0.75	0.56	NA	0.91	0.58	0.91	0.84	0.90	
PHE	0.79		0.58		0.82	0.59			0.96	0.69	0.58	0.91	NA	0.83	0.97	0.96	0.97	
ANT					0.93				0.87			0.58	0.83	NA	0.84	0.91	0.86	
FLA	0.70				0.79				0.94			0.91	0.97	0.84	NA	0.98	0.99	
PYR	0.65				0.86				0.95			0.84	0.96	0.91	0.98	NA	0.98	
RET	0.66				0.83				0.96			0.90	0.97	0.86	0.99	0.98	NA	
Lev								0.57			0.54							

Table 2.6. Concentrations of pesticides and polychlorinated biphenyls (PCBs) (pg/g dry weight) and their percent difference in burned and un-burned soil from the B&B complex fire in the Deschutes National Forest.

	Un-burned soil pg/g dw	Burned soil pg/g dw	% difference
Trifluralin	2.62	1.73	34
Hexachlorobenzene	140.45	22.51	84
HCH, alpha	1231.28	35.78	97
HCH, gamma (Lindane)	98.96	0.00	100
Heptachlor	2.25	0.00	100
Dacthal	61.98	5.92	90
Chlorpyrifos oxon	10.62	0.00	100
Heptachlor epoxide	23.24	0.00	100
Chlordane, trans	24.62	5.63	77
Nonachlor, trans	27.49	5.05	82
Dieldrin	519.42	0.00	100
Endosulfan II	13.87	6.20	55
Endosulfan sulfate	184.18	6.35	97
PCB 153 (hexa)	62.73	9.52	85
PCB 138 (hexa)	89.22	17.46	80
PCB 187 (hepta)	31.74	4.76	85
PCB 183 (hepta)	10.62	2.16	80

CHAPTER 3. CHIRAL SIGNATURES OF ORGANOCHLORINE PESTICIDES IN ASIAN, TRANS-PACIFIC AND WESTERN U.S. AIR MASSES

Susan A. Genualdi[1], Staci L. Massey Simonich[1,2*], Toby K. Primbs[1], Terry F. Bidleman[3], Liisa M.M. Jantunen[3], Keon-Sang Ryoo[4], Wang, Feng[5], Tong Zhu[5]

[1]Department of Chemistry, Oregon State University, Corvallis, Oregon
[2]Department of Environmental and Molecular Toxicology, Oregon State University, Corvallis, Oregon
[3]Centre for Atmospheric Research Experiments, Egbert, ON
[4]Andong National University, Seoul, South Korea
[5]College of Environmental Science, Peking University, Beijing, China
* Corresponding Author, staci.simonich@orst.edu, v: (541)737-9194, f: (541)737-0497

ABSTRACT

Chiral signatures of organochlorine pesticides were measured in air masses on Okinawa Japan and three remote locations in the Pacific Northwestern U.S.: Cheeka Peak Observatory (CPO), a coastal site on the Olympic Peninsula of Washington at 500 m; Mary's Peak Observatory (MPO), a site at 1250 m in Oregon's Coast range; and Mt. Bachelor Observatory (MBO), a site at 2300 m in Oregon's Cascade range. The chiral signature of composite soil samples collected from agricultural areas in China and South Korea were also measured. Racemic alpha-HCH was measured in Asian air masses and soil from China and South Korea. Non-racemic (enantiomer fraction (EF) = 0.528 ± 0.0048) alpha-HCH was measured in regional air masses at CPO, a marine boundary layer site, and may reflect volatilization from the Pacific Ocean and regional soils. However, during trans-Pacific transport events at CPO, the EFs were significantly (p-value <0.001) more racemic (EF = 0.513 ± 0.0003). Racemic alpha-HCH was consistently measured in trans-Pacific air masses at MPO and MBO. The alpha-HCH EFs in CPO, MPO, and MBO air masses were positively correlated (p-value = 0.0017) with the amount of time the air mass spent above the boundary layer along the 10-day back air mass trajectory prior to being sampled. This suggests that the alpha-HCH in the free troposphere is racemic. The racemic signatures of cis and trans chlordane in air masses at all four air sampling sites suggest that Asian and U.S. urban areas continue to be sources of chlordanes that have not yet undergone biotransformation.

INTRODUCTION

Organochlorine pesticides (OCPs) are semi-volatile, undergo long-range atmospheric transport and are persistent in the environment [1]. Although most OCPs

have been banned in the U.S. for many years, they continue to be measured in ambient air [2]. Re-volatilization of OCPs from contaminated soils is considered to be a significant source of OCPs to the atmosphere [1, 2]. In addition, several OCPs are classified as Persistent Organic Pollutants (POPs), and are being phased out by the United Nations Environmental Program (UNEP) [1]. In order to eliminate OCPs and other POPs from the atmosphere, their source regions need to be identified [1].

Chiral pesticides are composed of two enantiomers that have the same physical and chemical properties. Therefore, abiotic (hydrolysis, photolysis, etc.) and transport processes (volatilization, deposition, etc.) processes affect the enantiomers equally [3]. OCPs are manufactured and used in racemic form. However, microorganisms in soil and water selectively degrade one enantiomer over the other resulting in a non-racemic signature that can volatilize to the overlying air [1]. The enantiomer fractions of chiral OCPs in air masses can provide information about whether a pesticide has been transported from an area where it is currently being used or has not yet been biotransformed (a racemic signature) or has been transported from an area after historic use and biotransformation (a non-racemic signature).

The trans-Pacific and regional atmospheric transport of OCPs has been reported at sites in Asia and in the Pacific Northwestern U.S. [4-9]. The objectives of this research were to use the chiral signatures of OCPs to distinguish between air masses influenced by trans-Pacific and regional atmospheric transport and to determine if the sources of OCPs to the Pacific Northwestern U.S. were from current or historic use.

EXPERIMENTAL

Air Sampling

The air sampling sites included Hedo Station Observatory (HSO) on Okinawa, Japan (26.8^{o}N, 128.2^{o}E, 60 m) [6], Cheeka Peak Observatory (CPO) in Washington State (48.3^{o}N, 124.6^{o}W, 500 m) [7], Mary's Peak Observatory (MPO) in Oregon's Coast Range (44.5^{o}N, 123.6^{o}W, 1249 m) [7], and Mt. Bachelor Observatory (MBO) in Oregon's Cascade Range (43.9^{o}N, 121.7^{o}W, 2763 m) [4, 5] (Figure 3.1). The distance from HSO to the East China Sea is 0.2 km, while the distance of CPO, MPO, and MBO to the Pacific Ocean is approximately 3 km, 26 km, and 120 km, respectively. HSO, CPO and MBO are all well-established sites [4-7, 9].

Hi-volume air samples were collected at HSO during the spring of 2004 (18 samples) [6], at CPO during 2003 (12 samples) [7], at MPO during 2003 (14 samples) [7], and at MBO during 2004, 2005, and the spring of 2006 (69 samples) [4, 5]. Detailed information on the sample collection, OCP extraction procedures and analysis, including solvents and standards used, were previously reported [4-7, 10]

Soil Sampling

Soil samples were collected from four rice paddy fields in China (Nanjing, Tianjin, Guangzhou, and Tangdian) in the summer of 2006 (Figure 3.1). The sampling sites were chosen based on their proximity to intense agricultural regions, including the Yangtze and Pearl River Deltas. Rice paddies were chosen because of the large amount of technical hexachlorocyclohexane (HCH) historically used in these areas. In 1980, 53.2% of the HCH applied to agricultural fields in China was applied to rice paddies [11]. Technical HCH was banned in China in 1983 and in South Korea in 1985. A previous study estimated the historical contamination level of technical HCH in China to be extremely high (usage density > 40 t / kha) and in South Korea to be very high (usage

density is 10-40 t / kha) [12]. Soil samples were collected from 7 agricultural fields containing beans and hot peppers in provinces in South Korea (Kyeongbuk, Gangwon, Chungnam, Jeonbuk, Jeonnam, Kyeongnam, Ulsan City) in the spring of 2007. The latitude, longitude, and elevation of each of the soil sampling locations can be found in Table 3.1.

Twenty composite soil samples were collected in China, while twenty-one samples were collected from South Korea. Each composite soil sample was collected from $100m^2$ x $100m^2$ agricultural plots and consisted of 5 random surface (0 – 20cm) samples combined and mixed thoroughly. The samples collected were representative of 200,000 m^2 (China) and 210,000 m^2 (South Korea) of land. Additional information on the soil extraction and OCP analysis is given in the Supporting Information.

Chiral Analysis

Chiral analysis was performed using an Agilent 6890 GC and 5973N MSD (GC/MS) in electron capture negative ionization mode (ECNI). A DB-5MS (28m, 0.25mm id., 0.25um film thickness, J&W Scientific, USA) column connected to a BGB 172 chiral column (10m, 0.25mm id, 0.25um film thickness, BGB Analytik, Germany) was used for the enantiomer separation of alpha-HCH, heptachlor epoxide, oxychlordane, cis-chlordane, trans-chlordane, and o,p-DDT. The DB-5 column minimized interferences during the chiral separation on the BGB 172 column. Extracts were injected (2uL) using splitless injection with an initial oven temperature of 90^oC. Following a 1 minute hold, the following temperature program was used; 15^oC/min to 140, 55 min hold, 2^oC/min to 180, 40 min hold, 15^oC/min to 240^oC, 10 min hold resulting in a total run time of 133

minutes. The temperatures of the ion source and quadrupole were both 150^{o}C and the methane gas was 60%.

The following ions were monitored in selective ion monitoring (SIM) mode: alpha-HCH (m/z 253, 255, 257), heptachlor epoxide (m/z 316, 318), oxychlordane (m/z 350, 352) cis and trans chlordane (m/z 408, 410, 412), and o,p'-DDT (m/z 246, 248). The enantiomer elution order was determined for α-HCH and cis and trans chlordane using enantiomer (+) pure standards (Dr. Ehrenstorfer, D-86199 Augsburg, Germany). Enantiomer pure standards were not available for heptachlor epoxide or oxychlordane. The concentration of OCPs in field and lab blanks were below the detection limit for chiral analysis (S/N < 3:1).

Enantiomer fractions (EFs) are calculated using the following: Area (+)/(Area (+) + Area (-)), where Area (+) and Area (-) corresponds to the peak areas of the (+) and (-) enantiomers respectively. For heptachlor epoxide and oxychlordane, EFs were calculated using: Area (1)/(Area (1) + Area (2)), where Area (1) and Area (2) correspond to the peak areas of the 1st and 2nd eluting enantiomers, respectively. A macro was used to smooth the chromatograms in MSD ChemStation (G1701DA) before manual integration was performed. Seven replicate injections of racemic standards (25pg/uL) were used to determine the racemic ranges (95% confidence intervals) for alpha-HCH (0.499 ± 0.0095), trans chlordane (0.499 ± 0.0052), and cis chlordane (0.497 ± 0.0059). Because the EF precision of the standards was four decimal places, all EFs are reported to 3 decimal places. To ensure there were no interferences, ion ratios were monitored and required to fall within 20% of the standards. The detection limit for chiral analysis was defined as a S:N ratio > 3:1.

Air mass back trajectories and source region impact factors (SRIFs)

4-day (HSO) and 10-day (CPO, MPO, MBO) air mass back trajectories were calculated for each of the sampling dates using NOAA's Hybrid Single-Particle Lagrangian Integrated Trajectory model (HYSPLIT). Source region impact factors (SRIFs) were calculated to assess the impact of Asia, Siberia, and agriculturally intense areas in Eastern Washington, the Willamette Valley in Oregon, and the Central Valley in California on sampled air masses. The SRIFs for all air masses have been previously reported and are given in Table 3.2 [4-7]. The air mass back trajectories were also used to assess the influence of boundary layer (<1000m) and free tropospheric (>1000m) air on air masses sampled at MBO and have been previously reported for the air masses sampled at MPO and CPO (Table 3.2) [7].

RESULTS

Chiral Signatures of Alpha- HCH

Asia

Six of the eighteen HSO air masses sampled during the spring of 2004 had EFs above the detection limit (S/N > 3:1) and racemic signatures (Table 3.2). Source region impact factors (SRIFs) were previously calculated to identify the source regions that influenced each air mass and these included China, Korea, Japan, Russia, and ocean/local [6]. The concentrations of alpha-HCH ranged from 5.94 to 36.2 pg/m^3, and elevated concentrations were measured in air masses associated with China [6]. Of the 6 air masses with alpha-HCH EFs above the detection limit, 3 were primarily from China, (Apr 1-2, Apr 2-3, Apr 3-4, 2004) and the other 3 were primarily from Ocean/local

influence (Mar 30-31, Apr 26-27, Apr 27-28). This suggests that the alpha-HCH outflow from China and Japan is racemic.

Racemic alpha-HCH signatures were also measured above the detection limit in 10 of 20 composite soil samples taken from rice paddies in China and in 4 of 21 samples from agricultural fields in South Korea (Table 3.1). The alpha-HCH concentrations ranged from <DL to 474 pg/g dry weight (dw), with a median value of 156 pg/g dw in the Chinese soils, and 30 pg/g dw to 934 pg/g dw with a median value of 150 pg/g dw in the Korean soils. A previous study measured the alpha-HCH concentrations and EFs in soils in southern China that ranged from <DL to 3480 pg/g dw with a median of 800 pg/g (in crops), <DL to 2760 pg/g dw with a median of 780 pg/g dw (in rice paddies), <DL to 1460 pg/g dw with a median of 170 pg/g dw (in uncultivated soils) [13]. The rice paddy soils had racemic alpha-HCH signatures, while the crop and uncultivated soils had non-racemic alpha-HCH signatures indicating preferential degradation of the (-) enantiomer (EFs > 0.5) [13].

Technical HCH is composed of many isomers, including alpha-HCH, and was banned in China in 1983, in Korea in 1979, and in Japan in 1971. [11] The composition of technical HCH includes 60-70% alpha-HCH and 10-12% gamma-HCH [14]. Although technical HCH has been banned in most Asian countries, gamma-HCH (lindane) is still registered for use [15]. Technical HCH has an alpha/gamma ratio from 4 to 10 and this ratio can be used to identify HCH sources [16]. The HSO air masses had an average alpha/gamma ratio of 2.3 ± 0.3 when the source region was identified as China [6]. When the air mass was from the Japan/Korea/Russia source region, the alpha/gamma HCH ratio was as high as 5.9 [6]. Previous studies in urban and rural areas

of China measured alpha/gamma HCH ratios between 1.6 and 2.9 in air, indicating current-use of lindane [15]. Ratios measured in urban air in Japan and Korea ranged from 3.5 to 6, indicating past use of technical HCH [15]. Racemic alpha-HCH was measured in all HSO air masses and in all Chinese and South Korean soil samples above the EF detection limit. This suggests that the primary source of alpha-HCH in Asian air masses is due to relatively fresh sources of alpha-HCH and/or limited biotransformation of alpha-HCH since it was discontinued for use in Asia.

Pacific Northwestern United States

Because of their respective elevations, but relatively close proximity to each other, the three air sampling locations in the U.S.; CPO at 500m, MPO at 1249m, and MBO at 2300m, are influenced by boundary layer and free troposheric air masses to varying degrees. Figure 3.2 shows a significant negative correlation (p-value = 0.0017) between the percentage of time the 10-day air mass back trajectories spent above the boundary layer (>1000m) and the alpha-HCH EFs measured in the air masses at CPO, MPO, and MBO. This suggests that, in the Pacific Northwestern U.S., non-racemic alpha-HCH is present in the boundary layer, while racemic alpha-HCH is present in the troposphere. A previous study suggested that the racemic alpha-HCH in rain collected over Lake Ontario was due to racemic alpha-HCH scavenged from air masses above the boundary layer prior to equilibration with the non-racemic alpha-HCH measured in air masses below the boundary over the lake [17].

Each of the air masses sampled at CPO, MPO, and MBO were previously characterized for the relative influence of regional and trans-Pacific source regions for the transport of ~83 semi-volatile organic compounds (SOCs), including polycyclic aromatic

hydrocarbons (PAHs), current and historical use pesticides, and polychlorinated biphenyls (PCBs) [4-7]. The concentration of alpha-HCH ranged from <DL to 29.8 pg/m^3 at CPO, 3.84 pg/m^3 to 53.1 pg/m^3 at MPO, and 2.03 pg/m^3 to 42.7 pg/m^3 at MBO. Representative alpha-HCH EFs and 10-day air mass back trajectories for regional and trans-Pacific air masses are given in Figure 3.3 for CPO, MPO, and MBO. Trans-Pacific air masses typically spent higher percentages of time above the boundary layer than regional air masses (Table 3.2) [7]. Racemic alpha-HCH was measured in trans-Pacific air masses at MPO and MBO (Table 3.2). At CPO (the lowest elevation site), the trans-Pacific air masses contained non-racemic alpha-HCH (0.513 ± 0.0027) (Table 3.2). However, this EF was significantly lower (p-value < 0.001) than the alpha-HCH EF in regional air masses at CPO (0.528 ± 0.0048). Because the CPO trans-Pacific air masses spent larger percentages of time above the boundary layer and had a lower EF than regional CPO air masses, this is consistent with our conclusion that the free troposphere may be a significant source of racemic alpha- HCH.

A principal component analysis (PCA) biplot was created using the SRIFs for the Pacific Northwestern U.S. air masses (CPO, MPO, and MBO) and the alpha-HCH measured in each air mass was labeled as racemic or non-racemic (Figure 3.4). These first two components retained 97.5% of the original variation. Based on all of the CPO, MPO, and MBO data, when the air mass SRIFs indicated a strong source contribution from Siberia and Asia, often during trans-Pacific transport, the alpha-HCH was racemic. This provides additional support for our conclusion that the alpha-HCH in Asian air masses is due to relatively fresh sources of alpha-HCH and/or limited biotransformation of alpha-HCH since it was discontinued for use in Asia.

All CPO air masses contained non-racemic alpha-HCH with selective degradation of the (-) enantiomer at this low elevation, marine site. A previous study measured non-racemic signatures of alpha-HCH, with selective degradation of the (-) enantiomer, in air at low elevation, marine sites on the West coast of Canada in British Columbia [18]. The Canadian sites were far from agricultural source regions and the authors suggested that the sources of non-racemic alpha-HCH to these sites were volatilization of non-racemic alpha-HCH from the Pacific Ocean and/or trans-Pacific transport [18]. However, our data suggests that trans-Pacific air masses contain racemic alpha-HCH.

At CPO, the Clausius Clapeyron equation indicated a significant correlation (r^2= 0.81, p-value = 0.0004) between the concentration of ln (alpha-HCH) and inverse site temperature, indicating that volatilization from a local source influenced alpha-HCH concentrations in air. The CPO air sampler was located ~3 m above ground level in an open clearing and a composite soil sample was taken nearby and in a nearby forest. The CPO soil alpha-HCH EF in the clearing was non-racemic (0.544), and the alpha-HCH concentration in the forest soil was below the chiral detection limit (Table 3.1). A previous study measured the alpha-HCH EF in soils and in air at four different heights (5, 35, 75, and 140 cm) above the soil in the Fraser Valley, British Columbia [19]. Both the air (EF at 5 cm height above soil = 0.574) and soil (EF = 0.579) samples were preferentially depleted in the (-) enantiomer [19]. However, at greater heights above the soil (75 and 140 cm) the air EFs decreased (EF = 0.552 and 0.543, respectively) [19].

The alpha-HCH EF of the Pacific Ocean is not well characterized. Previous studies have measured the alpha-HCH EFs in the Bering, Chukchi, and Greenland Seas [20]. Because the Pacific Ocean flows into the Bering and Chukchi Seas, the Pacific

Ocean and the Bering and Chukchi Seas likely have similar alpha-HCH EFs [18]. The average alpha-HCH EF of the Bering and Chukchi Seas was non-racemic (0.521 ± 0.0058) and similar to the average alpha-HCH EF measured in CPO air masses (0.525 ± 0.007) [20]. This suggests that the Pacific Ocean likely has a non-racemic alpha-HCH signature and that sources of alpha-HCH to CPO likely include volatilization of non-racemic alpha-HCH from the Pacific Ocean.

In two CPO air masses (June 2, 2003 and August 4, 2003), the alpha-HCH EF was significantly lower than the CPO average (p-value < 0.001). These two air masses have been previously identified as being influenced by trans-Pacific transport from Siberian biomass burning emissions [7]. Trans-Pacific transport usually involves mid-latitude cyclones exporting Asian boundary layer air into the free troposphere [21]. During these two trans-Pacific events at CPO, the observed decrease in the alpha-HCH EF may be due to greater influence of racemic alpha-HCH from the free troposphere and the Asian boundary layer

4 of 10 MPO air masses had racemic alpha-HCH signatures, while 6 of 10 MPO air masses had non-racemic alpha-HCH signatures that were depleted in the (-) enantiomer (Table 3.2). During the concurrent sampling at CPO and MPO of trans-Pacific air masses (June 2 and August 4, 2003), alpha-HCH was racemic at both sites. In addition, the Clausius Clapeyron equation indicated no significant correlation between alpha-HCH concentration and inverse temperature at MPO. This suggests that the alpha-HCH measured at MPO was likely due to long-range transport and not local volatilization. The alpha-HCH EF could not be measured in the MPO composite soil sample because the concentration was below the chiral detection limit (Table 3.1).

16 of 20 MBO air masses had racemic alpha-HCH signatures (Table SI.2). However, 4 of 20 MBO air masses had non-racemic alpha-HCH signatures that were depleted in the (-) enantiomer (Table 3.2). The Clausius Clapeyron equation revealed a correlation between alpha-HCH concentration and inverse temperature ($r^2 = 0.42$, p-value = 0.003). MBO air mass back trajectories with a high percentage of air from the free troposphere (>80%) had racemic alpha-HCH signatures, suggesting that the free troposphere was a source of racemic alpha-HCH (Figure 3.2). Non-racemic alpha-HCH signatures in MBO air masses were only measured during the winter months (Table 3.2). Volatilization of non-racemic alpha-HCH from surrounding site soil during the winter is unlikely because of snow cover.

The ratio of alpha HCH/gamma HCH in MBO air masses has been previously used to distinguish between trans-Pacific and regional air masses (2.9 ± 0.3) and Pacific Ocean and Siberian air masses (5.2 ± 0.8). Out of the four MBO air masses with non-racemic signatures, three had alpha HCH/gamma HCH ratios of 5.3, 5.4, and 4.5, providing additional evidence that the Pacific Ocean is a likely source of these non-racemic signatures. Regional air masses at MBO typically had racemic signatures, and our data suggest that Asia and the free troposphere are sources of racemic alpha-HCH, while the Pacific Ocean is a source of non-racemic alpha-HCH to the Pacific Northwestern U.S.

Chiral Signatures of Chlordanes

Asia

Technical chlordane is composed of two major isomers (cis and trans), as well as other chlorine containing compounds [22]. Chlordane has been previously used in China

and Japan as an agricultural pesticide. This usage is now banned in Japan and China, but both countries currently hold exemptions for the use of chlordane as a termiticide [23]. Chlordane is also banned in all other countries in central and north east Asia, including South Korea [23].

Racemic cis and trans chlordane were measured in all of the air masses above the chiral detection limit at HSO (Table 3.2). The chlordane concentrations ranged from <DL to 5.40 pg/m^3 for cis chlordane and 0.448 pg/m^3 to 8.16 pg/m^3 for trans chlordane at HSO. The ratio of trans chlordane to cis chlordane (TC/CC) in HSO air masses (1.2 ± 0.3) did not vary based on source region influences and reflected the ratio (1 – 1.26) of the technical mixture [6]. The racemic chlordane signatures and TC/CC ratio suggest that Asian air masses are influenced by relatively fresh sources of chlordane and/or limited biotransformation of chlordane has occurred since it was it was discontinued for use in Asia.

The sum of chlordane concentrations ranged from 16.9 pg/g dw to 197 pg/g dw in the South Korean soil and < DL to 2.00 pg/g dw in the Chinese soil. Previous studies measured chlordane concentrations ranging from <DL to 1370 pg/g in crop, paddy, and uncultivated soils from the Pearl River Delta region of China [13]. Non-racemic signatures of cis and trans-chlordane were measured in all of the South Korean agricultural soils (Table 3.1); however, the chlordane concentrations in the Chinese agricultural soils were below the detection limit for chiral analysis. Trans-chlordane was typically depleted in the (+) enantiomer, while cis-chlordane was depleted in the (-) enantiomer in the Korean soil samples. The same enantioselectivity has been measured

in agricultural soils from Alabama, the Midwestern U.S., Connecticut, Hawaii, and the U.K. [2].

Pacific Northwestern United States

Chlordane was used as an agricultural pesticide and termiticide until 1983 in the U.S., and until 1988 for the control of subterranean termites [24]. The concentration of trans-chlordane ranged from <DL to 0.38 pg/m^3 at CPO, <DL to 2.45 pg/m^3 at MPO, and <DL to 4.94 pg/m^3 at MBO, while the concentrations of cis-chlordane were below the detection limit at CPO and MPO, and ranged from <DL to 3.31 pg/m^3 at MBO. The trans-chlordane EFs were above the chiral detection limit in 36% of the CPO, 69% of the MPO, and 57% of the MBO air masses sampled and for cis-chlordane 27% of the CPO, 31% of the MPO, and 33% of the MBO air masses sampled were above the chiral detection limit. Of the air masses with EFs above the detection limit, 50% at CPO, 89% at MPO, and 92% at MBO had racemic signatures for cis and trans-chlordane (Table 3.2). Unlike alpha-HCH, a significant correlation was not observed between the trans-chlordane or cis chlordane EF and the percentage of time the air mass spent above the boundary layer at CPO, MPO, and MBO (Figure 3.2). Although, like alpha-HCH, when the air mass spent > 80% of time above the boundary layer prior to being sampled, trans-chlordane was racemic, indicating the free troposphere may also be a source of trans-chlordane (Figure 3.2).

During trans-Pacific transport events to CPO, MPO, and MBO, the concentration of alpha-HCH was enhanced in these air masses, while trans and cis-chlordane were not enhanced at CPO and MPO, so the EFs of trans and cis-chlordane at these sites may not indicate the source of chlordane in these air masses. At MBO, during a strong trans-

Pacific event on April 25-26, 2004 enhanced racemic chlordane was observed, which indicates that trans-Pacific transport may also be a source of racemic chlordane to MBO.

The Clausius Clapeyron equation indicated that the chlordane concentrations at MBO were significantly correlated with inverse site temperature ($r^2 = 0.14$, p-value = 0.005) and only slightly correlated at MPO ($r^2 = 0.26$, p-value = 0.076). There were too few samples above the chiral detection limit at CPO to use the Clausius Clapeyron equation. Racemic cis and trans-chlordane have been measured in the Bering and Chukchi Seas [25]. This suggests that volatilization of racemic chlordane from the Pacific Ocean may be a source to these sites. Composite soil samples taken from agricultural soils in the Willamette Valley of Oregon and at MPO indicated non-racemic cis and trans-chlordane signatures (Table 3.2). However, urban air in South Carolina and Alabama and house foundation soils in Connecticut are dominated by racemic chlordanes [2].

At MBO, elevated cis and trans-chlordane concentrations were measured in air masses associated with urban California source regions (May 7-8, 12-13, 27-29, 2005 and Apr 4-6, 13-14, 2006). A PCA biplot of source region impact factors (SRIFs) indicated that air masses with high Asian influence also had racemic chlordane signatures (Figure 3.4). This suggests that U.S. urban areas and Asia are sources of racemic chlordanes to MBO.

Our findings suggest that Asian and U.S. air masses that pass over urban areas in the Western U.S. contain racemic chlordane due to volatilization from urban soils and/or limited biotransformation. Agricultural soils in South Korea, as well as the Western U.S., contain non-racemic chlordane signatures, with trans-chlordane depleted in the (+)

enantiomer and cis-chlordane depleted in the (-) enantiomer. Finally, the Pacific Ocean appears to have a racemic chlordane signature.

ACKNOWLEDEMENTS

This work was made possible by funding from the National Science Foundation CAREER (ATM-0239823), NSF EAPSI China 2006, and also the National Institutes of Health (P30ES00210). We would also like to thank Wang Xiaoping and his colleagues at the Guangzhou Institute of Geochemistry, Haibo Zhang and the Institute of Soil Science at the Chinese Academy of Science in Nanjing, and the students and staff, including Jen Krenz, Gao Dong, and Xie Hang at Yunnan Agricultural University in Kunming, China for their assistance with soil sampling in China.

LITERATURE CITED

1. Kurt-Karakus, P. B.; Bidleman, T. F.; Jones, K. C., Chiral organochlorine pesticide signatures in global background soils. *Environmental Science & Technology* **2005,** *39*, (22), 8671-8677.
2. Bidleman, T. F., Leone, A.D. Falconer, R.L., Harner, T., Jantunen, L.M., Wiberg, K., Helm, P.A., Diamond, M.L., Loo, B., Chiral Pesticides in Soil and Water and Exchange with the Atmosphere. *The Scientific World* **2002,** *2*, 357-373.
3. Bidleman, T. F.; Falconer, R. L., Using enantiomers to trace pesticide emissions. *Environmental Science & Technology* **1999,** *33*, (9), 206A-209A.
4. Primbs, T., Wilson, G., Schmedding, D., Higginbotham, C., Simonich, Staci Massey, Influence of Asian and Western United States Agricultural Areas and Fires on the Atmospheric Transport of Pesticides in the Western United States. *Environ. Sci. Technol.* **2008,** *Submitted and Accepted to ES&T, May 2008*.
5. Primbs, T.; Piekarz, A.; Wilson, G.; Schmedding, D.; Higginbotham, C.; Field, J.; Simonich, S. M., Influence of Asian and Western United States Urban Areas and Fires on the Atmospheric Transport of Polycyclic Aromatic Hydrocarbons, Polychlorinated Biphenyls, and Fluorotelomer Alcohols in the Western United States. *Environ. Sci. Technol.* **2008**.
6. Primbs, T.; Simonich, S.; Schmedding, D.; Wilson, G.; Jaffe, D.; Takami, A.; Kato, S.; Hatakeyama, S.; Kajii, Y., Atmospheric Outflow of Anthropogenic Semivolatile Organic Compounds from East Asia in Spring 2004. *Environ. Sci. Technol.* **2007,** *41*, (10), 3551-3558.
7. Genualdi, S.; Primbs, T.; Killin, R.; Woods, J.; Wilson, G.; Schmedding, D.; Simonich, S., Trans-Pacific and Regional U.S. Atmospheric Transport of PAHs and Pesticides in Biomass Burning Emissions *Submitted to ES&T* **2008**.

8. Harner, T.; Shoeib, M.; Kozma, M.; Gobas, F. A. P. C.; Li, S. M., Hexachlorocyclohexanes and endosulfans in urban, rural, and high altitude air samples in the Fraser Valley, British Columbia: Evidence for trans-Pacific transport. *Environmental Science & Technology* **2005,** *39*, (3), 724-731.
9. Killin, R. K.; Simonich, S. L.; Jaffe, D. A.; DeForest, C. L.; Wilson, G. R., Transpacific and regional atmospheric transport of anthropogenic semivolatile organic compounds to Cheeka Peak Observatory during the spring of 2002. *Journal of Geophysical Research-Atmospheres* **2004,** *109*, (D23).
10. Primbs, T.; Genualdi, S.; Simonich, S., Solvent Selection for Pressurized Liquid Extraction of Polymeric Sorbents Used in Air Sampling. *Environmental Toxicology and Chemistry* **2008,** *27*, (2008), 1267-1272.
11. Li, Y. F.; Cai, D. J.; Singh, A., Technical hexachlorocyclohexane use trends in China and their impact on the environment. *Archives of Environmental Contamination and Toxicology* **1998,** *35*, (4), 688-697.
12. Li, Y. F., Global technical hexachlorocyclohexane usage and its contamination consequences in the environment: from 1948 to 1997. *Science of the Total Environment* **1999,** *232*, (3), 121-158.
13. Li, J.; Zhang, G.; Qi, S. H.; Li, X. D.; Peng, X. Z., Concentrations, enantiomeric compositions, and sources of HCH, DDT and chlordane in soils from the Pearl River Delta, South China. *Science of the Total Environment* **2006,** *372*, (1), 215-224.
14. Willett, K. L.; Ulrich, E. M.; Hites, R. A., Differential Toxicity and Environmental Fates of Hexachlorocyclohexane Isomers. *Environ. Sci. Technol.* **1998,** *32*, (15), 2197-2207.
15. Lammel, G.; Ghim, Y. S.; Grados, A.; Gao, H. W.; Huhnerfuss, H.; Lohmann, R., Levels of persistent organic pollutants in air in China and over the Yellow Sea. *Atmospheric Environment* **2007,** *41*, (3), 452-464.
16. *Regionally Based Assessment of Persistent Toxic Substances*; Global Environmental Facility: December 2002, 2002.
17. Ridal, J. J.; Bidleman, T. F.; Kerman, B. R.; Fox, M. E.; Strachan, W. M. J., Enantiomers of alpha-hexachlorocyclohexane as tracers of air-water gas exchange in Lake Ontario. *Environmental Science & Technology* **1997,** *31*, (7), 1940-1945.
18. Shen, L.; Wania, F.; Lei, Y. D.; Teixeira, C.; Muir, D. C. G.; Bidleman, T. F., Hexachlorocyclohexanes in the north American atmosphere. *Environmental Science & Technology* **2004,** *38*, (4), 965-975.
19. Finizio, A.; Bidleman, T. F.; Szeto, S. Y., Emission of chiral pesticides from an agricultural soil in the Fraser Valley, British Columbia. *Chemosphere* **1998,** *36*, (2), 345-355.
20. Jantunen, L. M.; Bidleman, T., Air-water gas exchange of hexachlorocyclohexanes (HCHs) and the enantiomers of alpha-HCH in arctic regions. *Journal of Geophysical Research-Atmospheres* **1996,** *101*, (D22), 28837-28846.
21. Liang, Q.; Jaegle, L.; Wallace, J. M., Meteorological indices for Asian outflow and transpacific transport on daily to interannual timescales. *Journal of Geophysical Research-Atmospheres* **2005,** *110*, (D18), -.
22. Dearth, M. A.; Hites, R. A., Complete Analysis of Technical Chlordane Using Negative Ionization Mass-Spectrometry. *Environmental Science & Technology* **1991,** *25*, (2), 245-254.

23. *Regionally Based Assessment of Persistent Toxic Substances*; Global Environmental Facility: 2002 http://www.chem.unep.ch/pts/regreports/C&NE%20Asia%20full%20report.pdf.
24. Leone, A. D.; Ulrich, E. M.; Bodnar, C. E.; Falconer, R. L.; Hites, R. A., Organochlorine pesticide concentrations and enantiomer fractions for chlordane in indoor air from the US cornbelt. *Atmospheric Environment* **2000,** *34*, (24), 4131-4138.
25. Jantunen, L. M. M.; Bidleman, T. F., Organochlorine pesticides and enantiomers of chiral pesticides in Arctic Ocean water. *Archives of Environmental Contamination and Toxicology* **1998,** *35*, (2), 218-228.
26. Bidleman, T. F.; Wong, F.; Backe, C.; Sodergren, A.; Brorstrom-Lunden, E.; Helm, P. A.; Stern, G. A., Chiral signatures of chlordanes indicate changing sources to the atmosphere over the past 30 years. *Atmospheric Environment* **2004,** *38*, (35), 5963-5970.
27. Gouin, T.; Jantunen, L.; Harner, T.; Blanchard, P.; Bidleman, T., Spatial and temporal trends of chiral organochlorine signatures in great lakes air using passive air samplers. *Environmental Science & Technology* **2007,** *41*, (11), 3877-3883.

Figure 3.1. Map of air and soil sampling locations in Asia and the Pacific Northwestern United States

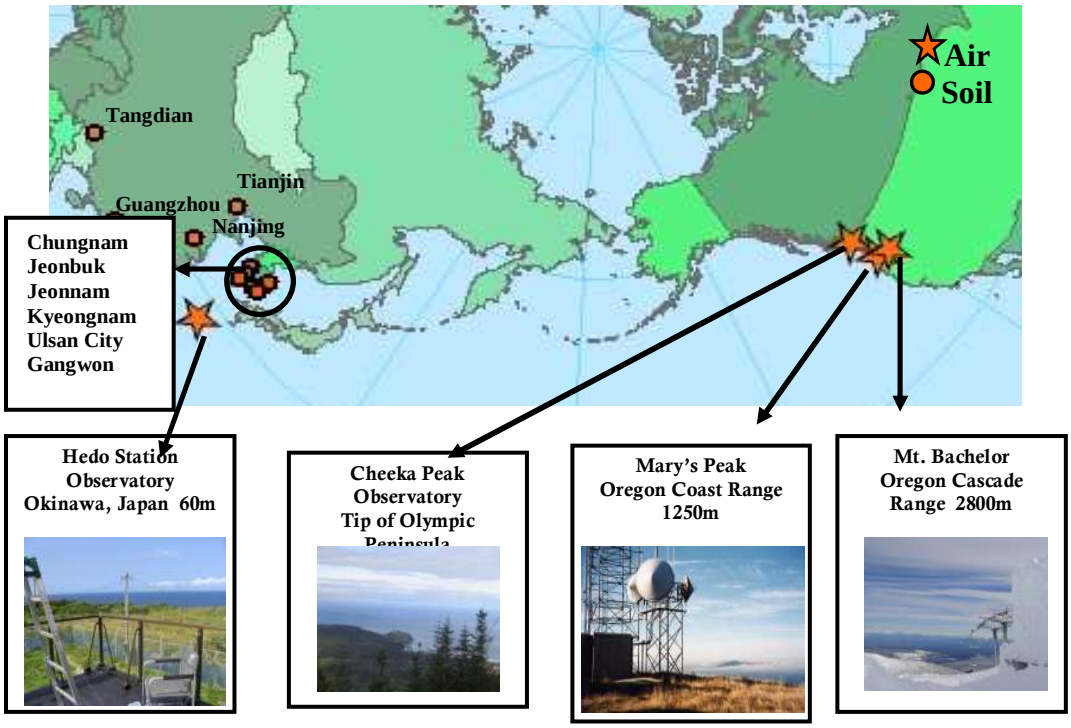

Figure 3.2. A) Alpha-HCH B) trans-chlordane and C) cis chlordane. EFs versus percentage of time air mass back trajectories spent above the boundary layer. The shaded regions represent the racemic range for alpha-HCH, trans-chlordane, and cis-chlordane.

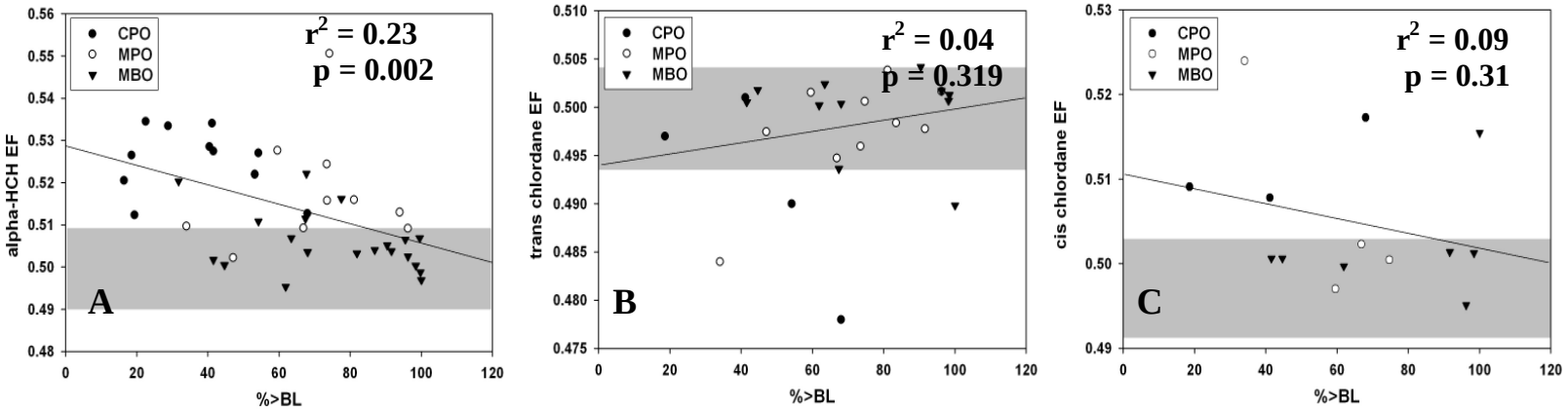

Figure 3.3. Representative alpha-HCH EFs and 10 day air mass back trajectories for regional and trans-Pacific air masses at CPO, MPO, and MBO

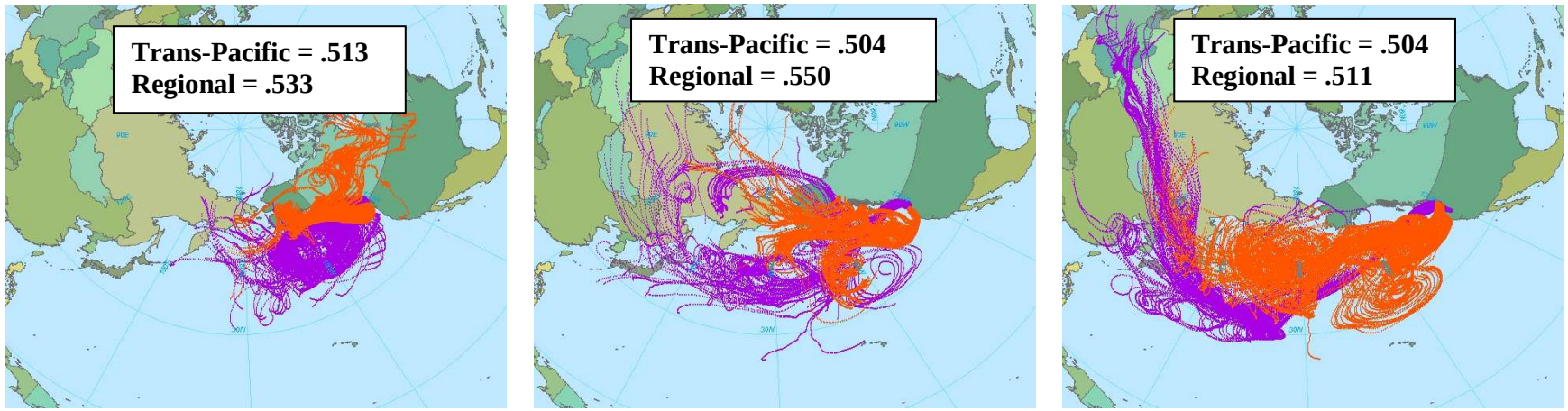

Figure 3.4. Principal Component Analysis (PCA) biplot of SRIFs for air masses sampled at CPO, MPO, and MBO. Numbers correspond to sample numbers in Table SI.2. The "NR" indicates non-racemic and "R" indicates racemic signatures for A. alpha-HCH and B. trans chlordane were measured in this air mass.

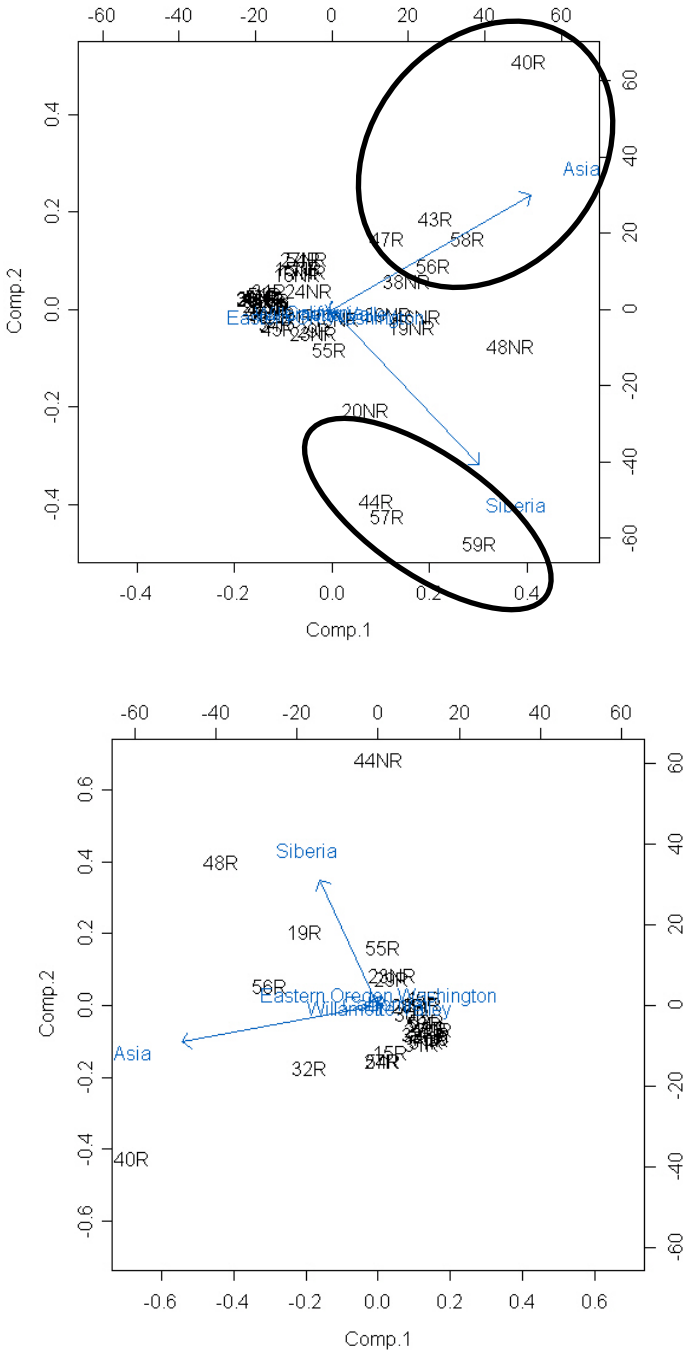

Table 3.1. Alpha-HCH and cis and trans-chlordane enantiomer fractions (EFs) in soil from sampling sites in China, South Korea, CPO, MPO, and the Willamette Valley, Oregon. Composite samples for each site were collected at the latitude, longitude, and elevation given. The mean EF and 95% confidence interval of the racemic standards are given below the name of the OCP.

	Sampling Site	*Latitude*	*Longitude*	*Elevation (m)*	*α-HCH 0.499 ±0.0095*	*trans chlordane 0.499 ±0.0052*	*cis chlordane 0.497 ±0.0059*
1	***Tangdian, China***	23.33 ^{o}N	103.09 ^{o}E	1136	0.500	<DL	<DL
2	***Tangdian, China***				0.499	<DL	<DL
3	***Tangdian, China***				0.5	<DL	<DL
4	***Tangdian, China***				<DL	<DL	<DL
5	***Tangdian, China***				<DL	<DL	<DL
6	***Nanjing, China***	31.83 ^{o}N	118.8^{o}E	13	0.498	<DL	<DL
7	***Nanjing, China***				0.502	<DL	<DL
8	***Nanjing, China***				<DL	<DL	<DL
9	***Nanjing, China***				<DL	<DL	<DL
10	***Nanjing, China***				0.497	<DL	<DL
11	***Guangzhou, China***	23.28 ^{o}N	113.34 ^{o}E	24	0.506	<DL	<DL
12	***Guangzhou, China***				0.497	<DL	<DL
13	***Guangzhou, China***				<DL	<DL	<DL
14	***Guangzhou, China***				<DL	<DL	<DL
15	***Guangzhou, China***				<DL	<DL	<DL
16	***Tianjin, China***	39.08 ^{o}N	117.12 ^{o}E	NA	0.497	<DL	<DL
17	***Tianjin, China***				0.507	<DL	<DL

18	***Tianjin, China***				<DL	<DL	<DL
19	***Tianjin, China***				<DL	<DL	<DL
20	***Tianjin, China***				<DL	<DL	<DL
21	***Kyeongbuk*** *Yeongdeok Ganggu-myeon Sowol-ri*	36.21°N	129.22 °E	7	<DL	<DL	<DL
22	***Kyeongbuk*** *Yeongdeok Ganggu-myeon Samsa-ri*				<DL	0.480	<DL
23	***Kyeongbuk*** *Yeongdeok Ganggu-myeon Namho-ri*				<DL	0.382	0.588
24	***Gangwon*** *Samchok Geundeok-myeon Chogok-ri*	37.18 °N	129.17 °E	8	<DL	0.490	<DL
25	***Gangwon*** *Samchok Jeongla-dong*				<DL	0.499	<DL
26	***Gangwon*** *Samchok Gyo-dong*				<DL	<DL	<DL
27	***Chungnam*** *Taean Sonwon-myeon Manlipobeach*	36.47 °N	126.08 °E	18	<DL	<DL	<DL
28	***Chungnam*** *Taean So-myeon Uihang-ri*				0.505	0.356	0.567
29	***Chungnam*** *Taean Cheonlipobeach*				<DL	0.489	<DL
30	***Jeonbuk*** *Buan Haseo-myeon Nakwonsusan*	35.42 °N	126.35 °E	6	<DL	<DL	<DL
31	***Jeonbuk*** *Buan Haseo-myeon*				<DL	0.465	<DL
32	***Jeonbuk*** *Buan Jinseo-myeon*				<DL	<DL	<DL
33	***Jeonnam*** *Wando Wando-eup Jukcheong-ri*	34.22 °N	126.43 °E	4	<DL	0.551	0.532
34	***Jeonnam*** *Wando Wando-eup Gunoe-myeon*				<DL	<DL	<DL
35	***Jeonnam*** *Wando Gunoe-myeon Namseon-ri*				<DL	<DL	<DL
36	***Kyeongnam*** *Jinhae Pungho-dong*	35.05 °N	128.43 °E	6	0.508	0.404	0.547
37	***Kyeongnam*** *Jinhae Ungcheon-dong*				<DL	0.498	<DL
38	***Kyeongnam*** *Jinhae Ungcheon-dong Jinhae*				<DL	0.474	0.507
39	***Ulsan City*** *Donggu Bangeo-dong*	35.28 °N	129.25 °E	6	0.503	0.434	0.540
40	***Ulsan City*** *Donggu Hajeong-dong*				0.504	0.358	<DL
41	***Ulsan City*** *Bukgu Youngpo-dong*				<DL	0.472	<DL
42	***Cheeka Peak tower soil***	48.3 °N	124.6 °W	500	0.544	<DL	<DL
43	***Cheeka Peak forest background soil***	48.3 °N	124.6 °W	500	<DL	<DL	<DL
44	***Mary's Peak tower soil***	44.5 °N	123.6 °W	1249	<DL	0.597	0.434
45	***HYSLOP Wheat soil***	44.38 °N	123.12 °W	76	<DL	0.398	0.579
46	***HYSLOP Wheat soil***	44.38 °N	123.12 °W	76	<DL	0.377	0.574

Table 3.2. Alpha-HCH and cis and trans-chlordane enantiomer fractions (EFs) in air masses sampled from Okinawa, Japan (HSO), Cheeka Peak Observatory (CPO), Mary's Peak Observatory (MPO), and Mt. Bachelor Observatory (MBO). Source region impact factors (SRIFs) and %<BL and %>BL have been previously reported [2, 3]. <DL refers to concentrations with a signal/noise ratio less than 3:1. The mean EF and 95% confidence interval of the racemic standards are given below the name of the OCP.

	Sampling Site	*Sampling dates*	*α-HCH 0.499 ±0.0095*	*trans chlordane 0.499 ±0.0052*	*cis chlordane 0.497 ±0.0059*
1	***HSO***	Mar 25-26, 2004	<DL	0.497	<DL
2	***HSO***	Mar 29-30, 2004	<DL	0.499	0.503
3	***HSO***	Mar 30-31, 2004	0.503	0.501	0.495
4	***HSO***	Apr 2-3, 2004	0.499	0.499	0.498
5	***HSO***	Apr 3-4, 2004	0.502	<DL	0.501
6	***HSO***	Apr 4-5, 2004	0.495	0.496	<DL
7	***HSO***	Apr 12-13, 2004	<DL	0.496	0.507
8	***HSO***	Apr 20-21, 2004	<DL	0.497	0.504
9	***HSO***	Apr 24-25, 2004	<DL	0.502	0.501
10	***HSO***	Apr 25-26, 2004	<DL	0.502	0.497
11	***HSO***	Apr 27-28, 2004	0.504	0.502	0.510
12	***HSO***	Apr 28-29, 2004	0.508	0.500	<DL
13	***HSO***	Apr 29-30, 2004	<DL	0.502	<DL
14	***HSO***	May 1-2, 2004	<DL	0.501	0.505

	Sampling Site	Sampling dates	α-HCH 0.499 ±0.0095	trans chlordane 0.499 ±0.0052	cis chlordane 0.497 ±0.0059	% < BL	%>BL	Willamette Valley	California	Eastern OR/WA	Siberia	Asia
15	**CPO**	Jan 28-30, 2003	0.534	0.501	0.508	58.8	41.2	0.79	0.00	0.00	0.57	7.23
16	**CPO**	Mar 1-3, 2003	0.529	<DL	<DL	59.5	40.5	0.00	0.00	0.00	1.03	6.66
17	**CPO**	Mar 13-15, 2003	0.534	<DL	<DL	77.4	22.6	0.22	0.14	0.00	1.46	7.68
18	**CPO**	Mar 24-26, 2003	0.522	<DL	<DL	46.8	53.2	0.35	0.00	0.00	9.59	8.51
19	**CPO**	Apr 11-13, 2003	0.527	0.497	0.509	81.4	18.6	0.74	0.00	1.51	17.8	17.9
20	**CPO**	Apr 21-23, 2003	0.527	<DL	<DL	58.4	41.6	1.12	0.00	0.00	22.1	5.41
21	**CPO**	May 2-4, 2003	0.533	<DL	<DL	71.2	28.8	0.00	0.17	0.00	0.00	0.00
22	**CPO**	Jun 2-4, 2003	0.513	0.478	0.517	32.0	68.0	0.00	0.00	0.00	1.20	0.16
23	**CPO**	Jun 16-18, 2003	0.527	0.490	<DL	45.8	54.2	0.00	0.00	0.00	8.85	4.38
24	**CPO**	July 7-9, 2003	0.521	<DL	<DL	83.5	16.5	0.02	0.00	0.00	3.93	6.93
25	**CPO**	Aug 4-6, 2003	0.512	<DL	<DL	80.6	19.4	0.00	0.00	0.00	1.71	0.00
26	**MPO**	May 11-13, 2003	0.516	0.504	<DL	18.9	81.1	7.14	0.00	3.97	0.00	0.00
27	**MPO**	May 26-28, 2003	0.516	0.496	<DL	26.5	73.5	0.49	0.00	0.00	0.14	8.92
28	**MPO**	May 30 - June 1, 2003	0.528	0.502	0.497	40.5	59.5	1.78	0.00	0.00	4.81	2.83
29	**MPO**	Jun 2-4, 2003	0.509	0.502	<DL	3.78	96.2	2.21	0.00	0.00	8.55	4.66
30	**MPO**	Jun 22-24, 2003	<DL	0.501	0.500	25.3	74.7	0.73	0.00	0.00	3.75	2.39
31	**MPO**	Jul 4-6, 2003	0.509	0.495	0.502	33.1	66.9	0.92	0.00	0.00	0.06	1.73
32	**MPO**	Jul 22-24, 2003	<DL	0.498	<DL	16.5	83.5	1.77	0.00	0.00	2.87	21.4
33	**MPO**	Aug 2-4, 2003	0.510	0.484	0.524	66.0	34.0	0.79	0.00	0.00	0.75	0.56
34	**MPO**	Aug 4-5, 2003	0.502	0.497	<DL	52.9	47.1	0.62	0.00	0.00	4.17	0.00
35	**MPO**	Aug 8-10, 2003	0.551	<DL	<DL	25.8	74.2	0.76	0.00	0.00	2.60	0.21
36	**MPO**	Aug 12-14, 2003	0.524	<DL	<DL	26.6	73.4	2.92	0.00	0.00	0.00	0.00
37	**MPO**	Sep 4-5, 2003	<DL	<DL	<DL	56.2	43.8	2.49	0.00	2.48	3.25	0.31
38	**MPO**	Sep 21-22, 2003	0.504	<DL	<DL	6.04	94.0	1.86	0.00	0.00	12.6	20.9

39	***MBO***	Apr 21-22, 2004	0.511	<DL	<DL	45.8	54.2	1.03	0.00	0.00	14.2	15.7
40	***MBO***	Apr 25-26, 2004	0.504	0.498	0.501	8.35	91.7	1.42	0.00	0.00	1.77	54.1
41	***MBO***	May 17-18, 2004	0.502	0.502	0.495	3.75	96.2	0.86	0.00	0.08	0.00	0.00
42	***MBO***	May 21-22, 2004	<DL	0.501	<DL	1.78	98.2	4.24	0.00	0.86	1.25	0.00
43	***MBO***	May 30-31, 2004	0.503	<DL	<DL	18.1	81.9	0.37	0.00	0.00	8.98	29.5
44	***MBO***	Jun 19-20, 2004	0.497	0.490	0.515	0.0	100	2.98	0.00	5.19	32.6	0.03
45	***MBO***	Jul 11-12, 2004	0.505	0.504	<DL	9.58	90.4	0.06	0.00	0.00	4.88	0.00
46	***MBO***	Dec 7-8, 2004	0.522	<DL	<DL	32.3	67.7	0.00	0.17	0.00	17.4	19.4
47	***MBO***	Dec 22-23, 2004	0.504	<DL	<DL	13.1	86.9	0.85	0.00	0.00	6.28	21.5
48	***MBO***	Jan 9-10, 2005	0.511	0.494	<DL	32.5	67.5	0.00	0.00	0.00	29.7	29.7
49	***MBO***	Feb 6-7, 2005	0.516	<DL	<DL	22.5	77.5	1.05	0.00	0.00	2.79	0.00
50	***MBO***	Feb 20-21, 2005	0.505	<DL	<DL	68.2	31.8	0.00	6.81	0.00	0.00	0.34
51	***MBO***	May 7-8, 2005	0.500	0.502	0.501	55.3	44.7	0.00	1.23	0.00	0.00	0.76
52	***MBO***	May 12-13, 2005	0.495	0.500	0.500	38.1	61.9	2.45	4.60	5.48	1.85	0.42
53	***MBO***	May 27-28, 2005	0.504	0.500	<DL	32.0	68.0	0.82	2.02	4.01	1.85	0.85
54	***MBO***	Aug 9-10, 2005	0.500	0.501	0.501	1.58	98.4	2.78	0.00	0.00	0.00	8.72
55	***MBO***	Apr 4-5, 2006	0.502	0.501	0.501	58.4	41.6	0.37	7.65	0.00	12.2	5.20
56	***MBO***	Apr 13-14, 2006	0.507	0.502	<DL	36.5	63.5	1.56	0.15	1.76	13.6	25.6
57	***MBO***	May 8-9, 2006	0.499	<DL	<DL	0.22	99.8	2.93	0.00	0.00	35.3	0.14
58	***MBO***	May 11-12, 2006	0.507	<DL	<DL	4.50	95.5	1.00	0.00	0.00	14.1	32.2
59	***MBO***	May 12-13, 2006	0.507	<DL	<DL	0.47	99.5	0.02	0.00	0.00	47.3	10.3

SUPPORTING INFORMATION

An aliquot of approximately 25 grams of soil was taken from each homogenized composite soil sample. The soil was ground with 150 grams of sodium sulfate and spiked with 15 uL of a 10 ng/uL solution containing 23 isotopically labeled SOCs [1]. SOCs were extracted using the Accelerated Solvent Extraction 300 (ASE®) (Dionex, Sunnyvale, CA, USA) with 2 cycles of 75:25 hexane:acetone. The ASE parameters during extraction were 1500psi, 100^{o}C, and a 50% flush of the cell volume. Samples were purified using 20 grams of silica (Varian, Palo Alto, CA) with 75:25 hexane:acetone as the elution solvent, concentrated to 300 uL using a stream of N_2 gas (Turbovap II, Caliper Life Sciences, Massachusetts), and spiked with 15 uL of a 10ng/uL solution containing 4 isotopically labeled SOCs [1]. Samples were analyzed using an Agilent 6890 GC interfaced with an Agilent 5973N mass selective detector (GC/MS). A DB-5ms column (30m, 0.25mm id., 0.25um film thickness, J&W Scientific, USA) was used with an oven temperature program that varied based on the ionization mode of the mass selective detector [1]. Details on the GC temperature programs for both electron capture negative ionization (ECNI) and electron impact ionization (EI), as well as the ions monitored, have been previously reported [1]. The mode of ionization chosen for each SOC was based on which ionization technique gave the lowest detection limit [1]. SOC recoveries for this method ranged from 21% to 115%, and the concentrations of the chiral compounds were below the detection limit in the method blank. All concentrations are reported in pg/g dry weight of soil. Aliquots of each soil sample were weighed in aluminum boats and then dried in an oven for 24 hours at a temperature of 205^{o}C. After

24 hours, the samples were re-weighed and a ratio to convert from wet weight to dry weight was calculated.

1. Usenko, S.; Hageman, K. J.; Schmedding, D. W.; Wilson, G. R.; Simonich, S. L., Trace analysis of semivolatile organic compounds in large volume samples of snow, lake water, and groundwater. *Environmental Science & Technology* **2005,** *39*, (16), 6006-6015.
2. Genualdi, S.; Primbs, T.; Killin, R.; Woods, J.; Wilson, G.; Schmedding, D.; Simonich, S., Trans-Pacific and Regional U.S. Atmospheric Transport of PAHs and Pesticides in Biomass Burning Emissions *Submitted to ES&T* **2008**.
3. Primbs, T., Wilson, G., Schmedding, D., Higginbotham, C., Simonich, Staci Massey, Influence of Asian and Western United States Agricultural Areas and Fires on the Atmospheric Transport of Pesticides in the Western United States. *Environ. Sci. Technol.* **2008,** ASAP on line.

CHAPTER 4. SOURCES AND FATE OF CHIRAL ORGANOCHLORINE PESTICIDES IN WESTERN U.S. NATIONAL PARK ECOSYSTEMS

Susan A. Genualdi[1], Kimberly Hageman[2], Luke Ackerman[3], Sascha Usenko[4] Staci L. Massey Simonich[1,5*],

[1]Department of Chemistry, Oregon State University, Corvallis, Oregon
[2] Department of Chemistry, University of Otago, Dunedin, New Zealand
[3] FDA Center for Food Safety & Applied Nutrition, College Park, MD
[4] Department of Environmental Science, Baylor University, Waco, Texas
[5]Department of Environmental and Molecular Toxicology, Oregon State University, Corvallis, Oregon
* Corresponding Author, staci.simonich@orst.edu, v: (541)737-9194, f: (541)737-0497

ABSTRACT

The enantiomer fractions (EFs) of chiral organochlorine pesticides (OCPs) were measured in snow, sediment, and trout samples collected from high elevation and high latitude lake catchments in seven western U.S. national parks in order to investigate the sources and fate of these compounds in the ecosystems. The non-racemic alpha-HCH signatures measured in seasonal snow pack from continental U.S. national parks (Sequoia, Rocky Mountain, Mount Rainier, Glacier) were significantly different from the racemic alpha-HCH signatures measured in seasonal snow pack from the Arctic parks (Noatak and Gates of the Arctic), confirming the influence of regional agricultural sources (non-racemic) and long-range transport (racemic) sources to these sites. The alpha-HCH EFs measured in trout collected from Pear Lake in Sequoia, Matcharak Lake in Gates of the Arctic (Matcharak lake), and Burial Lake in Noatak were similar to the alpha-HCH EFs measured in seasonal snow pack collected from the same lake catchments. This indicates that these fish did not biotransform alpha-HCH enantioselectively. Racemic cis-chlordane was measured in seasonal snow pack in Sequoia because of its past use as a termiticide in the surrounding urban areas, while non-racemic cis-chlordane was measured in seasonal snow pack in Rocky Mountain because of its past use on regional agricultural soils. Racemic cis-chlordane was measured in the sediment of Sequoia and Mount Rainier, the two lake catchments with the highest population density within 300 km of the park, and was non-racemic at Rocky Mountain reflecting the signature measured in snow. The fish from all lake catchments showed preferential degradation of the (+) enantiomer of cis-chlordane and preferential biotransformation of the (-) enantiomer of trans-chlordane.

INTRODUCTION

Organochlorine pesticides (OCPs) are persistent in the environment and have been shown to undergo long range atmospheric transport and accumulation in remote high elevation and high latitude ecosystems [1-4]. Identifying the sources of OCPs to these sensitive ecosystems is of interest because many OCPs are toxic and have the potential to bioaccumulate in food webs.

A major objective of the Western Airborne Contaminants Assessment Project (WACAP) was to determine the sources of semi-volatile organic contaminants to high elevation and high latitude ecosystems in Western U.S. national parks [3]. OCPs have been measured in seasonal snow pack, lake water, sediment, vegetation and fish from these ecosystems [1-4]. Snow is a major route of OCP deposition to these ecosystems because it is an effective scavenger of both gas and particulate phase OCPs from the atmosphere [2]. The melting of the seasonal snowpack results in the release of OCPs to the aquatic ecosystem and is a major source of OCPs to the lake sediment and fish.

The enantiomer fractions (EFs) of chiral OCPs have been used to identify the sources and biotransformation of these contaminants in food webs [5-7]. Chiral pesticides are composed of two enantiomers and are manufactured in racemic form. The enantiomers have the same physiochemical properties and are affected by abiotic processes in the same way [8]. However, biotic processes, involving enzymatic activity, may result in the preferential degradation of one enantiomer over the other [8]. As a result, recent use or non-enantioselective biodegradation or biotransformation will result in a racemic signature, while enantioselective biodegradation or biotransformation will result in a non-racemic signature.

The objectives of this research were to identify sources and assess the pathway of chiral OCPs in high elevation and high latitude ecosystems in Western U.S. national parks with respect to the EFs of source regions and enantioselective biotransformation in fish.

EXPERIMENTAL

Sampling sites

Seasonal snowpack, sediment cores, and fish: brook trout (*Salvelinus fontinalis*) and lake trout (*Salvelinus namaycush*), and on occasion cutthroat trout (*Oncorhynchus clarki*) and rainbow trout (*Oncorhynchus mykiss*) were collected from Emerald and Pear Lake catchments in Sequoia National Park (SEKI), Lone Pine and Mills Lake catchments in Rocky Mountain National Park (ROMO), LP19 and Golden Lake catchments in Mount Rainier National Park (MORA), Oldman and Snyder Lake catchments in Glacier National Park (GLAC), Wonder Lake catchment in Denali National Park (DENA), Burial Lake catchment in Noatak National Preserve (NOAT), and Matcharak Lake catchment in Gates of the Arctic National Park and Preserve (GAAR) between 2003 and 2005 as part of the US National Park Service's Western Airborne Contaminants Assessment Project (WACAP) (Figure 4.1) [1-4]. Seasonal snow pack samples were collected from 1-3 sites at each park at the end of the snow accumulation season in 2003, 2004, and 2005 [2]. Sediment cores were collected from the deepest point in each lake, sectioned, and dated using ^{210}Pb and ^{137}Cs [4] and ten fish per lake were collected and analyzed [1]. Site and sampling procedure details have been previously reported [1-4].

Analysis of Chiral OCPs

The analytical methods for the extraction, cleanup, and instrumental analysis of semi-volatile organic compounds (SOCs) in snow, sediment, and fish were previously reported along with the chemicals, standards, and solvents used [1-4, 9]. The concentrations of SOCs in each of these matrices was determined using isotope dilution gas chromatography-mass spectrometry (GC-MS) and are reported elsewhere [1-4].

Chiral analysis the OCPs was performed using GC-MS with electron capture negative ionization and a 30m DB-5 column in tangent with a 15m BGB Analytik chiral column. Details on the GC temperature program, instrumental parameters, and ions monitored have been reported elsewhere [10]. This column can separate the enantiomers of alpha, HCH, oxychlordane, trans chlordane, cis chlordane, heptachlor epoxide and o,p, DDT. All of these chiral OCPs could be measured above the chiral detection limit except o,p, DDT. Pure enantiomer standards were used to determine the elution order of alpha-HCH and cis and trans-chlordane (Dr. Ehrenstorfer, D-86199 Augsburg, Germany). However, pure enantiomer standards were not available for heptachlor epoxide and oxychlordane.

The enantiomer fractions (EFs) of the chiral OCPs were calculated using the following formula: Area (+)/(Area (+) + Area (-)); where Area (+) and Area (-) correspond to the peak areas of the (+) and (-) enantiomers, respectively. For heptachlor epoxide and oxychlordane, the elution order of the enantiomers could not be determined and EFs were calculated using the following formula: Area (1)/(Area (1) + Area (2)); where Area (1) and Area (2) correspond to the peak areas of the first and second eluting enantiomers, respectively. An EF of 0.5 indicates a racemic mixture.

Manual peak integration was performed using macro smoothed chromatograms in MSD ChemStation (G1701DA). The racemic ranges of the chiral OCPs were calculated from seven replicate injections of the racemic standard (25 pg/uL). The 95% confidence intervals for the racemic ranges were 0.499 ± 0.0095 for alpha-HCH, 0.499 ± 0.0052 for trans-chlordane, and 0.497 ± 0.0059 for cis-chlordane. The EFs were reported to 3 decimal places because the racemic standards had a precision of four decimal places. Ion ratios were monitored in each sample to ensure there were no matrix interferences and the ratios were required to be within 20% of the ratios of the standards. Ion ratios in the sediment extracts and some of the fish extracts indicated a matrix interference with the (+) enantiomer of trans-chlordane. This limited trans-chlordane interpretation to seasonal snow pack.

Because of the relatively low OCP concentrations and significant matrix interferences in these samples, the samples with the highest chiral OCP concentrations within a park were analyzed first. If the concentrations in these samples were above the chiral detection limit then additional samples of that matrix from the park were analyzed. The detection limit for chiral analysis was a signal to noise ratio of 3:1 [11] and was approximately 0.05 ng/L for alpha-HCH in snow and, 0.01 ng/L in snow, 0.07 ng/g in sediment, and 0.09 ng/g in fish for trans-chlordane and 0.02ng/g in fish for cis-chlordane. The EFs of cis-chlordane were also measured in snow and sediment; however, a chiral detection limit could not be determined because the concentrations were below the detection limit for SOC analysis. All lab and field blanks had concentrations below the detection limit for chiral analysis.

RESULTS AND DISCUSSION

Sources of Chiral Pesticides

The EFs of alpha-HCH, cis and trans chlordane measured in seasonal snow pack did not vary from year to year when the snow was collected from the same location in the same park each year (Table 4.1). The EFs were more variable when the sampling sites were different year to year in each park, such as Mount Rainier where the EFs of alpha-HCH varied from 0.520 to 0.562. Although the EFs were variable, the non-racemic signatures observed within a park were still depleted in the same enantiomer.

The deposition of historic use pesticides (HUPs) in seasonal snowpack to WACAP sites was determined to be influenced by volatilization from regional agricultural soils and atmospheric transport to parks with high regional cropland intensity (Sequoia, Glacier, and Rocky) and long-range atmospheric transport to parks with low regional cropland intensity (Rainier, Denali, Gates of the Arctic, Noatak) [2]. A t-test revealed a significant difference (p-value < 0.001) between the racemic alpha-HCH signatures (0.505 ± 0.0057) measured at Noatak and Gates of the Arctic and the non-racemic alpha-HCH signatures (0.529 ± 0.0131) measured at Sequoia, Glacier, Mount Rainer, and Rocky Mountain (Figure 4.2, Table 4.1).

The alpha-HCH EF in seasonal snow pack was negatively correlated with site latitude ($r = 0.396$, p-value = 0.007), but positively correlated with site elevation ($r = 0.282$, p-value = 0.028) and mean site winter temperature ($r = 0.677$, p-value = 0.002) (Figure 4.3). The alpha-HCH EF in seasonal snow pack became more racemic at higher latitude, lower elevation, and lower temperature sites. The positive correlation of alpha-HCH EF with site elevation may be an artifact of the highest elevation sites being located at the lowest latitude sites [2]. The concentrations of alpha-HCH in agricultural and

background soils are relatively low because of its relatively low octanol-air partition coefficient and it has been suggested that the Pacific Ocean may be a major reservoir of non-racemic alpha-HCH [10, 12]. Passive air samplers, located at two Arctic sites where it was thought that ice cover prevented re-volatilization from the Arctic Ocean, had racemic alpha-HCH signatures that were attributed to long-range atmospheric transport [12]. Asian and Western U.S. air masses influenced by trans-Pacific transport have been previously shown to contain racemic alpha-HCH signatures [10]. These studies indicate that the racemic alpha-HCH measured in seasonal snowpack at the Alaskan sites (Noatak and Gates of the Arctic) is due to long-range atmospheric transport.

Non-racemic alpha-HCH enhanced in the (+) enantiomer was measured in seasonal snow pack at Sequoia, Glacier, Mount Rainier and Rocky Mountain are likely due to re-volatilization of alpha-HCH from regional agricultural soils, background soils, or the Pacific Ocean. Non-racemic alpha-HCH (enhanced in the (+) enantiomer) was also measured at a remote, marine site on the coast of Washington, and the non-racemic signature of alpha-HCH was attributed to background soil at the site and/or re-volatilization from the Pacific Ocean [10].

Technical chlordane has been banned from use in the US as an agricultural pesticide since 1983 and as a termiticide since 1988 [13]. The major sources of chlordane to the atmosphere are thought to be from agricultural soils in rural areas (a non-racemic signature) and soils surrounding the foundations of homes in urban areas (a racemic signature) [14]. Racemic cis- and trans-chlordane were measured in seasonal snowpack from Sequoia, while non-racemic cis- and trans-chlordane were measured in Glacier, Noatak, and Gates of the Arctic (Table 4.1). The chlordane concentrations in

seasonal snowpack from Rocky and Mount Rainier were below the chiral detection limit. The non-racemic cis and trans chlordane signatures measured in seasonal snowpack from Glacier, Noatak, and Gates of the Arctic followed the same enantioselective degradation that has been previously observed in agricultural soils [15]. This suggests that the racemic chlordane signature in seasonal snowpack at Sequoia was due to its past regional use as a termiticide around homes, while the non-racemic chlordane signature in snow pack at Glacier was due to volatilization from regional agricultural soils. Of all the WACAP parks, Sequoia has the highest population density within 300 km of the park (13 million people) [3]. As part of a global passive air sampling study, some of the highest chlordane concentrations in the world were measured near Los Angeles, CA at a site ~250 km south of Sequoia National Park [16]. Previous studies in the Western U.S. have also measured racemic cis- and trans-chlordane signatures in air masses influenced by California [10].

Because the cropland intensity and population was low surrounding the Alaskan parks [2], the non-racemic chlordane signature measured in Noatak and Gates of the Arctic seasonal snowpack was likely due to long-range transport from agricultural soils in Asia and North America.

No significant correlations were observed between the trans-chlordane EF and site latitude, elevation, or temperature (Figure 4.3). These correlations were not calculated for cis-chlordane because of the limited number of detections. These data suggest that the chiral signature of chlordanes in seasonal snow pack at WACAP sites is influenced by the site's proximity to urban centers (racemic in Sequoia), regional transport from

agricultural soils (non-racemic in Glacier), and long-range transport from agricultural soils (non-racemic in Noatak and Gates of the Arctic).

Occurence of Chiral Pesticides in Ecosystems

Sediment

The chiral pesticide EF in seasonal snow pack should be reflected in the surficial sediment of the associated lake catchment if the snow pack is a major contributor to the pesticide deposition in the lake catchment and there was no enantioselective biotransformation of the chiral pesticide in the water column or sediment. Cis-chlordane was the only chiral pesticide that was measured above the chiral detection limit in both seasonal snow pack and sediment and only at Pear Lake in Sequoia.

Previous studies have measured racemic cis-chlordane in surficial sediment and archived sediment cores from Long Island Sound, New York [17]. This study determined that either the biodegradation of chlordane in sediment is non-enantioselective or that biodegradation in sediment is inhibited due to anaerobic conditions. These findings were confirmed in a different study that observed a lack of chlordane biodegradation in flooded soils under anaerobic conditions [17, 18]. These studies suggest that the chiral signature of chlordane in lake sediment should reflect the chiral signature entering the lake catchment and not enantioselective biodegradation after deposition.

Racemic cis-chlordane was measured in seasonal snowpack and sediment from both Emerald and Pear lake catchments in Sequoia NP (Figure 4.2 and Figure 4.4). There was insufficient data to make this comparison at the other National Parks because cis-chlordane was below the chiral detection limit in snow at all of the other parks. Racemic

cis-chlordane was also measured in sediment from Golden Lake in Mount Rainier (Figure 4.4). Of the national parks studied, Mount Rainier has the second highest population density within 300 km of the park at 9 million people. Although the cis-chlordane EF in the seasonal snow pack at Mount Rainier was below the chiral detection limit, the sediment from Mount Rainier suggests that the park receives racemic chlordane based on it's proximity to urban areas like Sequoia.

A one-way analysis of variance (ANOVA) indicated that the mean cis-chlordane EFs in sediment collected from the different parks were not equal. In addition, Scheffe confidence intervals revealed that the non-racemic cis-chlordane EFs in Mills Lake and Lone Pine Lake sediment in Rocky Mountain were not significantly different from each other. However, the non-racemic cis-chlordane EF in Mills Lake was significantly different from the EFs of cis-chlordane in sediment from Emerald Lake and Pear Lake in Sequoia and Golden Lake in Mount Rainier (Figure 4.5). Non-racemic cis-chlordane, depleted in the (-) enantiomer, was measured in sediment from both Mills and Lone Pine lakes in Rocky Mountain. This same cis-chlordane depletion pattern was measured in agricultural soils from Alabama, the Midwestern U.S., Connecticut, Hawaii, and the U.K. [15]. This suggests that the source of non-racemic cis-chlordane to Rocky Mountain is revolatilization of chlordane from regional agricultural soils, while the source of racemic cis-chlordane to Sequoia and Mount Rainier is volatilization from urban areas where chlordane was used as a termiticide.

Fish

Aquatic organisms are exposed to chiral pesticides through the water column, diet, and sediment [5]. For hydrophobic pesticides with log octanol-water partition

coefficients greater than 5, such as chlordane, pesticide uptake by fish from the water column is insignificant compared to uptake via the food web [5]. Alpha-HCH has a log K_{ow} of 3.8 [19] and is the most abundant OCP in air and water in northern latitudes [20]. In general, the EFs of chiral pesticides increase in their deviation from racemic in the following order: air < water < soil < biota because of increasing enantioselective biotransformation [6].

Wong et al. measured racemic alpha-HCH signatures in rainbow trout fed a diet of racemic alpha-HCH and chlordane throughout the course of a 40-day study, followed by a depuration period of 238 days [21]. This study suggested that trout do not enantioselectively biotransform alpha-HCH and that non-racemic residues of alpha-HCH in rainbow trout are due to uptake of non-racemic alpha-HCH through the food [21]. In this same study, cis and trans-chlordane EFs in the same fish were significantly non-racemic after only 13 days. In our study, alpha-HCH was above the chiral detection limit in 9 out of the 33 trout from all of the parks (Table 4.1, Figure 4.6). The alpha-HCH EFs in fish in our study ranged from 0.309 to 0.507, while the trans-chlordane and cis-chlordane EFs ranged from 0.582 to 0.900 and 0.021 to 0.466, respectively. These results confirm that trans- and cis-chlordane are enantioselectively biotransformed in these trout species to a greater extent than alpha-HCH. The fish at Wonder Lake in Denali had alpha-HCH EFs ranging from 0.309 to 0.348, indicating enhanced degradation compared to the other parks. The age, species, and gender of the fish at Denali compared to other parks offered no explanation.

Non-racemic cis and trans-chlordane were measured in fish from all parks, with depletions in the (+) enantiomer and (-) enantiomer, respectively (Figure 4.7). This

suggests that the non-racemic chlordane signatures in the fish were due, at least in part, to biotransformation in the rainbow trout. The alpha-HCH EFs in fish reflected the alpha-HCH EFs in seasonal snow pack collected from the same lake catchment. However, the cis and trans-chlordane EFs in fish did not necessarily reflect the chlordane EFs in snow because of enantioselective biotransformation in the fish and/or enantioselective uptake through the food web.

Oxychlordane was measured in 29 out of 33 fish samples and the EF averaged 0.499 ± 0.027 (Figure 4.7). Previous studies with fish fed food with racemic chlordane measured oxychlordane a few days after trans-chlordane was significantly non-racemic, and the concentrations of oxychlordane remained constant over the course of the study [21]. Heptachlor epoxide was measured in 12 out of 33 fish samples and the EF averaged 0.619 ± 0.137 (Figure 4.7). Previous studies have measured EFs in Lake Ontario air (0.65), and Lake Superior (0.67), and surface water of the North Pole (0.62) [6]. Although the EF of heptachlor epoxide was below the chiral detection limit in snow, the EF of heptachlor epoxide in the fish indicates that the formation of this metabolite is not enantioselective in these species.

Finally, no significant correlations were observed between the alpha-HCH, oxychlordane, cis-chlordane, and trans-chlordane EFs measured in fish and fish age, weight, or trout species. In addition, a t-test revealed that there was no significant difference between the alpha-HCH, oxychlordane, cis-chlordane, and trans-chlordane EFs measured in male and female fish. This suggests that the enantioselective biotransformation of cis and trans-chlordane in fish from these high elevation and high latitude ecosystems is independent of fish age, weight, gender, or trout species.

ACKNOWLEDGEMENTS

The authors would like to thank Rachel Huber, Rebecca McElroy, and Dan Koch for their help in extracting and analyzing the snow, sediment and fish samples. This work was made possible by funding from the National Science Foundation CAREER (ATM-0239823) grant and also the National Institutes of Health (P30ES00210).

LITERATURE CITED

1. Ackerman, L. K.; Schwindt, A. R.; Simonich, S. L. M.; Koch, D. C.; Blett, T. F.; Schreck, C. B.; Kent, M. L.; Landers, D. H., Atmospherically deposited PBDEs, pesticides, PCBs, and PAHs in Western US National Park fish: Concentrations and consumption guidelines. *Environmental Science & Technology* **2008,** *42*, (7), 2334-2341.
2. Hageman, K. J.; Simonich, S. L.; Campbell, D. H.; Wilson, G. R.; Landers, D. H., Atmospheric deposition of current-use and historic-use pesticides in snow at national parks in the Western United States. *Environmental Science & Technology* **2006,** *40*, (10), 3174-3180.
3. Landers, D. H.; Simonich, S. L.; Jaffe, D. A.; Geiser, L. H.; Campbell, D. H.; Schwindt, A. R.; Schreck, C. B.; Kent, M. L.; Hafner, W. D.; Taylor, H. E.; Hageman, K. J.; Usenko, S.; Ackerman, L. K.; Schrlau, J. E.; Rose, N. L.; Blett, T. F.; Erway, M. M., The Fate, Transport, and Ecological Impacts of Airborne Contaminants in Western National Parks (USA). In EPA/600/R-07/138 .U.S. Environmental Protection Agency, O. o. R. a. D., Western Ecology Division, Corvallis, OR, Ed. 2008.
4. Usenko, S.; Landers, D. H.; Appleby, P. G.; Simonich, S. L., Current and historical deposition of PBDEs, pesticides, PCBs, and PAHs to rocky mountain national park. *Environmental Science & Technology* **2007,** *41*, (21), 7235-7241.
5. Borga, K.; Fisk, A.; Hoekstra, P.; Muir, D. C. G., Biological and Chemical Factors of Importance in the Bioaccumulation and Trophic Transfer of Persistent Organochlorine Contaminants in Arctic Marine Food Webs. *Environmental Toxicology and Chemistry* **2004,** *23*, (10), 2367-2385.
6. Hegeman, W. J. M.; Laane, R. W. P. M., Enantiomeric enrichment of chiral pesticides in the environment. *Reviews of Environmental Contamination and Toxicology, Vol 173* **2002,** *173*, 85-116.
7. Wiberg, K.; Letcher, R. J.; Sandau, C. D.; Norstrom, R. J.; Tysklind, M.; Bidleman, T. F., The enantioselective bioaccumulation of chiral chlordane and alpha-HCH contaminants in the polar bear food chain. *Environmental Science & Technology* **2000,** *34*, (13), 2668-2674.
8. Bidleman, T. F.; Falconer, R. L., Using enantiomers to trace pesticide emissions. *Environmental Science & Technology* **1999,** *33*, (9), 206A-209A.
9. Usenko, S.; Hageman, K. J.; Schmedding, D. W.; Wilson, G. R.; Simonich, S. L., Trace analysis of semivolatile organic compounds in large volume samples of snow, lake water, and groundwater. *Environmental Science & Technology* **2005,** *39*, (16), 6006-6015.

10. Genualdi, S.; Simonich, S. L.; Primbs, T.; Bidleman, T.; Jantunen, L.; Ryoo, K. S.; Feng, W.; Zhu, T., Chiral Signatures of Organochlorine Pesticides in Asian, Trans-Pacific and Western U.S. Air Masses. *In preparation for ES&T* **2008**.
11. Eitzer, B. D.; Mattina, M. I.; Iannucci-Bercer, W., Compositional and chiral profiles of weathered chlordane residues in soil. *Environmental Toxicology and Chemistry* **2001,** *20*, (10), 2198-2204.
12. Shen, L.; Wania, F.; Lei, Y. D.; Teixeira, C.; Muir, D. C. G.; Bidleman, T. F., Hexachlorocyclohexanes in the north American atmosphere. *Environmental Science & Technology* **2004,** *38*, (4), 965-975.
13. Leone, A. D.; Ulrich, E. M.; Bodnar, C. E.; Falconer, R. L.; Hites, R. A., Organochlorine pesticide concentrations and enantiomer fractions for chlordane in indoor air from the US cornbelt. *Atmospheric Environment* **2000,** *34*, (24), 4131-4138.
14. Bidleman, T. F.; Wong, F.; Backe, C.; Sodergren, A.; Brorstrom-Lunden, E.; Helm, P. A.; Stern, G. A., Chiral signatures of chlordanes indicate changing sources to the atmosphere over the past 30 years. *Atmospheric Environment* **2004,** *38*, (35), 5963-5970.
15. Bidleman, T. F., Leone, A.D. Falconer, R.L., Harner, T., Jantunen, L.M., Wiberg, K., Helm, P.A., Diamond, M.L., Loo, B., Chiral Pesticides in Soil and Water and Exchange with the Atmosphere. *The Scientific World* **2002,** *2*, 357-373.
16. Harner, T.; Shoeib, M.; Kozma, M.; Gobas, F. A. P. C.; Li, S. M., Hexachlorocyclohexanes and endosulfans in urban, rural, and high altitude air samples in the Fraser Valley, British Columbia: Evidence for trans-Pacific transport. *Environmental Science & Technology* **2005,** *39*, (3), 724-731.
17. Li, X. Q.; Yang, L. J.; Jans, U.; Melcer, M. E.; Zhang, P. F., Lack of enantioselective microbial degradation of chlordane in Long Island Sound sediment. *Environmental Science & Technology* **2007,** *41*, (5), 1635-1640.
18. Sethunathan, M., Microbial degradation of insecticides in flooded soil and in anaerobic cultures. *Residue Rev.* **1973,** *47*, 143-165.
19. Mackay, D.; Shiu, W.-Y.; Ma, K.-C., *Illustrated Handbook of Physical-Chemical Properties and Environmental Fate for Organic Chemicals*. Lewis Publishers: 1997 Vol. Pesticide Chemicals.
20. Falconer, R. L.; Bidleman, T. F.; Gregor, D. J.; Semkin, R.; Teixeira, C., Enantioselective Breakdown of Alpha-Hexachlorocyclohexane in a Small Arctic Lake and Its Watershed. *Environmental Science & Technology* **1995,** *29*, (5), 1297-1302.
21. Wong, C. S.; Lau, F.; Clark, M.; Mabury, S. A.; Muir, D. C. G., Rainbow trout (Oncorhynchus mykiss) can eliminate chiral organochlorine compounds enantioselectively. *Environmental Science & Technology* **2002,** *36*, (6), 1257-1262.

Figure 4.1 Map of National park sampling locations

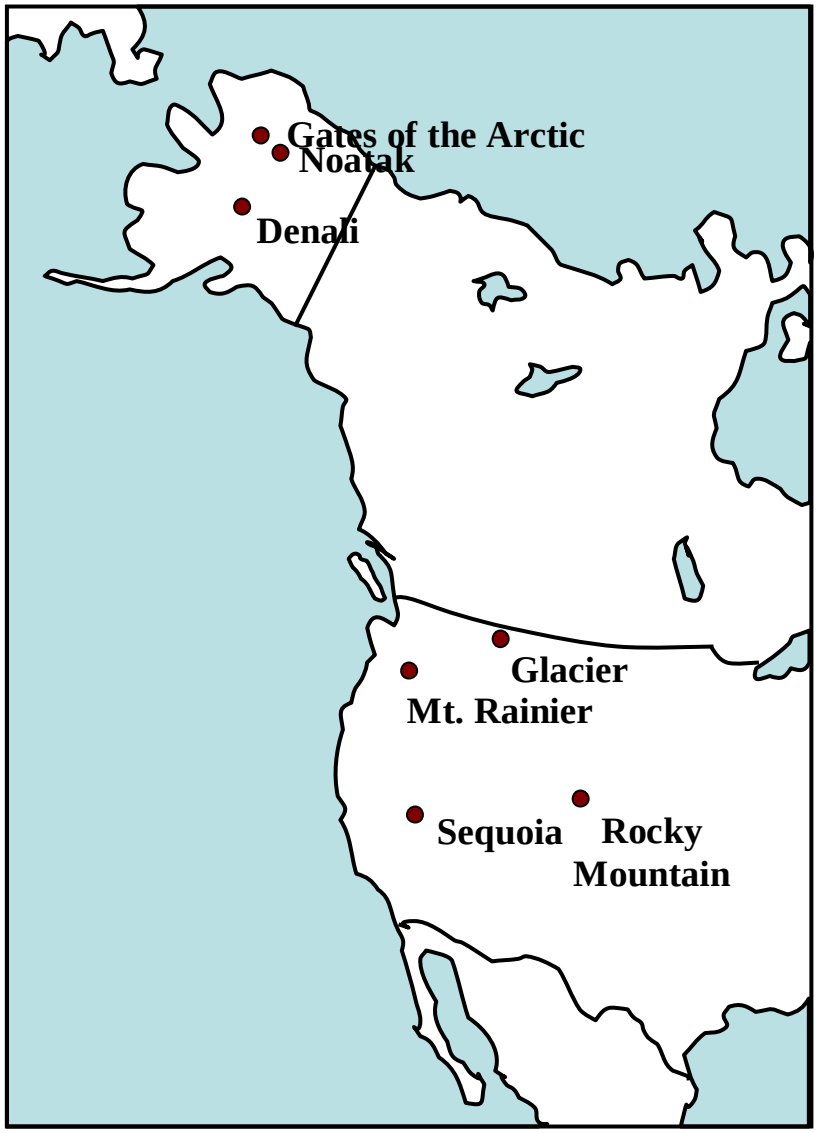

Figure 4.2. A. Alpha-HCH and B. trans and C. cis chlordane enantiomer fractions (EFs) in seasonal snowpack collected from SEKI (Sequoia), ROMO (Rocky Mountain), MORA (Mount Rainier), GLAC (Glacier), DENA (Denali), and NOAT and GAAR (Noatak and Gates of the Arctic). The dots in each box represent the median, and the limits of the box are the 25th and 75th quartiles. The black lines represent the 95% confidence interval of the racemic standard.

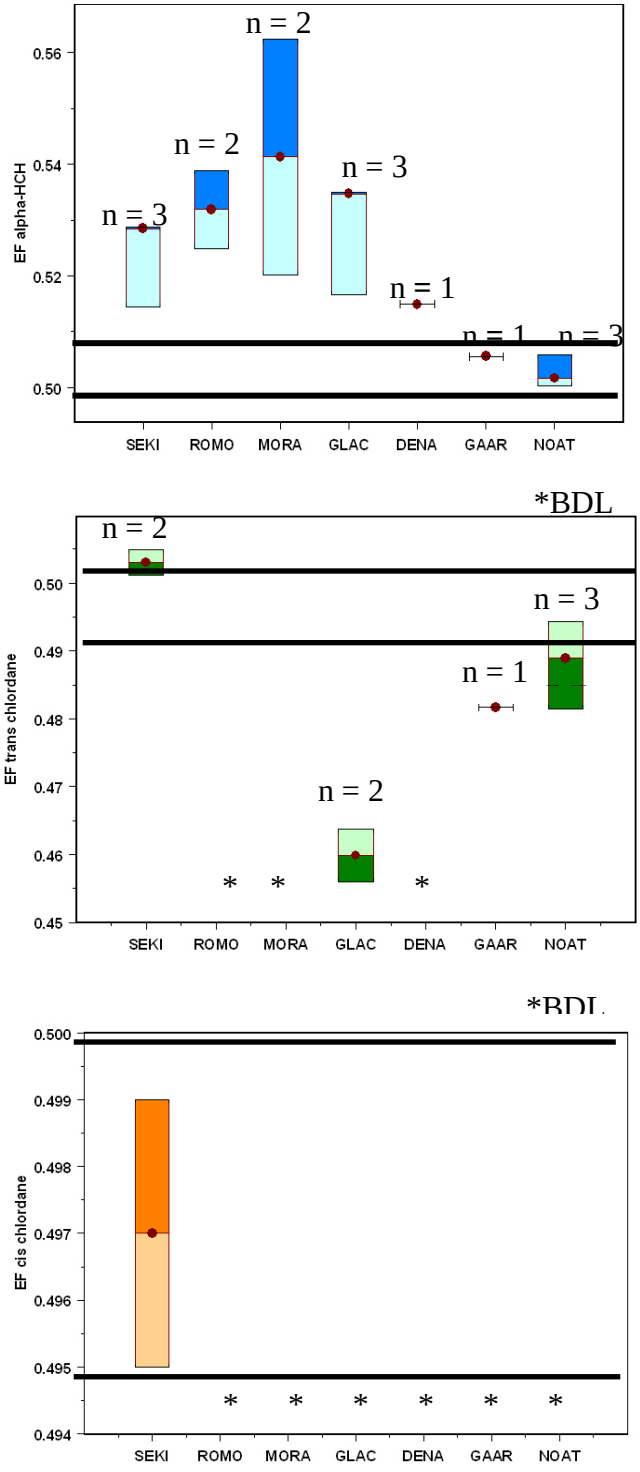

Figure 4.3. Correlations between the alpha-HCH and trans chlordane EFs in seasonal snow pack with latitude and elevation. The shaded box represents the 95% confidence interval for the racemic range of the standard.

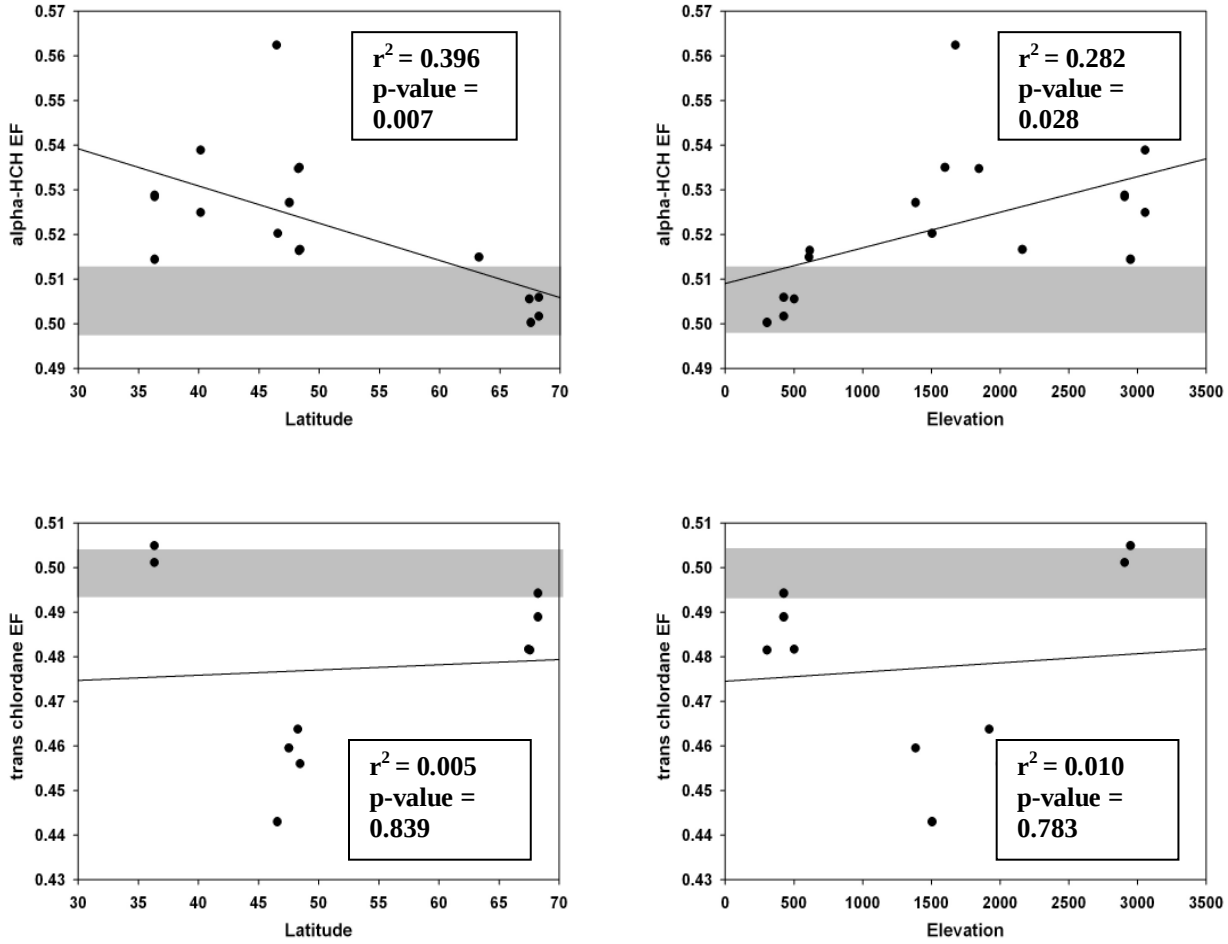

Figure 4.4. Cis-chlordane enantiomer fractions (EFs) in surficial and core sediment collected from SEKI (Sequoia), ROMO (Rocky Mountain), MORA (Mount Rainier), GLAC (Glacier), DENA (Denali), and NOAT and GAAR (Noatak and Gates of the Arctic) The black lines indicate the racemic range for the cis-chlordane standard. Cis chlordane was below the chiral detection limit (BDL) in Glacier (Oldman lake), Denali (Wonder lake), Gates of the Arctic (Matcharak lake), and Noatak (Burial lake). The dots in each box represent the median, while the upper and lower limits of the box represent the 75th and 25th quartiles, respectively.

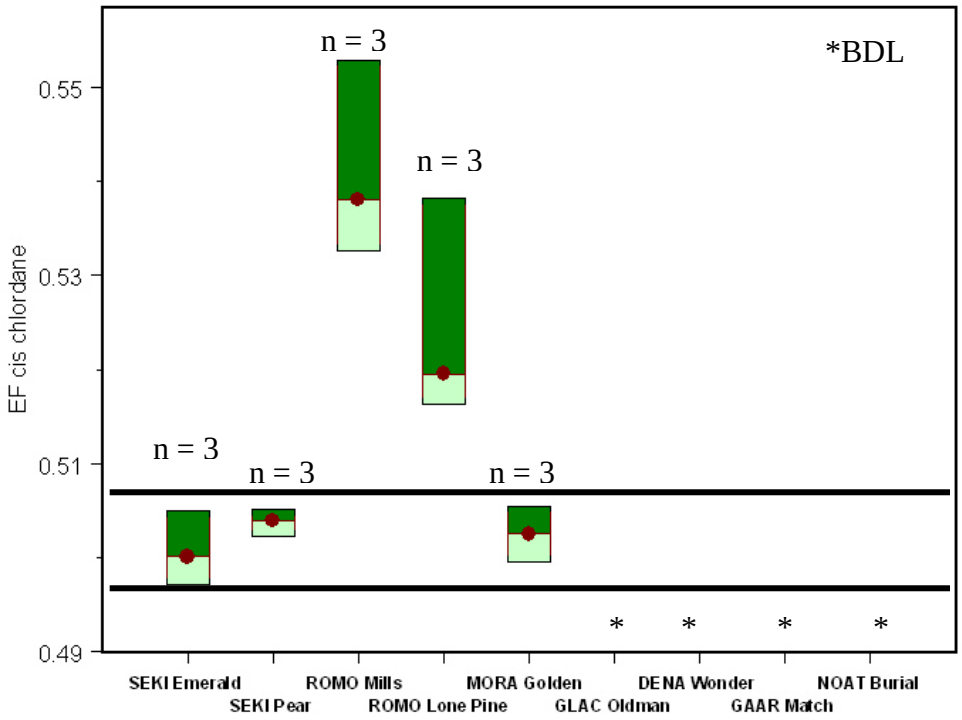

Figure 4.5. Scheffe confidence intervals of cis-chlordane enantiomer fractions (EFs) of cis chlordane measured in sediment at Sequoia (Emerald and Pear lakes), Rocky Mountain (Mills and Lone Pine lakes), and Glacier (Golden lake) lake catchments. If the confidence interval crosses zero, then there is no significant difference between those two lake catchments, however, if the confidence interval does not cross zero then the means of those two catchments are significantly different from each other.

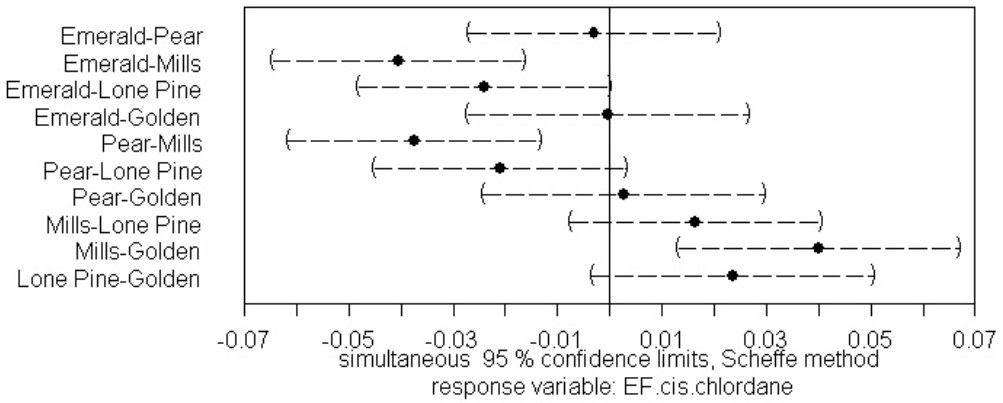

Figure 4.6. Alpha-HCH and trans-chlordane EFs in seasonal snow pack, sediment, and fish from lake catchments in Sequoia NP (SEKI), Rocky Mountain NP (ROMO), Mount Rainier NP (MORA), Glacier NP (GLAC), Denali NP (DENA), Gates of the Arctic (GAAR), and Noatak (NOAT)

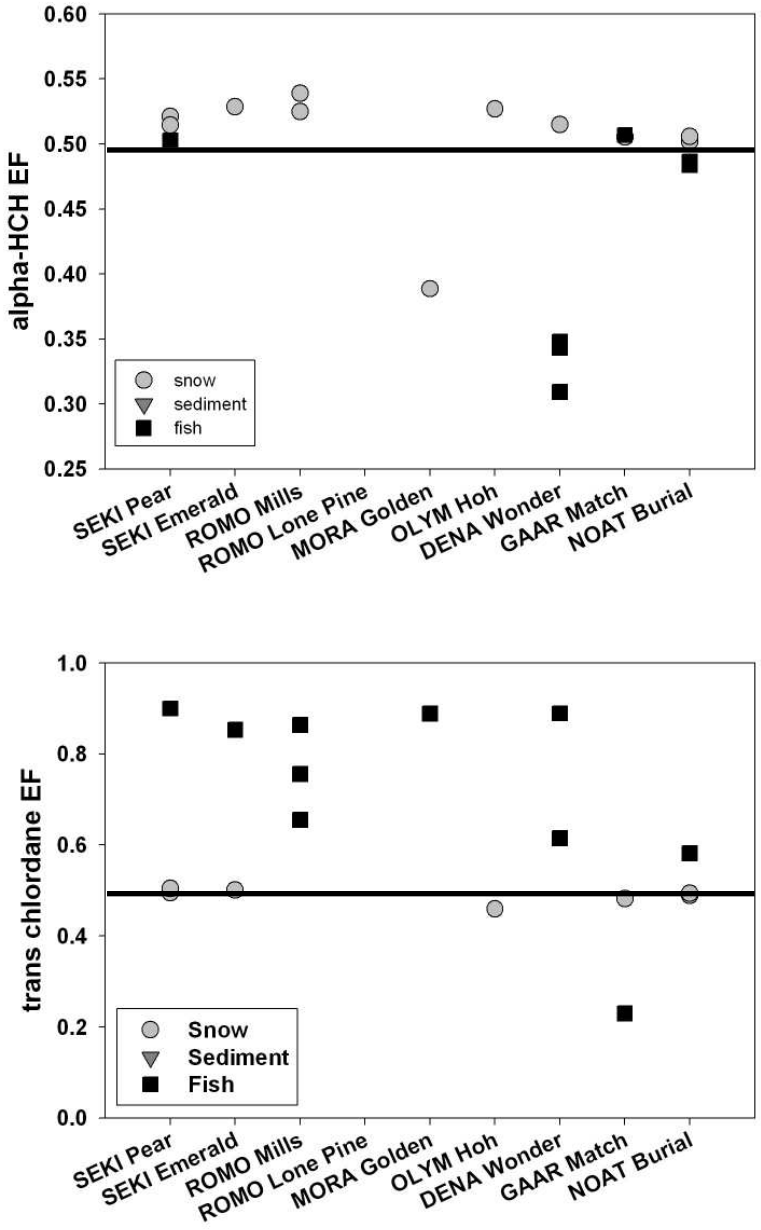

Figure 4.7. Oxy, trans, cis chlordane, alpha-HCH, and heptachlor epoxide enantiomer fractions (EFs) in fish collected from SEKI (Sequoia), ROMO (Rocky Mountain), MORA (Mount Rainier), GLAC (Glacier), DENA (Denali), NOAT (Noatak) and GAAR (Gates of the Arctic). The black line represents a racemic EF of 0.5. Racemic ranges vary for each analyte and are not displayed in this figure.

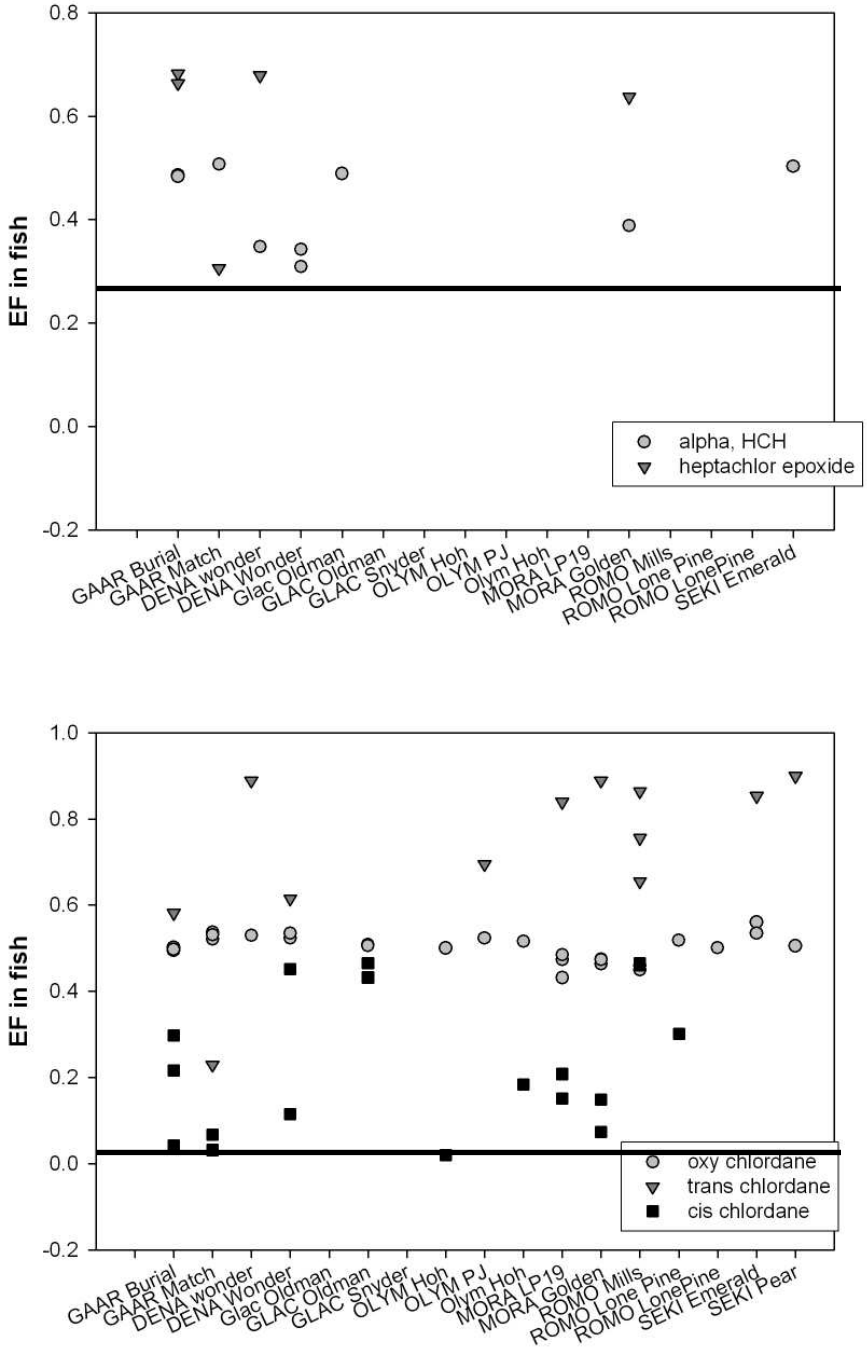

Table 4.1 Enantiomer Fractions (EFs) of alpha-HCH (aHCH), trans chlordane (TC), and cis chlordane (CC) in snow, sediment, and fish at WACAP sites. < DL indicated the sample was below the chiral detection limit and int indicates there was an interference and the ion ratios for the compound were greater than 20%.

			snow	sediment	fish		snow	sediment	fish		snow	sediment	fish
Park	**Catchment**		**aHCH**	**aHCH**	**aHCH**		**TC**	**TC**	**TC**		**CC**	**CC**	**CC**
SEKI	***Pear***		0.521	<DL	0.503		0.495	int	0.900		0.499	0.505	int
SEKI	***Pear***		<DL	<DL	<DL		<DL	int	<DL		<DL	0.504	<DL
SEKI `	***Pear***		0.514	<DL	<DL		0.505	int	<DL		0.495	0.502	<DL
SEKI	***Emerald***		0.528	<DL	<DL		0.501	int	0.853		<DL	0.505	int
SEKI	***Emerald***		<DL	<DL	<DL		<DL	int	<DL		<DL	0.497	<DL
SEKI	***Emerald***		<DL	<DL	<DL		<DL	int	<DL		<DL	0.500	<DL
ROMO	***Irene***		0.475	<DL	<DL		<DL	int	<DL		<DL	<DL	<DL
ROMO	***Mills***		0.539	<DL	<DL		<DL	int	0.655		<DL	0.533	0.466
ROMO	***Mills***		<DL	<DL	<DL		<DL	int	0.864		<DL	0.553	0.461
ROMO	***Mills***		0.525	<DL	<DL		<DL	int	0.756		<DL	0.538	<DL
ROMO	***Lone Pine***		<DL	<DL	<DL		<DL	int	int		<DL	0.516	0.302
ROMO	***Lone Pine***		<DL	<DL	<DL		<DL	int	<DL		<DL	0.538	int
ROMO	***Lone Pine***		<DL	<DL	<DL		<DL	int	<DL		<DL	0.520	<DL
MORA	***LP19***		<DL	<DL	<DL		<DL	int	0.840		<DL	<DL	0.209
MORA	***LP19***		<DL	<DL	<DL		<DL	int	int		<DL	<DL	0.152
MORA	***Golden***		<DL	<DL	<DL		<DL	int	0.889		<DL	0.503	0.149
MORA	***Golden***		<DL	<DL	<DL		<DL	int	int		<DL	0.500	0.074
MORA	***Golden***		<DL	<DL	<DL		<DL	int	<DL		<DL	0.506	int
MORA	***Fell fields***		<DL	<DL	<DL		<DL	int	<DL		<DL	<DL	<DL
MORA	***Sugarloaf***		<DL	<DL	<DL		<DL	int	<DL		<DL	<DL	<DL
MORA	***Edith***		<DL	<DL	<DL		<DL	int	<DL		<DL	<DL	<DL
MORA	***Paradise***		0.562	<DL	<DL		<DL	int	<DL		<DL	<DL	<DL
MORA	***Mowic***		0.520	<DL	<DL		<DL	int	<DL		<DL	<DL	<DL
MORA	***Paradise***		<DL	<DL	<DL		<DL	int	<DL		<DL	<DL	<DL

GLAC	***Oldman***	[redacted]	<DL	<DL	<DL	[redacted]	<DL	<DL	<DL	[redacted]	<DL	<DL	0.432
GLAC	***Oldman***	[redacted]	<DL	<DL	0.489	[redacted]	<DL	<DL	<DL	[redacted]	<DL	<DL	0.465
GLAC	***Granite Park***	[redacted]	<DL	<DL	<DL	[redacted]	0.456	<DL	<DL	[redacted]	<DL	<DL	<DL
GLAC	***Aster***	[redacted]	<DL	<DL	<DL	[redacted]	0.464	<DL	<DL	[redacted]	<DL	<DL	<DL
GLAC	***Preston***	[redacted]	<DL	<DL	<DL	[redacted]	<DL	<DL	<DL	[redacted]	<DL	<DL	<DL
GLAC	***Preston***	[redacted]	0.517	<DL	<DL	[redacted]	<DL	<DL	<DL	[redacted]	<DL	<DL	<DL
GLAC	***Aster***	[redacted]	0.535	<DL	<DL	[redacted]	<DL	<DL	<DL	[redacted]	<DL	<DL	<DL
GLAC	***Snyder***	[redacted]	0.535	<DL	<DL	[redacted]	<DL	<DL	<DL	[redacted]	<DL	<DL	<DL
GLAC	***Preston***	[redacted]	<DL	<DL	<DL	[redacted]	<DL	<DL	<DL	[redacted]	<DL	<DL	<DL
DENA	***Wonder***	[redacted]	<DL	<DL	0.348	[redacted]	<DL	<DL	0.889	[redacted]	<DL	<DL	0.452
DENA	***Wonder***	[redacted]	<DL	<DL	0.309	[redacted]	<DL	<DL	0.615	[redacted]	<DL	<DL	0.115
DENA	***Wonder***	[redacted]	<DL	<DL	0.343	[redacted]	<DL	<DL	int	[redacted]	<DL	<DL	int
DENA	***McLeod***	[redacted]	<DL	<DL	<DL	[redacted]	<DL	<DL	<DL	[redacted]	<DL	<DL	<DL
DENA	***Wonder***	[redacted]	<DL	<DL	<DL	[redacted]	<DL	<DL	<DL	[redacted]	<DL	<DL	<DL
GAAR	***Match***	[redacted]	0.506	<DL	0.507	[redacted]	0.482	<DL	0.230	[redacted]	<DL	<DL	0.068
GAAR	***Match***	[redacted]	<DL	<DL	<DL	[redacted]	<DL	<DL	<DL	[redacted]	0.491	<DL	0.032
NOAT	***Burial***	[redacted]	<DL	<DL	0.487	[redacted]	<DL	<DL	0.582	[redacted]	<DL	<DL	0.298
NOAT	***Burial***	[redacted]	0.502	<DL	0.484	[redacted]	0.489	<DL	int	[redacted]	0.510	<DL	0.217
NOAT	***Burial***	[redacted]	0.506	<DL	<DL	[redacted]	0.494	<DL	<DL	[redacted]	0.513	<DL	0.043
NOAT	***Kanglipack***	[redacted]	0.500	<DL	<DL	[redacted]	0.481	<DL	<DL	[redacted]	<DL	<DL	<DL

CHAPTER 5. CONCLUSION

Semi-volatile organic compounds (SOCs) were measured in air masses in the Pacific Northwestern U.S. in 2003 and were used to distinguish between regional and trans-Pacific atmospheric transport. During this time period, Cheeka Peak Observatory (CPO) in Washington State and Mary's Peak Observatory (MPO) in Oregon were both influenced by Siberian and regional biomass burning emissions. The historic-use pesticide, dieldrin and alpha-HCH, concentrations were enhanced during the Siberian fire events, while the current-use pesticide, dacthal and endoulfan, concentrations were enhanced during regional fire events. The concentrations of particulate phase polycyclic aromatic hydrocarbons (PAHs) were enhanced at MPO and gas phase PAHs were enhanced at CPO in air masses influenced by trans-Pacific atmospheric transport. The analysis of forest soils collected from a burned and unburned area of a regional forest fire, separated by a two lane road, indicated that 34 to 100% of the pesticide mass was lost from the soil due to volatilization and/or degradation during the burning process. This suggested that the elevated pesticide concentrations measured in air masses influenced by regional and Siberian fires was due to volatilization of historically deposited pesticides from soils and vegetation during the fire event.

Chiral organochlorine pesticides (OCPs) were measured in Asian air masses on Okinawa, Japan and in trans-Pacific and regional air masses at Cheeka Peak Observatory (CPO), WA, Mary's Peak Observatory (MPO), OR, and Mt. Bachelor Observatory (MBO), OR. Chiral OCPs were also measured in

agricultural soils collected from China, South Korea, and the Willamette Valley of Oregon.

Asian air masses and Asian soil contained racemic alpha-HCH. At CPO, non-racemic alpha-HCH was measured in regional air masses and was significantly different (p-value <0.001) from the racemic alpha-HCH measured in trans-Pacific air masses. CPO is located at 500 m elevation and 3 km from the Pacific Ocean in the marine boundary layer of the atmosphere. During trans-Pacific transport events to MPO and MBO (located at 1249 m and 2300 m elevation, respectively), racemic signatures of alpha-HCH were measured. The alpha-HCH enantiomer fractions (EFs) in CPO, MPO, and MBO air masses were positively correlated with the amount of time the air mass spent above the boundary layer, along the 10-day air mass back trajectory, prior to being sampled. This indicates that the marine boundary layer is influenced by non-racemic alpha-HCH due to re-volatilization of non-racemic alpha-HCH from soil and water bodies, such as the Pacific Ocean, while the free troposphere is a source of racemic alpha-HCH. Racemic cis and trans-chlordane were measured in Okinawa, MPO, and MBO air masses, indicating that urban areas in Asia and the U.S. continue to be sources of chlordane that has not yet undergone enantioselective biotransformation.

Non-racemic alpha-HCH was measured in seasonal snowpack from Western U.S. national parks (Sequoia, Glacier, and Rocky Mountain) due to revolatilization from regional agricultural soils. Racemic alpha-HCH was

measured in seasonal snowpack in Noatak and Gates of the Arctic due to long-range atmospheric transport.

At Sequoia, racemic cis and trans-chlordane were measured in seasonal snowpack, while non-racemic cis and trans-chlordane were measured in Glacier, Noatak National Preserve, and Gates of the Arctic. Of the national parks studied, Sequoia has the highest population density within 300 km of the park (12,841,589 people) and the racemic chlordane measured in this park is likely due to the parks close proximity to urban areas. Racemic cis-chlordane was measured in seasonal snowpack and sediment cores from Pear and Emerald Lakes in Sequoia. Scheffe confidence intervals indicated that the sources of cis-chlordane to Mills Lake in Rocky Mountain were different from the sources of cis-chlordane to Emerald and Pear Lakes in Sequoia.

The alpha-HCH EFs in fish from Sequoia, Gates of the Arctic, and Noatak reflected the alpha-HCH EFs in seasonal snowpack, indicating that the fish in these parks do not enantioselectively biotransform alpha-HCH. No significant correlations were observed between the alpha-HCH, trans-chlordane, cis-chlordane, and oxychlordane EFs in fish and fish age, weight, sex, or species suggesting that cis and trans-chlordane were enantioselectively biotransformed by fish *in vivo*.

Future work should include the characterization of Asian, North American, and Pacific Ocean air masses over a longer time period to assess the sources associated with seasonal variability. Episodic events such as trans-Pacific transport and forest fires were suggested to be significant sources of OCPs to the

Pacific Northwest, and chiral analysis has shown to be an effective technique that can be used to help characterize their sources. More measurements of SOCs are needed during these episodic events to confirm the origins of the enhanced SOCs observed in these air masses.

The Pacific Ocean was suggested to be a major reservoir of non-racemic alpha-HCH, although the enantiomer fraction (EF) of alpha-HCH in the Pacific Ocean has never been measured. Also, agricultural and background soils in the Pacific Northwest are not well characterized for OCP concentrations and chiral signatures. The emission of chiral OCPs to the atmosphere from background versus agricultural soils is also not well understood. In order to gain a better assessment of the sources of OCPs to the Pacific Northwest, more measurements in background soil, agricultural soil, and the Pacific Ocean need to be made. Also, in order to better assess the distribution of OCPs in different layers of the atmosphere, further studies should be done at one of the sampling locations along an elevational gradient with a sites in both the boundary layer and the free troposphere.

.

APPENDICES

Appendix A: SOC Concentrations (pg/m^3) for all 2003 CPO samples

	Trif	HCB	Hept	Dact	a-HCH	b-HCH	g-HCH	d-HCH
Jan 28-30	0.12	5.55	<DL	0.04	13.52	<DL	<DL	<DL
Mar 1-3	<DL	19.32	0.91	0.03	13.38	<DL	<DL	<DL
Apr 11-13	0.41	38.65	<DL	9.44	13.55	<DL	4.57	<DL
Apr 21-23	<DL	43.31	<DL	0.11	15.57	<DL	5.06	<DL
May 2-4	<DL	36.21	<DL	8.79	14.40	<DL	6.70	<DL
Jun 2-4	<DL	17.06	<DL	0.58	21.49	<DL	6.35	<DL
Jun 16-18	<DL	26.21	<DL	2.04	29.85	<DL	14.92	<DL
Jul 7-9	<DL	13.66	<DL	0.29	<DL	<DL	4.64	<DL
Jul 30 - Aug 1	<DL	<DL	<DL	<DL	<DL	<DL	<DL	<DL
Aug 4-6	<DL	28.63	<DL	0.07	22.86	<DL	4.66	<DL

	Trial	Metr	Ald	Chlorp	Chlorp ox	Hept epox	oxy-chlor	t-chlor	Endo 1
Jan 28-30	<DL	<DL	<DL	<DL	0.41	<DL	<DL	0.09	1.51
Mar 1-3	<DL	<DL	<DL	<DL	<DL	<DL	<DL	<DL	1.83
Apr 11-13	6.31	<DL	<DL	<DL	<DL	<DL	<DL	0.28	12.11
Apr 21-23	<DL	<DL	<DL	<DL	<DL	<DL	<DL	0.23	2.53
May 2-4	2.40	<DL	<DL	<DL	<DL	<DL	<DL	0.22	6.49
Jun 2-4	<DL	<DL	<DL	<DL	<DL	<DL	<DL	0.27	3.24
Jun 16-18	<DL	<DL	<DL	<DL	<DL	<DL	<DL	0.38	3.50
Jul 7-9	<DL	<DL	<DL	<DL	<DL	<DL	<DL	0.06	0.83
Jul 30 - Aug 1	<DL	<DL	<DL	<DL	<DL	<DL	<DL	<DL	<DL
Aug 4-6	<DL	<DL	<DL	<DL	0.32	<DL	<DL	0.18	3.29

	cis-chlor	NT	Dield	PCB 74	PCB 101	PCB 118	Endrin	Endo 2	CN
Jan 28-30	<DL	0.24	2.63	<DL	<DL	0.08	<DL	<DL	<DL
Mar 1-3	<DL	<DL	<DL	<DL	<DL	0.23	<DL	<DL	<DL
Apr 11-13	<DL	0.28	3.00	<DL	<DL	0.06	<DL	<DL	<DL
Apr 21-23	<DL	0.21	6.46	<DL	<DL	<DL	<DL	<DL	<DL
May 2-4	<DL	0.25	11.73	<DL	<DL	0.04	<DL	<DL	<DL
Jun 2-4	<DL	0.29	13.74	<DL	<DL	0.24	<DL	<DL	<DL
Jun 16-18	<DL	0.00	40.08	<DL	<DL	<DL	<DL	<DL	<DL
Jul 7-9	<DL	0.08	7.13	<DL	<DL	<DL	<DL	<DL	<DL
Jul 30 - Aug 1	<DL	<DL	<DL	<DL	<DL	<DL	<DL	<DL	<DL
Aug 4-6	<DL	0.17	10.01	<DL	<DL	0.12	<DL	0.34	<DL

	End ald	Endo sulf	PCB 153	PCB 138	PCB 187	PCB 183	ACE	FLO
Jan 28-30	2.08	0.04	0.10	0.07	0.04	0.03	<DL	<DL
Mar 1-3	<DL	<DL	<DL	<DL	<DL	<DL	<DL	<DL
Apr 11-13	<DL	<DL	<DL	<DL	<DL	<DL	<DL	52.22
Apr 21-23	<DL	<DL	<DL	<DL	<DL	<DL	<DL	32.35
May 2-4	<DL	<DL	<DL	<DL	<DL	<DL	<DL	22.20
Jun 2-4	<DL	<DL	0.13	<DL	<DL	<DL	<DL	11.70
Jun 16-18	<DL	<DL	<DL	<DL	<DL	<DL	<DL	5.87
Jul 7-9	<DL	<DL	<DL	<DL	<DL	<DL	<DL	<DL
Jul 30 - Aug 1	<DL	<DL	<DL	<DL	<DL	<DL	<DL	<DL
Aug 4-6	<DL	<DL	0.33	<DL	<DL	<DL	<DL	3.07

	PHE	ANT	FLA	PYR	RET	BaA	CT
Jan 28-30	<DL	<DL	<DL	<DL	<DL	<DL	<DL
Mar 1-3	<DL	<DL	<DL	<DL	<DL	<DL	<DL
Apr 11-13	34.65	<DL	8.34	0.35	<DL	3.01	1.42
Apr 21-23	45.21	<DL	11.22	7.24	<DL	<DL	<DL
May 2-4	55.75	<DL	10.36	7.26	<DL	<DL	<DL
Jun 2-4	38.72	<DL	19.21	19.38	8.65	<DL	<DL
Jun 16-18	34.85	<DL	22.79	26.85	9.64	<DL	<DL
Jul 7-9	62.33	<DL	18.41	19.26	<DL	<DL	<DL
Jul 30 - Aug 1	64.52	<DL	35.48	<DL	<DL	<DL	<DL
Aug 4-6	35.46	<DL	22.50	30.13	8.85	<DL	<DL

	BbF	BkF	BeP	BaP	IcdP	BghiP
Jan 28-30	<DL	<DL	<DL	<DL	<DL	<DL
Mar 1-3	<DL	<DL	<DL	<DL	<DL	<DL
Apr 11-13	<DL	<DL	<DL	<DL	<DL	<DL
Apr 21-23	2.95	<DL	1.03	<DL	<DL	<DL
May 2-4	4.43	<DL	<DL	<DL	<DL	<DL
Jun 2-4	<DL	2.34	<DL	<DL	<DL	<DL
Jun 16-18	<DL	<DL	<DL	<DL	<DL	<DL
Jul 7-9	<DL	<DL	<DL	<DL	<DL	<DL
Jul 30 - Aug 1	<DL	<DL	<DL	<DL	<DL	<DL
Aug 4-6	<DL	<DL	<DL	<DL	<DL	<DL

Appendix B: SOC Concentrations (pg/m^3) for all 2003 MPO samples

	HCB	a-HCH	g-HCH	Trial	Dact	Chlorp Ox	Chlorp	t-chlor	Endo	TN	Dield
May 11-13	<DL	<DL	<DL	<DL	<DL	<DL	<DL	<DL	<DL	<DL	<DL
May 21-23	3531.71	3532.65	3533.12	<DL	3533.77	<DL	3536.76	3538.45	3539.48	3539.57	3540.04
May 26-28	284.47	300.00	300.00	<DL	<DL	<DL	268.19	167.82	167.82	83.91	<DL
Jun 1-3	<DL	<DL	<DL	<DL	<DL	<DL	<DL	<DL	<DL	<DL	<DL
June 4-6	<DL	<DL	<DL	<DL	<DL	<DL	<DL	<DL	<DL	<DL	<DL
June 22-24	<DL	<DL	<DL	<DL	<DL	<DL	<DL	<DL	<DL	<DL	<DL
July 4-6	31.90	32.45	10.98	12.60	39.42	37.53	13.25	50.73	14.26	7.84	<DL
July 24-26	21.31	23.86	6.87	<DL	28.91	<DL	10.25	36.97	9.30	8.55	53.09
Aug 2-4	8.93	5.90	<DL	<DL	7.73	<DL	<DL	<DL	<DL	<DL	<DL
Aug 4-5	19.82	<DL	<DL	<DL	<DL	<DL	0.99	<DL	<DL	<DL	<DL
Aug 10-12	55.23	3.70	<DL	<DL	0.29	<DL	0.67	3.67	0.03	0.74	5.65
Aug 12-14	<DL	<DL	<DL	<DL	0.00	<DL	67.87	<DL	<DL	<DL	<DL
Sept 4-5	6.38	16.07	1.33	<DL	13.99	<DL	40.61	8.31	<DL	4.54	4.84
Sept. 9-22	2.16	3.44	0.82	<DL	<DL	<DL	1.19	3.57	<DL	0.00	1.51

	PCB 118	Endrin	Endo II	CN	Endo Sulf	PCB 153	PCB 138	PCB 187	PCB 183	EPTC	Etridiazole	Pebulate
May 11-13	<DL	<DL	<DL	<DL	<DL	<DL	<DL	<DL	<DL	<DL	<DL	<DL
May 21-23	3540.41	<DL	3544.06	<DL	<DL	<DL	<DL	<DL	<DL	<DL	<DL	<DL
May 26-28	167.82	<DL	<DL	<DL	<DL	<DL	<DL	<DL	<DL	<DL	<DL	<DL
Jun 1-3	<DL	<DL	<DL	<DL	<DL	<DL	<DL	<DL	<DL	<DL	<DL	<DL
June 4-6	<DL	<DL	<DL	<DL	<DL	<DL	<DL	<DL	<DL	<DL	<DL	<DL
June 22-24	<DL	<DL	<DL	<DL	<DL	<DL	<DL	<DL	<DL	<DL	<DL	<DL
July 4-6	46.69	<DL	25.07	<DL	<DL	<DL	<DL	<DL	<DL	<DL	<DL	<DL
July 24-26	44.85	<DL	25.18	<DL	<DL	<DL	<DL	<DL	<DL	<DL	<DL	<DL
Aug 2-4	<DL	<DL	4.16	<DL	<DL	<DL	<DL	<DL	<DL	<DL	<DL	<DL
Aug 4-5	<DL	<DL	<DL	<DL	<DL	<DL	<DL	<DL	<DL	<DL	<DL	<DL
Aug 10-12	5.31	<DL	<DL	<DL	<DL	<DL	<DL	<DL	<DL	<DL	<DL	<DL
Aug 12-14	<DL	<DL	<DL	<DL	<DL	<DL	<DL	<DL	<DL	<DL	<DL	<DL
Sept 4-5	7.84	<DL	2.60	<DL	<DL	<DL	<DL	<DL	<DL	<DL	<DL	<DL
Sept. 9-22	1.90	<DL	2.45	<DL	<DL	<DL	<DL	<DL	<DL	<DL	<DL	<DL

	Acenaphthylene	ACE	FLO	Phorate	Demeton	Propachlor	Atrazine desisoproply	Atrazine desethyl	Carbofuran	Simazine
May 11-13	<DL	<DL	1720	<DL	<DL	<DL	<DL	<DL	<DL	<DL
May 21-23	<DL	<DL	2903.8	<DL	<DL	<DL	<DL	<DL	<DL	<DL
May 26-28	<DL	<DL	610.28	<DL	<DL	<DL	<DL	<DL	<DL	<DL
Jun 1-3	<DL	<DL	325.87	<DL	<DL	<DL	<DL	<DL	<DL	<DL
June 4-6	<DL	774	1906.1	<DL	<DL	<DL	<DL	<DL	<DL	<DL
June 22-24	<DL	<DL	511.48	<DL	<DL	<DL	<DL	<DL	<DL	<DL
July 4-6	<DL	<DL	1078.8	<DL	<DL	<DL	<DL	<DL	<DL	<DL
July 24-26	<DL	888	3264.8	<DL	<DL	<DL	<DL	<DL	<DL	<DL
Aug 2-4	<DL	22	482.45	<DL	<DL	<DL	<DL	<DL	<DL	<DL
Aug 4-5	<DL	215	759.07	<DL	<DL	<DL	<DL	<DL	<DL	<DL
Aug 10-12	<DL	822	1057.6	<DL	<DL	<DL	<DL	<DL	<DL	<DL
Aug 12-14	<DL	526	1580	<DL	<DL	<DL	<DL	<DL	<DL	<DL
Sept 4-5	<DL	1288	1588.2	<DL	<DL	<DL	<DL	<DL	<DL	<DL
Sept. 9-22	<DL	<DL	823.04	<DL	<DL	<DL	<DL	<DL	<DL	<DL

	Prometon-	Atrazine	Cyanazine	PHE	ANT	Diazinon	Disulfoton	Acetochlor	Alachlor	Metolachlor	Triallate
May 11-13	<DL	<DL	<DL	2926	<DL	<DL	<DL	<DL	<DL	<DL	<DL
May 21-23	<DL	<DL	<DL	6989	<DL	<DL	<DL	<DL	<DL	<DL	<DL
May 26-28	<DL	<DL	<DL	940	<DL	<DL	<DL	<DL	<DL	<DL	<DL
Jun 1-3	<DL	<DL	<DL	863	<DL	<DL	<DL	<DL	<DL	<DL	<DL
June 4-6	<DL	<DL	<DL	4055	<DL	<DL	<DL	<DL	<DL	<DL	<DL
June 22-24	<DL	<DL	<DL	1841	<DL	<DL	<DL	<DL	<DL	<DL	<DL
July 4-6	<DL	150.1	<DL	1720	<DL	<DL	<DL	<DL	<DL	<DL	<DL
July 24-26	<DL	<DL	<DL	7814	<DL	<DL	<DL	<DL	<DL	<DL	<DL
Aug 2-4	<DL	<DL	<DL	1121	<DL	<DL	<DL	<DL	<DL	<DL	<DL
Aug 4-5	<DL	<DL	<DL	1200	<DL	<DL	<DL	<DL	<DL	<DL	<DL
Aug 10-12	<DL	<DL	<DL	5054	153	<DL	<DL	<DL	<DL	<DL	<DL
Aug 12-14	<DL	<DL	<DL	6058	0	<DL	<DL	<DL	<DL	<DL	<DL
Sept 4-5	<DL	<DL	<DL	7799	375	<DL	<DL	<DL	<DL	<DL	<DL
Sept. 9-22	<DL	<DL	<DL	2887	0	<DL	<DL	<DL	<DL	<DL	<DL

	Carbaryl	Malathion	Methyl parathion	Parathion	Ethion	FLA	PYR	RET	o,p'-DDE	p,p'-DDE	o,p'-DDD
May 11-13	<DL	<DL	<DL	<DL	<DL	398.5	744	446	<DL	<DL	<DL
May 21-23	<DL	<DL	<DL	<DL	<DL	888.3	1036	762	<DL	<DL	<DL
May 26-28	<DL	<DL	<DL	<DL	<DL	105.5	226	170	<DL	<DL	<DL
Jun 1-3	<DL	<DL	<DL	<DL	<DL	20.27	300	14	<DL	<DL	<DL
June 4-6	<DL	<DL	<DL	<DL	<DL	327.6	352	278	<DL	21.05	<DL
June 22-24	<DL	<DL	<DL	<DL	<DL	140	248	276	<DL	<DL	<DL
July 4-6	<DL	<DL	<DL	<DL	<DL	283.5	437	301	<DL	<DL	<DL
July 24-26	<DL	<DL	<DL	<DL	<DL	1481	2295	986	<DL	<DL	<DL
Aug 2-4	<DL	<DL	<DL	<DL	<DL	189.2	375	<DL	<DL	<DL	<DL
Aug 4-5	<DL	<DL	<DL	<DL	<DL	198.7	368	263	<DL	<DL	<DL
Aug 10-12	<DL	<DL	<DL	<DL	<DL	621	1616	500	<DL	<DL	<DL
Aug 12-14	<DL	<DL	<DL	<DL	<DL	628	1594	532	<DL	<DL	<DL
Sept 4-5	<DL	<DL	<DL	<DL	<DL	998.6	3238	959	<DL	<DL	<DL
Sept. 9-22	<DL	<DL	<DL	<DL	<DL	170.2	243	197	<DL	12.35	<DL

	p,p'-DDD	o,p'-DDT	p,p'-DDT	Methoxychlor	TPB	BaA	CT	BbF	BkF	BeP	BaP	IcdP	DahA	BghiP
May 11-13	<DL	<DL	<DL	<DL	230	45	41	<DL	<DL	<DL	<DL	<DL	<DL	40.36
May 21-23	<DL	<DL	<DL	<DL	154	58	41	<DL	<DL	<DL	<DL	<DL	<DL	50.83
May 26-28	<DL	<DL	<DL	<DL	63	<DL	<DL	<DL	<DL	<DL	<DL	<DL	<DL	11.04
Jun 1-3	<DL	<DL	<DL	<DL	6.3	<DL	<DL	<DL	<DL	17	<DL	25.9	<DL	10.78
June 4-6	<DL	<DL	<DL	<DL	405	<DL	129	91	349	147	<DL	146	<DL	79.87
June 22-24	<DL	<DL	<DL	<DL	102	<DL	<DL	<DL	<DL	<DL	<DL	<DL	<DL	8.55
July 4-6	<DL	<DL	<DL	<DL	71	52	<DL	<DL	<DL	<DL	<DL	22	<DL	29.11
July 24-26	<DL	<DL	<DL	<DL	175	<DL	<DL	<DL	<DL	<DL	<DL	<DL	<DL	<DL
Aug 2-4	<DL	<DL	<DL	<DL	8.4	<DL	<DL	<DL	<DL	18	<DL	18.5	<DL	11.94
Aug 4-5	<DL	<DL	<DL	<DL	127	<DL	<DL	<DL	<DL	15	<DL	<DL	<DL	12.66
Aug 10-12	<DL	<DL	<DL	<DL	131	<DL	13	<DL	<DL	312	<DL	<DL	<DL	14.25
Aug 12-14	<DL	<DL	<DL	<DL	121	<DL	<DL	<DL	<DL	<DL	<DL	25.7	<DL	24.31
Sept 4-5	<DL	<DL	<DL	<DL	233	<DL	<DL	<DL	<DL	959	60	<DL	<DL	17.83
Sept. 9-22	<DL	<DL	<DL	<DL	112	60	15	<DL	<DL	32	105	26.6	<DL	28.2